UNIVERSITY OF CALIFORNIA
RIVERSIDE

Global Change and Mountain Lakes
Establishing Nutrient Criteria and Critical Loads for Sierra Nevada Lakes

A Dissertation submitted in partial satisfaction
of the requirements for the degree of

Doctor of Philosophy

in

Environmental Sciences

by

Andrea Michelle Heard

August 2013

Dissertation Committee:
Dr. James O. Sickman, Chairperson
Dr. Michael Anderson
Dr. Edith Allen

Copyright by
Andrea Michelle Heard
2013

The Dissertation of Andrea Michelle Heard is approved:

Committee Chairperson

University of California, Riverside

ACKNOWLEDGEMENTS

I would like to first acknowledge my advisor and committee members, Drs. James Sickman, Michael Anderson, Edith Allen, David Parker, William Walton, and Louis Santiago for their guidance and support through this process. I would like to thank Jim for all the time and enthusiasm he directs towards mentoring graduate students. My research and personal growth benefitted immensely from Jim's knowledge, expertise, and, especially, his enthusiasm for science. I would like to thank Dr. Neil Rose at the University College London for sharing his expertise and data and inviting me into his lab to learn the intricacies of spheroidal carbonaceous particles. This dissertation and subsequent manuscripts have greatly benefitted from Neil's reviews. Dr. David Clow with the U.S. Geological Survey provided guidance, especially with the spatial analysis.

I would like to acknowledge my colleagues at the Sierra Nevada Network, National Park Service (NPS) who have provided tremendous support during this journey. I could never have done this without the support of my supervisors, Linda Mutch and Alice Chung-MacCoubrey. They supported me in many ways, including, but not limited to, providing me the flexibility I needed to balance work and school, back-filling for my position, and contributing resources directly to my field work. I could not have completed the GIS work without Sandy Graban's guidance and work. Thank you to Jennie Skancke, Les Chow, Jenny Matsumoto, Jonny Nesmith, Tani Meadows, Annie Esperanza, and Jim Roche.

There were many people that helped out with field work. I would like to thank my NPS crews (Dena Paolilli, Lindsay Belt, Scott Roberts, Cat Fong, Natalie Rouse, Josh

Baccei, Scott Cereghino, Harrison Forrester, Nathan Ernster, Rich Thiel, Ari Sarzotti, and SIEN staff mentioned above), UCR colleagues (Pete Homyak, Thomas Martin, Paul Koster, Amanda and Marcus James, Dee Lucero, Joy McCullough, Will Vicars, and Kristy Richardson), USFS colleague (Tracy Weddle), and family (Alice Heard).

I would like to thank Dee Lucero, Dave Thomason, and Woody Smith for the guidance and help in the lab. I also would like to thank Ahmed Haggag and Amanda James for their lab support.

This research was funded by the University of California, Riverside, National Park Service, USDA Forest Service, and Geological Society of America.

DEDICATION

I dedicate this dissertation to my family and friends who have supported and inspired me in so many ways. To my parents, Stuart and Alice, for their encouragement through all my years of education. To Rich for his love and support and with whom I share this achievement. To my brother, Steve, for his unconditional support, interest, and enthusiasm in my endeavors and sister-in-law, Kristyn, with whom I enjoyed sharing the grad school experience with during holiday runs. To my good friend Meryl Rose for always being only a phone call away. I can't mention everyone here as I am so fortunate to have a large and supportive family and close network of friends – but I truly dedicate this dissertation to all of you.

ABSTRACT OF THE DISSERTATION

Global Change and Mountain Lakes
Establishing Nutrient Criteria and Critical Loads for Sierra Nevada Lakes

by

Andrea Michelle Heard

Doctor of Philosophy, Graduate Program in Environmental Sciences
University of California, Riverside, August 2013
Dr. James O. Sickman, Chairperson

Increased inputs of nutrients and acid anions to oligotrophic mountain lakes are contributing to ANC depression, elevated nitrate concentrations, shifts in nutrient limitation, and changes in the productivity and structure of aquatic communities. A need for stricter standards based on measurable ecological effects has been identified as an important step toward the long-term protection of mountain lakes. The objectives of this research were to link atmospheric deposition with acidification and eutrophication effects, develop critical loads and nutrient criteria, and assess status and trends of Sierra Nevada lakes. Investigation of multiple proxies of deposition, climate, acidification, and eutrophication indicated that early 20th century ANC decline in a Sierra Nevada lake is attributed to atmospheric deposition and the subsequent recovery in the late 20th century is attributed to the success of the Clean Air Act. Correlation analysis indicated ANC was correlated with atmospheric deposition indicators, but was not correlated with climate

measures or productivity proxies. However, analyses looking more broadly across the landscape found a correlation with present day indicators of atmospheric deposition (SCPs) and ANC. These results indicate that not all lakes have fully recovered from acid deposition and stricter regulatory standards are needed. I aimed to link atmospheric deposition indicators with effects of eutrophication and acidification at a landscape scale and found that atmospheric deposition indicators were correlated with acidification, but not with eutrophication. Quantifying the relationship between nitrogen deposition and eutrophication across complex mountain landscapes is presently challenging, leading to the conclusion that critical loads based on acidification are a more robust approach. An acidification critical load was calculated based on 20th century ANC and acid deposition patterns and is 73.9 eq ha^{-1} yr^{-1} for acid anions, which translates to 0.68 kg-N ha^{-1} yr^{-1} and 1.2 kg-SO_4 ha^{-1} yr^{-1}. Nitrogen criteria were calculated and ranged from were 0.33 – 0.89 μM (10% ED), 1.0 – 4.0 μM (50% ED), and 3.1 – 18 μM (90% ED). Application of criteria to Sierra Nevada lakes indicated the 10% effective dose was exceeded by 28-37 %, the 50% effective dose was exceeded by 18-29%, and the 90% effective dose was exceeded by 0.0-21%.

Table of Contents

Chapter 1: Introduction 1

Chapter 2: 20th Century Atmospheric Deposition and Lake Acidification Trends in Western Mountain Lakes (USA): Importance of the Clean Air Act 6

2.1 Abstract 6

2.2 Introduction 7

2.3 Methods 11

2.3.1 Site Description 11
2.3.2 Sediment Core Sampling Methods 12
2.3.3 Sediment Core Laboratory Analysis 13
2.3.4 Sediment Core Data Analysis 14
2.3.5 Emerald Lake ANC Trends 16
2.3.6 Critical Load Calculation 16

2.4 Results 19

2.4.1 Spheroidal Carbonaceous Particles 19
2.4.2 ANC Comparison 19
2.4.3 Biogenic Silica and Stable Carbon Isotopes 21
2.4.4 PCA Bi-plot 21
2.4.5 Emerald Lake ANC Trends 21
2.4.6 Critical Load 22

2.5 Discussion 23

2.6 Tables and Figures 34

Chapter 3: Landscape Analysis Correlating Atmospheric Deposition and Chemical Indicators of Acidification and Eutrophication to Inform Critical Load Development.... 43

3.1 Abstract 43

3.2 Introduction 44

3.3 Methods 47

3.3.1 Study Area 47
3.3.2 Sample Design 47
3.3.3 Sample Collection and Analysis 48

3.3.4 Basin Characteristics 50
3.3.5 Data Analysis 51

3.4 Results 52

3.5 Discussion 54

3.5.1 Spheroidal Carbonaceous Particles 54
3.5.2 Lake Nitrate $\delta^{18}O$ and $\delta^{15}N$ 60
3.5.3 Implications for Critical Loads 63

3.6 Conclusions 65

3.7 Tables and Figures 66

Chapter 4: Nutrient Criteria Development and Application to Sierra Nevada Lakes .. 79

4.1 Abstract 79

4.2 Introduction 80

4.3 Methods 85

4.3.1 Limnocorral Experiments 86
4.3.2 Cubitainer Experiments 87
4.3.3 Survey Data 89
4.3.4 Data Analysis 90

4.4 Results 92

4.4.1 Chemistry and Chlorophyll a 92
4.4.2 Modeling 95
4.4.3 Application of Criteria to Survey Data 98

4.5 Discussion 98

4.5.1 Response to Nutrient Additions 98
4.5.2 Modeling 101
4.5.3 Application of Criteria 105

4.6 Tables and Figures 108

Chapter 5: Conclusion 126

Chapter 6: References 130

List of Tables

Table 2.1: Total annual precipitation and deposition at Emerald Lake.. 34

Table 2.2: Mean critical load (CL) results. 35

Table 2.3: Maximum SCP concentrations from a selection of lakes in Canada, Chile, Europe, Russia, United Kingdom, and United States. 36

Table 3.1: Summary statistics for SCPs, $\delta^{18}O$ (NO_3^-), $\delta^{15}N$ (NO_3^-), ANC, DIN:TP, and nitrate in the diatom and SIEN data sets. 66

Table 3.2: Diatom data set Kendall tau correlation results for atmospheric deposition indicators, lake chemistry variables, and basin characteristics. 67

Table 3.3: SIEN data set Kendall tau correlation results for atmospheric deposition indicators, lake chemistry variables, and basin characteristics. 68

Table 3.4: SCP-ANC Kendall tau correlation results comparing the correlation for all data to data stratified by low and high sulfate concentrations. 69

Table 4.1: Descriptions of each experiment 108

Table 4.2: Logistics function modeling results. 109

Table 4.3: High and low criteria estimates and summary of effective dose results used to calculate criteria estimates. 110

Table 4.4: Percent of lakes in Sequoia, Kings Canyon, and Yosemite that exceed high and low criteria estimates. 110

List of Figures

Figure 2.1: Moat, Emerald, and Pear Lake locations in the Sierra Nevada, California.... 37

Figure 2: Sediment accumulation rates for Moat, Pear, and Emerald Lakes..... 38

Figure 2.3: a) Moat Lake SCP concentrations and reconstructed ANC, b) Pear Lake SCP concentrations, and c) Emerald Lake SCP concentrations. 39

Figure 2.4: Time series graphs for a) California mean annual air temperature presented as the 3-year moving average, b) California mean annual precipitation as the 3-year moving average, c) April 1st SWE at Donner Summit (DNS) and Virginia Lakes (VGL) presented as the 3-year moving averages, d) national NO_x and SO_2 emissions, and e) diatom reconstructed ANC..... 40

Figure 2.5: BSi and $\delta^{13}C$ profiles for Moat Lake..... 41

Figure 2.6: PCA bi-plot for Moat Lake sediment, emissions, and climate variables. 41

Figure 2.7: Residuals for regression between April 1st SWE and summer ANC graphed over time. 42

Figure 2.8: Reconstructed acid anion deposition trends for a) sulfate and b) nitrate. 42

Figure 3.1: Diatom and SIEN lake sites..... 70

Figure 3.2: SCP concentrations in Yosemite National Park, and Humboldt-Toiyabe and Inyo National Forests..... 71

Figure 3.3: SCP concentrations in Sequoia and Kings Canyon National Parks 72

Figure 3.4: ANC concentrations in Yosemite National Park, Humboldt-Toiyabe National Forest, and Inyo National Forest (diatom data set)..... 73

Figure 3.5: ANC concentrations in Sequoia and Kings Canyon National Parks (diatom data set). 74

Figure 3.6: Dual isotope plot for lake water nitrate samples collected at SIEN sites..... 75

Figure 3.7: DIN:TP nutrient ratios for Yosemite National Park. 76

Figure 3.8: DIN:TP nutrient ratios for Yosemite National Park. 77

Figure 3.9: $\delta^{18}O$ (NO_3^-) and $\delta^{15}N$ (NO_3^-) time series during the summer and fall of 2011 at Emerald Lake (EML) and Marble Fork of the Kaweah (MFK), ... 78

Figure 3.10: ANC vs. SCP concentration for study region. 78

Figure 4.1: Sierra Nevada study area. 111

Figure 4.2: Nutrient gradients for Moat and Hamilton limnocorral experiments in July and September. 112

Figure 4.3: Nitrate gradients for Moat, Topaz, Emerald-P, Emerald, and Aster cubitainer experiments. 113

Figure 4.4: Cation (Na^+ or K^+) gradients for the Moat and Hamilton limnocorral experiments. 114

Figure 4.5: Chlorophyll a concentrations for Moat and Hamilton limnocorral experiments. 115

Figure 4.6: Chlorophyll a concentrations for Moat, Topaz, Emerald-P, Emerald, and Aster cubitainer experiments. 116

Figure 4.7: Phosphate gradients for the sites where N was added (Moat-July and September, Hamilton-September) and the nitrate gradient at Hamilton-July where P was added. 117

Figure 4.8: TDP gradients for the cubitainer experiments. 118

Figure 4.9: Nutrient ratio, DIN:TP, gradients for the cubitainer experiments. 119

Figure 4.10: Monod (top) and dose response (bottom) curves for the Moat-July limnocorral experiment. 120

Figure 4.11: Monod (top) and dose response (bottom) curves for the Moat-September limnocorral experiment. 121

Figure 4.12: M-M (top) and dose response (bottom) curves for the Hamilton-July limnocorral experiment using phosphate uptake as an indicator of growth. 122

Figure 4.13: Monod (top) and dose response (bottom) curves for the Hamilton-July limnocorral experiment using particulate phosphorus as an indicator of growth. 123

Figure 4.14: Monod (top) and dose response (bottom) curves for the Moat cubitainer experiment..... 124

Figure 4.15: Monod (top) and dose response (bottom) curves for the Emerald-P cubitainer experiment..... 125

Chapter 1: Introduction

Mountain lakes are sensitive indicators of environmental change and often used for detecting changes from large-scale regional stressors such as air pollution and climate change (Seastedt et al. 2004). Increased rates of atmospheric deposition are altering biogeochemical cycles and ecological processes in remote mountain ecosystems (Fenn *et al.* 2003). The Sierra Nevada Mountains, California are exposed to air pollution that originates from agricultural, urban, and industrial sources in California's Central Valley, the San Francisco Bay Area, and as far away as Asia (Bytnerowicz *et al.* 2002; Vicars and Sickman 2011). Nutrients and acid anions are transported by air currents into the Sierra Nevada where they are deposited as wet and dry deposition.

Sensitivity of aquatic ecosystems to acidic deposition of sulfate and nitrate is well documented throughout the northern hemisphere (Driscoll et al. 2001; Henriksen et al. 1998; Melack et al. 1985). Adverse effects from acidification include chronic or episodic acid neutralizing capacity (ANC) depression and changes in the productivity and structure of biotic communities (Raddum et al. 2001; Sickman et al. 1999; Wigington Jr et al. 1992). Air pollution is also increasing nutrient inputs to mountain lakes. In contrast to the traditionally accepted paradigm that phosphorus (P) is the limiting nutrient in freshwater lake ecosystems (Schindler 1974), there is increasing evidence that many oligotrophic lakes in the northern hemisphere were once nitrogen (N) limited and shifted to P limitation as a result of increased anthropogenic N deposition (Bergström and Jansson 2006; Goldman 1988). Increased nutrient inputs are contributing to long-term

eutrophication, changes in nutrient cycles, and shifts in phytoplankton communities (Elser *et al.* 2009a; Goldman *et al.* 1993; Sickman *et al.* 2003b). Atmospheric deposition effects are often confounded by climate change effects. Climate change is altering hydrologic and temperature regimes in mountain lakes (Coats et al. 2006). The onset of spring warming and snowmelt is occurring earlier (Cayan et al. 2001; Hamlet et al. 2005). Algal community shifts are occurring in response to early lake ice-off from warming air temperatures (Douglas et al. 1994; Michelutti et al. 2003).

The Clean Air Act and Amendments (CAAA) is the primary policy in the United States aimed at improving air quality and reducing atmospheric deposition. Despite the protections afforded to many mountain lakes under the CAAA, a need for stricter standards based on measurable ecological effects has been identified as an important step towards the continued protection of high elevation lakes (National Research Council 2004). One approach is the critical load, which is defined as a quantitative estimate of an input or exposure to a pollutant at which unacceptable impacts occur to sensitive ecosystem components (Bull 1992). This approach, widely used in Europe for the last few decades (UNECE 1999), is gaining interest and application in the United States (Burns *et al.* 2008; Porter and Johnson 2007). There has been an increase in research to determine critical loads to protect sensitive Wilderness areas, including high-elevation lakes (Pardo *et al.* 2011; Saros *et al.* 2011). Critical load estimates identified from extensive research in Rocky Mountain National Park were incorporated into air quality policy in the State of Colorado (Porter and Johnson 2007). Critical loads may be based on ecological change from acidification or eutrophication (Baron *et al.* 2011). Critical

nitrogen loads for Sierra Nevada lakes have been estimated to range from 1.5 to 2.0 kg N ha^{-1} yr^{-1} for eutrophication, while there is limited information for acidification estimates (Baron *et al.* 2011; Saros *et al.* 2011). These initial estimates would benefit from continued research and efforts to revise them as more data become available (Baron *et al.* 2011).

In addition to the need to develop critical loads, basic nutrient criteria (in the form of lake nutrient concentrations) specific to high-elevation lake ecosystems are also lacking (Creager *et al.* 2006). Nutrient water quality criteria can be used to develop critical loads and is another tool that managers can use to assess status and trends of mountain lakes. Presently, the criteria available to compare Sierra Nevada waters against are state water quality standards described in Water Quality Control Plans. Current nutrient guidance is generally the same across the Sierra and falls under the objective for 'Biostimulatory Substances' (California Regional Water Quality Control Board - Central Valley Region 1995; 1998; California Regional Water Quality Control Board - Lahontan Region 1994). The concentrations of nitrogen and phosphorus that cause impairment or ecological change vary widely, which poses a challenge for developing numeric criteria for large regions. The Environmental Protection Agency (EPA) has recently been encouraging states to develop numeric criteria and the State of California is in the process of evaluating several approaches (Gibson *et al.* 2000; State Water Resources Control Board and California Environmental Protection Agency 2011). However, the approaches proposed by the State focus on more impaired downstream waters and are not based on

ecological change specific to Sierra Nevada lakes nor will they provide measures that are readily incorporated into existing lake survey and monitoring programs.

The overarching objective of my research was to gain greater understanding of how global change is affecting mountain lakes and how this information can be used to inform environmental policy to protect sensitive aquatic ecosystems. My focus was on linking atmospheric deposition with acidification and eutrophication effects, developing critical loads and nutrient criteria, and using this information to assess the status and trends of Sierra Nevada lakes. In Chapter 2, I started by investigating the extent that atmospheric deposition and climate explain 20th century trends in lake acidification and eutrophication. I used these results to assess the effectiveness of existing environmental policy (i.e. Clean Air Act and Amendments) and to develop future policy by developing a critical load for acidification. This aspect of my research focused on temporal trends in three Sierra Nevada lakes. In Chapter 3, I took a more spatial perspective and investigated factors contributing to spatial variation in acid and nutrient affected lakes to further inform critical load development. If critical loads are to be an effective and incorporated into air quality policy it is important to link atmospheric deposition to chemical lake effects and understand these relationships at a landscape scale, the scale at which policy is applied. My approach was to measure indicators of atmospheric deposition and basin characteristics to explain variation in lake ANC and nutrient limitation ratios across the Sierra Nevada landscape. In the final chapter, I developed quantitative nutrient criteria based on measurable ecological effects specific to high-elevation lakes and applied the nutrient criteria to survey data to assess regional

atmospheric deposition effects. The combined information of nutrient criteria, applied to lake chemistry data, and critical loads, applied to air quality data, will be a powerful tool for Sierra Nevada managers in protecting these ecosystems. This information can be used to inform local management decisions, develop state and federal environmental policy, and communicate the status of our natural resources to the public.

Chapter 2: 20th Century Atmospheric Deposition and Lake Acidification Trends in Western Mountain Lakes (USA): Importance of the Clean Air Act

2.1 Abstract

Sensitivity of aquatic ecosystems to acidic deposition of sulfate and nitrate is well documented throughout the northern hemisphere. Recent research suggests that remote mountain lakes in the Sierra Nevada, California may have been affected by acid deposition as early as 1920. We investigated multiple proxies to determine if observed changes in acid neutralizing capacity (ANC) at remote mountain lakes are a result of 20th century atmospheric deposition patterns or if the changes are better explained by climate variables. We further investigated potential eutrophication effects from atmospheric deposition and climate change by measuring proxies of algal productivity. The spheroidal carbonaceous particle (SCP) profile at Moat Lake indicated the first presence of SCPs was ca. 1870, the maximum SCP concentration was 2,400 gDM^{-1} occurring ca. 1990, and the present day SCP concentration is 590 gDM^{-1}. The SCP profile at Emerald Lake indicated the first presence of SCPs was ca. 1930, the maximum SCP concentration was 1,500 gDM^{-1} occurring ca.1960, and the present day SCP concentration is 1,200 gDM^{-1}. The SCP profile at Pear Lake indicated the first presence of SCPs was ca. 1840, the maximum SCP concentration was 1,800 gDM^{-1} occurring ca. 1970, and the present day SCP concentration is 560 gDM^{-1}. Biogenic silica (BSi) in Moat Lake ranged from 175.1 to 227.9 mg g^{-1} from 1834 to 2002 and $\delta^{13}C$ ranged from -22.25 to -19.22 ‰. Positive

temporal trends are observed throughout the 20th century for BSi and $\delta^{13}C$. Moat Lake ANC was negatively correlated with SCPs sulfur dioxide emissions. ANC was not correlated with air temperature, precipitation, snow water equivalent, $\delta^{13}C$, biogenic silica (BSi), or nitrogen oxides (NO_x) emissions. The productivity proxies, $\delta^{13}C$ and BSi, were positively correlated with air temperature and to a lesser extent precipitation and NO_x emissions. SCP profiles in Pear and Emerald Lakes further support patterns observed in Moat Lake. Emerald Lake chemistry data indicates an increasing trend in lake ANC concentrations over the last three decades, supporting the late 20th century positive trend observed in the Moat Lake sediment record. We used the 20th century sediment records and hindcasted deposition estimates to calculate a critical load for acid anions of 73.9 eq ha^{-1} yr^{-1}. Separate critical load estimates for nitrate and sulfate, based on present day nitrate and sulfate deposition ratios, were 0.68 kg-N ha^{-1} yr^{-1} and 1.2 kg-SO_4 ha^{-1} yr^{-1}. Our results indicated that Moat Lake early 20th century ANC decline is attributed to atmospheric deposition and the subsequent recovery in the late 20th century is attributed to the success of the Clean Air Act and Amendments. Although atmospheric deposition is the dominant driver of ANC in the 20th century, aquatic communities are responding to combined effects from acidification, climate change, and eutrophication.

2.2 Introduction

Mountain lakes are sensitive indicators of environmental change and are especially useful for detecting changes from large-scale regional stressors such as air pollution and climate change (Seastedt et al. 2004). Sensitivity of aquatic ecosystems to acidic deposition of sulfate and nitrate is well documented throughout the northern

hemisphere (Driscoll et al. 2001; Henriksen et al. 1998; Melack et al. 1985). Adverse effects from acidification include chronic or episodic acid neutralizing capacity (ANC) depression and changes in the productivity and structure of biotic communities (Raddum et al. 2001; Sickman et al. 1999; Wigington Jr et al. 1992). Air pollution is also increasing nutrient inputs to mountain lakes. There is increasing evidence that many oligotrophic lakes in the northern hemisphere were once nitrogen (N) limited and shifted to phosphorus limitation as a result of increased anthropogenic N deposition (Bergström and Jansson 2006; Goldman 1988). Increased nutrient inputs are contributing to long-term eutrophication, changes in nutrient cycles, and shifts in phytoplankton communities (Elser *et al.* 2009a; Goldman *et al.* 1993; Sickman *et al.* 2003b). Climate change is altering hydrologic and temperature regimes in mountain lakes (Coats et al. 2006). The onset of spring warming and snowmelt is occurring earlier (Cayan et al. 2001; Hamlet et al. 2005). Algal community shifts are occurring in response to early lake ice-off from warming air temperatures (Douglas et al. 1994; Michelutti et al. 2003).

The Clean Air Act (CAA) of 1970 is the primary policy in the United States aimed at improving air quality and reducing atmospheric deposition. 1977 Amendments to the Clean Air Act (42 USC 7470) provide additional protection to mountain lakes as the legislation includes requirements to prevent deterioration of air quality in National Parks, Monuments, Seashores, and Wilderness Areas. A large proportion of western mountain lakes are located in these protected areas and are thus afforded the highest protection under the CAA. Title IV-A in the 1990 Clean Air Act Amendment (CAAA)

provides additional protection as it targets improvements in acid deposition with the recovery of surface waters from acidification as one of the objectives.

Chemical recovery of lakes from acid deposition has been attributed to the CAAA, although, most of the published research and success stories have been in the northeastern United States where the effects have been most notable and acid deposition has received the most attention (Burns et al. 2011; Kahl et al. 2004). However, recent research suggests that Sierra Nevada lakes may have been affected by acid deposition as early as 1920. Sickman et al. (In press) reconstructed the last 1600 years of ANC using a lake sediment core from Moat Lake, a remote sub-alpine lake located in the eastern Sierra Nevada. Lake ANC was reconstructed using a diatom inference model developed from 41 calibration lakes. They observed a decrease in ANC from 1920 to 1970 that was a notable deviation from the historic sediment record. ANC concentrations increased after 1970 and returned to pre-1920 levels by 2005. The cause of the 20th century ANC pattern was uncertain as the biogeochemical processes in Sierra Nevada lakes have been affected by multiple stressors that can confound the palaeolimnological record, namely increased acid and nutrient deposition and climate change. Further investigation of additional proxies is needed to determine if the changes in ANC are a result of atmospheric deposition patterns or if other variables explain these trends. Multi-proxy approaches are recommended when investigating 20th century palaeolimnological records due to these complexities (Smol 2010).

Spheroidal carbonaceous particle (SCP) lake sediment profiles are used to investigate historic atmospheric deposition (Pla et al. 2009; Rose et al. 1999). SCPs are

porous spheroids composed primarily of elemental carbon that are chemically very resistant and well-preserved in lake sediments. They are unambiguous geochemical indicators of anthropogenic atmospheric deposition because they are only produced by industrial combustion of fossil fuels. There are no natural sources. Biogenic silica (BSi) and $\delta^{13}C$ are good proxies for algal productivity and are used to assess effects of nutrient inputs and climate change on lake ecosystems (Brenner et al. 1999; Colman et al. 1995). BSi is primarily a measure of the abundance of diatoms preserved in lake sediments and reflects lake primary productivity. An increase in the ratio of $^{13}C/^{12}C$, expressed as $\delta^{13}C$, indicates increased lake productivity. Phytoplankton energetically favor the lighter carbon isotope, ^{12}C. This results in the removal of ^{12}C from the water column as algae preferentially take-up ^{12}C and subsequently settle in lake bottom sediments. If productivity increases, the available inorganic carbon and ^{12}C become depleted in the water column. Fractionation is less pronounced and the ratio of $^{13}C/^{12}C$ increases. This increase is reflected in the $\delta^{13}C$ sediment record.

A multi-proxy paleolimnology study provides the opportunity to determine when and why biological and chemical changes first occurred in Sierra Nevada lakes. This information can be used to inform environmental policy through the development of critical loads. A critical load is a quantitative estimate of an input or exposure to a pollutant at which unacceptable impacts occur to sensitive ecosystem components (Bull 1992). The critical load approach is an effective policy tool as it quantitatively links atmospheric deposition to ecological effects. Initial development of critical loads and adoption of the approach began in the late 1980's, primarily in Europe and Canada

(Nilsson and Grennfelt 1988) and today is well-integrated into European air quality policy and transboundary agreements (UNECE 1999). More recently the approach is gaining interest and application in the United States, including with western land management agencies (Burns et al. 2008; Porter and Johnson 2007).

We investigated additional proxies to determine if the observed changes in ANC at Moat Lake are a result of 20th century atmospheric deposition patterns or if other variables may explain these trends. The aims of our research were to better understand historic atmospheric deposition in the Sierra Nevada and inform environmental policy by evaluating the effectiveness of the Clean Air Act in protecting Sierra Nevada lakes and contributing to the development of critical loads. Our research objectives were to 1) determine SCP sediment profiles for three Sierra Nevada lakes, 2) determine if changes in reconstructed ANC are attributed to atmospheric deposition by examining multiple lines of evidence (SCPs, climate variables, and emissions), 3) compare palaeolimnological data to measured lake chemistry trends, 4) calculate an acidification critical load for Sierra Nevada lakes, and 5) investigate additional changes that may be occurring in Sierra Nevada lakes using biogenic silica (BSi) and $\delta^{13}C$ as proxies for algal productivity.

2.3 Methods

2.3.1 Site Description

The study sites are three nitrogen-limited, sub-alpine lakes located in the Sierra Nevada, California, United States of America (Figure 2.1). Moat Lake (elevation 3224 m)

is located on the eastern slope of the Sierra Nevada 12.5 km west-northwest of Mono Lake on Toiyabe National Forest. The lake has a maximum depth of 7 m, lake surface area of 2.8 ha, and watershed area of 59.1 ha. A majority of the watershed is comprised of the western flank of Dunderberg Peak (elevation 3772 m), a rock and scree-covered slope with a mean angle of 35°. The bedrock geology of the watershed is dominated by metasedimentary rocks including quartzite and argillite. Less than 10% of the watershed is vegetated. Pear (elevation 2904) and Emerald (elevation 2800 m) Lakes are located adjacent to each other on the western slope of the Sierra Nevada in Sequoia National Park. Pear Lake has a maximum depth of 27 m, lake surface area of 7.3 ha, and watershed area of 136 ha. The bedrock geology of the watershed is dominated by granite and granodiorte. Less than 10% of the watershed is vegetated. Emerald Lake has a maximum depth of 10 m, lake surface area of 2.7 ha, and watershed area of 120 ha. The bedrock geology of the watershed is dominated by granite and granodiorite. Less than 10% of the watershed is vegetated.

2.3.2 Sediment Core Sampling Methods

At Moat Lake, We used a rod-corer to collect a single 210 cm core, which was sectioned every cm. All core sectioning was done in the field immediately after collection and samples were placed in Whirl-Pak bags. SCPs were analyzed to ca. 1650 (22 cm) well before the post-industrial time period. Pear and Emerald Lake cores were collected as part of the Western Airborne Contaminants Assessment Project (WACAP) using a gravity corer fitted with a Plexiglass tube. Cores were sectioned into 0.5 cm sections in the field and stored in 250-ml glass jars immediately following collection. Detailed field

methods for Pear and Emerald Lake cores are described in Landers et al. (2008). All samples were kept cool during transport and held at 5°C until analyzed.

2.3.3 Sediment Core Laboratory Analysis

The chronology of the Moat Lake sediment core was established with ^{210}Pb and ^{14}C dating as described in Sickman et al. (In press). The chronology of the Pear and Emerald Lake sediment cores was established using the ^{210}Pb method as described in Landers et al. (2008).

SCPs were measured through the full cores for Pear (31 cm) and Emerald (27 cm) Lakes and in the top 22 cm of the Moat Lake core. SCPs were extracted from sediment sub-samples using a sequential chemical attack to remove unwanted sediment fractions (Rose 1994). Sediment samples were dried, weighed and placed in 10 ml polypropylene tubes, and tubes were placed in an 80-90 ^{o}C water bath. Nitric acid, hydrofluoric acid, and hydrochloric acid were added sequentially to remove organic, siliceous, and carbonate materials, respectively. A known fraction of the remaining suspension was evaporated and mounted on a standard microscope slide. SCPs were then counted at 400x magnification under a light microscope using criteria described in Rose (2008) and converted to a concentration of SCPs per gram of dry mass sediment (gDM^{-1}). Reference sediments and blanks were included for quality control and quality assurance (Rose 2008).

Diatom biogenic silica and $\delta^{13}C$ were analyzed in the top 20 cm of the Moat Lake core. Dried sediment samples were analyzed for BSi using time-course (2, 3, and 4 hour) leaching with 1% sodium carbonate (Na_2CO_3) at 85 ^{o}C. Digested samples were

neutralized with hydrochloric acid and analyzed for dissolved silica using standard colorimetric techniques. The dissolved silica concentrations were charted over time using a least squares regression analysis and the diatom BSi calculated by extrapolating back to the y-intercept (Conley and Schelske 1993). $\delta^{13}C$ was analyzed using a Delta V isotope ratio mass spectrometer interfaced with an elemental analyzer. Filters were acid fumigated to remove trace amounts of inorganic carbon prior to analysis and a National Institute for Standards and Technology (NIST) standard (USGS 40) was included in the run. Isotope values are reported in per mil units (‰) relative to Pee Dee Belemnite.

2.3.4 Sediment Core Data Analysis

Sickman et al. (In press) describes the methods and results for reconstructing ANC for Moat Lake using a diatom transfer model. In this paper we compare Sickman et al.'s (In press) Moat Lake ANC reconstruction to SCP profiles and 20th century sulfur dioxide (SO_2) and nitrogen oxides (NO_x) emissions to investigate if ANC changes are correlated with atmospheric deposition and to mean air temperature, precipitation, and snow water equivalent (SWE) to investigate if changes in ANC are correlated with climate. We investigated the relationships between variables using core depth and time series graphs and principal component analysis (PCA).

Moat Lake SCPs and diatoms were analyzed from the same core and compared. In order to understand how temporal deposition patterns (i.e. SCP profiles) in Moat Lake compare to other lakes in the Sierra Nevada, we also compared the Moat Lake core results to SCP profiles in Pear and Emerald Lakes. Pear and Emerald Lakes provide a good comparison to Moat Lake because both sites are the focus of extensive watershed

and atmospheric deposition research for the past three decades. Since SCP concentrations were used we calculated sedimentation accumulation rates to assess the effect of sedimentation on SCP concentrations.

We compared Moat Lake ANC data to SO_2 and NO_x emissions trends for the 1850-2005 and 1900-2012 time periods, respectively. North American SO_2 emission trends were estimated by Smith et al. (2011) using a bottom-up mass balance method. National NO_x emissions were estimated by the U.S. Environmental Protection Agency using a combination of "top-down" methodologies and direct monitoring of emissions as described in EPA (2000).

Mean annual air temperature and precipitation were calculated from long-term climate data sets maintained by the California Department of Water Resources. We compared Moat Lake ANC to statewide trends since early 20th century data specific to the high-elevations in the Sierra Nevada are lacking. Data are presented as the three-year moving average. Mean California air temperature was calculated from 47 long-term stations with continuous annual records from 1900-2003. California annual mean precipitation was calculated from 191 stations (Goodridge 1997). All stations had a period of record from 1910 to 2011 that met a 90% completeness criteria. We used April 1st SWE data from the California Cooperative Snow Surveys' Donner Summit site (elevation 2103 m), located in the Northern Sierra Nevada in the Yuba River Basin and the Virgina Lakes site (2865 m) located within two miles of Moat Lake (http://cdec.water.ca.gov). The Donner Summit site was selected due to its long-term,

continuous record dating back to 1910 and the Virginia Lakes site due to its proximity to Moat Lake. The period of record at the Virginia Lakes site is 1947-2005.

2.3.5 Emerald Lake ANC Trends

Sickman et al. (In press) established a strong linear correlation between April 1st SWE and summer ANC concentrations at Emerald Lake (Sickman et al. In press). This strong correlation coupled with the high annual variability of SWE makes it challenging to detect trends in ANC from atmospheric deposition (or other drivers). We removed the effect of SWE by computing the residuals for the SWE-ANC linear regression, plotting the residuals in chronological order, and computing the linear regression for the residuals over time. We also used multiple linear regression (MLR) to predict ANC using time and SWE.

2.3.6 Critical Load Calculation

We calculated a critical load for acid deposition by hindcasting deposition back to 1900 and calculating a critical load for the time period (1920-1930) where change in ANC was initially observed by Sickman et al. (In press). We make the case in this paper that observed changes were attributed to atmospheric deposition thus justifying using deposition for the 1920-1930 time period as the critical load. Acid deposition was assumed to be the sum of nitrate and sulfate deposition. We estimated deposition rates for each constituent separately and summed them to get a final critical load presented as the sum of acid anions:

$$\text{CL as Sum of Acid Anions (eq ha}^{-1}\text{ yr}^{-1}) = \text{N Dep (eq ha}^{-1}\text{ yr}^{-1}) + \text{S Dep (eq ha}^{-1}\text{ yr}^{-1})$$

where CL is the critical load, N Dep is the mean nitrate deposition in the 1920 to 1930 time period and S Dep is the mean sulfate deposition in the 1920 to 1930 time period.

Nitrate deposition was hindcast back to 1900 using methods described in Baron (2006). Total nitrate deposition data collected from 1985-1999 at Emerald Lake were plotted over time. 1900 nitrate deposition was estimated as 0.15 kg ha^{-1} yr^{-1} (10.7 eq ha^{-1} yr^{-1}) (Holland et al. 1999) and used to anchor the plot. Deposition was modeled using an exponential function and nitrate deposition for the time period of change was computed using the trendline equation. The exponential function was determined to be the best fit by Baron (2006) as it is consistent with NO_x emissions data and population growth. Sulfate deposition was hindcast using a different approach because 20th century sulfate emissions data suggest that sulfate history is more complex and does not follow an exponential growth curve (EPA 2000). As a result, we calculated the relationship between mean sulfate deposition at Emerald Lake from 1985 – 1999 to mean sulfate emissions during the same time period. Then we used this relationship to compute sulfate deposition based on annual SO_2 emissions from the EPA (EPA 2000). 90% confidence intervals for estimated nitrate and sulfate are proportional to the confidence intervals computed for the measured deposition.

Total nitrate and sulfate deposition estimates were computed using wet and dry deposition data collected at or near Emerald Lake from 1985 – 1999. Methods are

described in detail in Sickman et al. (2001), so we only briefly describe them here. Precipitation was divided into two seasons and measured with methods appropriate for the season and dominant precipitation type. Winter precipitation was defined as approximately December through early April and non-winter precipitation was defined as approximately early-April through November. Winter precipitation depth was measured through intensive snow surveys (200-300 measurements annually) conducted throughout the Emerald watershed during the time of maximum snowpack (approximately April 1st). Snow samples for chemical analysis, representing both wet and dry deposition, were collected from snow pits during the early April snow surveys. Non-winter precipitation depth was measured using an Alter-shield equipped tipping bucket rain gage and samples for wet deposition chemical analysis were collected weekly in Aerochemetric samplers. Precipitation chemistry samples were analyzed for nitrate and sulfate on a DIONEX ion chromatograph. Non-winter dry deposition was computed using the dry-deposition inferential method (DDIM), which uses air-borne chemical concentrations and deposition velocities of SO_2 and HNO_3 to compute deposition rates (Hicks et al. 1991; Meyers et al. 1998). Air-borne chemical concentrations were collected by the National Oceanic and Atmospheric Administration (NOAA) - Atmospheric Integrated Research Monitoring Net- work (AIRMoN) at the Wolverton Meadow site located 6 km west of the Emerald watershed and at 2250 m elevation.

Once a critical load in terms of the sum of acid anions was computed we converted this critical load to nitrate and sulfate deposition using the ratio of nitrate to

sulfate in late 20th century deposition. A mean nitrate to sulfate ratio was computed using the 1985 – 1999 Emerald Lake deposition data.

2.4 Results

2.4.1 Spheroidal Carbonaceous Particles

Sedimentation accumulation rates in Moat Lake ranged from 0.016 to 0.083 g cm^{-2} yr^{-1} with a mean of 0.030 g cm^{-2} yr^{-1} (Figure 2). Sedimentation accumulation rates in Pear Lake ranged from 0.006 to 0.014 g cm^{-2} yr^{-1} with a mean of 0.008 g cm^{-2} yr^{-1}. Sedimentation accumulation rates in Emerald Lake ranged from 0.035 to 0.079 g cm^{-2} yr^{-1} with a mean of 0.047 g cm^{-2} yr^{-1}.

SCPs were first detected in 1869 ±96 in Moat Lake (excluding a measured SCP ca. 1725 discussed later in the chapter), 1842 ±33 in Pear Lake, and 1932 ±10 in Emerald Lake (Figure 2.3). Following initial detection, SCPs show an increasing trend at all three sites until the maximum SCP concentrations were reached in 1964 ±6 at Emerald Lake (1,500 gDM^{-1}, 90% CI [910, 2100]), 1972 ±9 at Pear Lake (1,800 gDM^{-1}, 90% CI[1200, 2400]), and 1988 ±4 at Moat Lake (2,400 gDM^{-1}, 90% CI [1700, 3100]). A decreasing trend in SCP concentrations is then observed through present day, with the exception of Emerald Lake where SCPs decrease, but then increase again after 2000. SCP concentrations measured in present day surface sediments are 560 gDM^{-1}, 90% CI [240, 870] in Pear Lake, 590 gDM^{-1},90% CI [260, 900] in Moat Lake, and 1,200 gDM^{-1}, 90% CI [480,1200] in Emerald Lake.

2.4.2 ANC Comparison

SCPs are observed in Moat Lake prior to any notable change in ANC (Figure 2.3). A decreasing trend in ANC began after 1920 and continued until the mid 1980s. The ANC decrease in1920-1985 coincided with increasing concentrations of SCPs in Moat Lake. ANC in Moat Lake switched to an increasing trend within the same decade that SCPs switched to a decreasing trend. Pear and Emerald Lake SCPs showed similar declines that also began around the 1970s.

California mean air temperature (moving 3-year average) range was 14.8 – 16.9 ^{o}C from 1900-2003 (Figure 2.4). Mean air temperature increased throughout the 20th century. Temperature did not correlate strongly with Moat Lake ANC throughout the 20th and early 21st centuries. The early 20th century decrease in ANC coincided with a slight warming trend observed at the same time period. However, temperature continued to rise through present day whereas Moat Lake ANC returned to early 20th century concentrations after 1980. California mean precipitation (moving 3-year average) range was 40 – 83 cm (Figure 2.4). The SWE (moving 3-year average) range at Donner Summit was 52.1 - 147.0 cm and at Virginia Lakes it was 11.4 – 101.9 cm (Figure 2.4). Moat Lake ANC patterns did not correlate with SWE and precipitation as no significant trends were observed with these two climate variables.

Moat Lake ANC patterns did correlate with SO_2 emissions data following 1920 (Figure 2.4). From 1920 – 1970 Moat Lake ANC decreased as SO_2 emissions increased. Moat Lake ANC increased after 1980, which coincided with decreasing SO_2 emissions observed from 1970 – 2005. Moat Lake ANC patterns also correlated with NO_x

emissions following 1920 through 1980 (Figure 2.4). Following 1980, the Moat Lake ANC increase is observed about two decades prior to a decrease in NO_x emissions, which occurred from 2000 through present.

2.4.3 Biogenic Silica and Stable Carbon Isotopes

Moat Lake BSi ranged from 175.1 to 227.9 mg g^{-1} from ca.1830 to ca. 2000 (Figure 2.5). We observed an initial increase in BSi between 1920 and 1930 and a second increase between 1980 and 2000. $\delta^{13}C$ ranged from -22.25 to -21.39 ‰ from ca. 1830 to ca. 1900 with no notable trend (Figure 2.5). We observed an increasing trend in $\delta^{13}C$ (i.e. more enriched ^{13}C) after 1900 through 2000 where $\delta^{13}C$ ranged from -21.89 to -19.22 ‰. In the analysis and discussion we focused on trends from ca. 1830 to ca. 1990 as diagenesis complicates interpretation for the most recent 5 to 10 years (Galman et al. 2009). By 1990, $\delta^{13}C$ had increased from the most depleted value of -22.25 ‰ in 1903 to -20.20 ‰.

2.4.4 PCA Bi-plot

The first principal component explained 34% of the variation and was correlated with SCPs and SO_2 emissions (using the data from the EPA and Smith et al. (2011)) (Figure 2.6). ANC was negatively correlated with SCPs and SO_2 emissions. The second principal component explained 30% of the variation and was correlated with precipitation, temperature, $\delta^{13}C$, biogenic silica, and to a lesser extent NO_x. SWE was not strongly correlated with either axis or other variables

2.4.5 Emerald Lake ANC Trends

The linear regression for SWE-ANC residuals plotted over time showed a

significant increasing trend (slope p=0.007) (Figure 2.7). ANC increased approximately 4 μeq L^{-1} between 1983 and 2011. MLR results confirmed that year (p=0.005) and SWE ($p<0.001$) are both significant predictors of ANC (R^2=0.89). The relationship between ANC and year was positive. The model equation is:

$$ANC = -245 + (0.142)(year) - (0.00814)(SWE)$$

2.4.6 Critical Load

Emerald watershed deposition chemistry was summarized for the 1985 – 1999 period (Table 2.1). Mean nitrate and sulfate deposition were 98.6 ± 17.2 eq ha^{-1} yr^{-1} and 51.5 ± 15.3 eq ha^{-1} yr^{-1}, respectively. The sum of acid anions (nitrate plus sulfate) was 150.2 ± 29.5 eq ha^{-1} yr^{-1}. Deposition was hindcast for nitrate and sulfate. Sulfate results, hindcast using the relationship between measured deposition and emissions, were a curve similar to emissions data with a deposition ranging from 13.1 to 75.5 eq ha^{-1} yr^{-1} (Figure 2.8). The resulting trendline equation from the nitrate hindcast used to compute deposition prior to 1985 was $y = 8 \times 10^{-19} e^{0.0232x}$ (Figure 2.8).

The critical load was computed using the estimates of nitrate and sulfate deposition for the time period of initial ANC decrease that coincided with increased SCPs and emissions. We identified this time period as 1920-1930. Mean nitrate deposition during this time period was 20.0 eq ha^{-1} yr^{-1}, 90% CI [18.4, 21.4] and mean sulfate deposition was 54.0 eq ha^{-1} yr^{-1}, 90% CI [47.2, 60.8] (Figure 2.8). Therefore, the critical load, presented as the sum of acid anions, was 73.9 eq ha^{-1} yr^{-1}, 90% CI [65.6, 82.22]. The 1985-1999 deposition data indicated that during the late 20th century nitrate contributed to 66.2 ± 5.3% of the total acid anions and the sulfate contribution was 33.8 ±

5.3% (Table 2.1). This was in contrast to 1900, where our estimates suggested that nitrate contributed 31% and sulfate 69%. Using the late 20th century percentages we also presented the critical load in terms of nitrate-nitrogen deposition and sulfate deposition. The nitrate-nitrogen critical load ranged from 0.61 to 0.76 kg ha^{-1} yr^{-1} with a mean of 0.68 kg ha^{-1} yr^{-1}. The sulfate critical load ranged from 1.1 to 1.3 kg ha^{-1} yr^{-1} with a mean of 1.2 kg ha^{-1} yr^{-1} (Table 2.2). Pre-industrial nitrate deposition was 0.15 kg ha^{-1} yr^{-1} (Holland et al. 1999).

2.5 Discussion

SCP concentration rates are sensitive to sedimentation rates, therefore, we examined sedimentation rates within cores. Moat Lake sedimentation rates were relatively consistent with the exception of an increase ca. 1925 resulting in relatively lower SCP concentrations during this time period. Pear Lake sedimentation rates were very consistent throughout the 20th century and likely had minimal effect on SCP concentrations. Emerald Lake sedimentation rates were also very consistent from ca. 1910 – 2001. Sedimentation rates were relatively higher ca. 1900, although this did not affect concentration measures because SCPs were below detection in all samples prior to 1930.

SCP profiles in Moat and Pear Lakes had very similar patterns. SCPs gradually increased in the mid to late 1800s and then increased at a faster rate in the early 1900s. In contrast, SCPs were not even detected until the early 1930s in Emerald Lake, although once detected they increased rapidly through the mid 1960s. The differences observed in

Emerald Lake were unexpected given that Emerald and Pear Lakes are in adjacent watersheds that have similar exposure and deposition rates (Sickman 1989). It is likely explained by the higher sedimentation rate in Emerald Lake. The mean sedimentation rate in Emerald Lake was 0.047 g cm^{-2} yr^{-1}, compared to 0.008 and 0.030 g cm^{-2} yr^{-1} in Pear and Moat Lakes, respectively (Figure 2). SCP detection limits are sensitive to sedimentation rates, especially in remote lakes that have relatively low SCP inputs. Increased sediment fluxes decrease the already low concentration of SCPs making it less likely an SCP will be present and detected in a sample.

SCPs in Pear and Moat Lakes began to decline ca. 1970 and ca. 1985, respectively, which suggest a decline in atmospheric inputs from industrial fossil fuel burning. Emerald Lake, again, showed a different pattern, after a marked decrease in SCPs, concentrations began to increase again after 2000. We were not clear on what caused the increase but offer two possible explanations. The first is higher variability in Emerald Lake due to mixing of sediments from avalanches. Avalanches in the Emerald Lake watershed can displace lake water and disturb sediments due to the lake's shallow depth and small lake area (Engle and Melack 1997). Second, it could reflect a change in deposition that has not yet been detected in Pear and Moat Lakes. The higher sedimentation rates in Emerald Lake provided higher resolution and thus Emerald Lake may have a more sensitive sediment profile, when SCPs are above detection. Rose et al. (1995) found that profiles can be remarkably consistent across regions as is observed in the Moat and Pear sediments. However, they also observed high variation between lakes

that were in close proximity and attributed the variation to differences in watershed and lake characteristics (e.g. vegetation cover, lake size, elevation. aspect).

The patterns observed in Moat and Pear Lakes which can be described as increased SCPs through the early and mid 20th century followed by a recovery in the later 20th century have been observed at other sites, including lakes in the United Kingdom (UK), Europe, Russia, and Chile (Chirinos et al. 2006; Rose 1995). The start of the SCP record in the Sierra was quite consistent with UK records, where SCPs were also typically first observed in the mid 19th century (Rose et al. 1995). In Moat Lake small concentrations were observed as early as the 1700s, decades prior to industrial fossil fuel combustion was occurring in the region. We concluded the SCPs were present in this layer due to mixing in the sediments and that SCPs likely did not show up until ca. 1870 (Figure 2.3). Rose et al. (1995) identified the period of rapid increase in SCPs to typically be between the 1950s or 1960s in the UK, although variation was observed. We observed the rapid increase in Moat and Pear Lakes after 1920. This increase was, however, relative to the Sierra profiles. The dramatic increases observed in the 1950 – 1960s in other regions typically resulted in SCP concentrations that are an order of magnitude larger than those observed in the Sierra. The remoteness of our sites along with lower regional inputs resulted in a less dramatic increase observed over a longer time period.

Sierra Nevada SCPs reached maximum concentrations in the 1960-1980 time period, which was consistent with sites in other regions including the UK, Europe, Northwestern United States, and Rocky Mountains (Landers *et al.* 2008; Rose *et al.* 1995; Rose *et al.* 1999) (Table 2.3). Maximum concentrations were similar to other sites in the

western United States, which ranged from 1,100 gDM^{-1} (Glacier National Park) to 3,700 gDM^{-1} (Mt. Rainer National Park) (unpublished concentration data; flux data published in Landers et al. 2008). Moat and Pear Lakes maximum concentrations were greater than very remote sites, such as Svalbard or the Canadian Athabasca Oil Sands (Curtis *et al.* 2010), suggesting a regional source of SCPs. However, Sierra SCP concentrations were much less relative to locations in Europe, UK, and Chile.

Present day SCP concentrations in Moat and Pear Lakes have recovered and are now within the range of Northern Hemisphere background concentrations, which range between 500-1000 gDM^{-1} (Rose 1995). Emerald Lake was also within the background concentration range in the 1980s and 1990s, however, after 2000 Emerald Lake has again exceeded 1000 gDM^{-1}. The effect of sedimentation rates should also be considered, as increased rates near the surface would also explain lower SCP concentrations. Surface sediments at these three sites were in the low to mid range for the Sierra Nevada. SCP analysis of surface sediments from 42 Sierra lakes ranged from below detection to 5,900 gDM^{-1} (A. M. Heard, unpubl.).

We compared reconstructed ANC to SCPs, climate, and emissions and concluded that changes in 20th century ANC were primarily attributed to atmospheric deposition, specifically increases in acid anions. We considered the influence of climate as diatom communities and ANC can be sensitive to climate variables, including temperature and precipitation (Curtis et al. 2009; Sickman et al. In press; Sorvari et al. 2002). Our results showed limited 20th century coherence with climate variables. The increasing temperature trends we observed using data from multiple California stations were consistent with

increasing temperature trends, especially post-1940, observed by Bonfils et al. (2008) for mountainous regions of the western United States and Edwards and Redmond (2011) for the Sierra Nevada. Porinchu et al. (2007) reconstructed historic Moat Lake water temperature using chironomid indicators and observed trends consistent with air temperature. They observed slight warming (less than 0.2 ^{o}C) in Moat Lake between the late 1800s and 1920 followed by a period of minimal temperature change from 1920-1970. Then, surface water temperature in Moat Lake increased from 1970 to 2000 (~ 0.8 ^{o}C). It is possible that increasing air and water temperature changes could have contributed to either the decrease in ANC prior to 1970 or the increase post 1970. Warmer temperatures have been shown to increase ANC due to increased weathering rates and productivity and thus could be contributing to ANC recovery (Rouillard et al. 2012). However, the linear temperature trend did not explain the complete decreasing-increasing ANC pattern and the PCA indicated correlation with different principal components (Figure 2.6).

State-wide precipitation and Donner Summit SWE data varied throughout the time period, but showed minimal linear trends. Precipitation slightly increased and SWE slightly decreased, although correlation coefficients were weak ($R^2 < 0.04$). The PCA indicated limited to no correlation with ANC. The SWE and ANC angle was less than 45°, but the SWE vector was not very strong. Studies have shown that April 1st SWE has been decreasing over much of the western United States due to increased warming. However, increasing SWE has been observed in the higher elevations of the Sierra Nevada due to moderate increasing trends in precipitation and lower sensitivity to

temperature changes (Hamlet et al. 2005; Kapnick and Hall 2012). The Virginia Lakes snow course indicated there was no trend in SWE from 1947 – 2005 suggesting minimal effects on Moat Lake ANC trends in the later 20th century. Sickman et al. (In press) has shown an inverse relationship between ANC and SWE. Therefore, at high-elevation lakes where SWE was increasing in the later 20th century, less recovery in ANC may be observed. However, the lack of SWE trends observed back to 1900 at Donner Summit and in the later 20th century at Virginia Lakes did not explain the decreasing-increasing ANC pattern we observed at Moat Lake.

The strong coherence between ANC and SCPs and ANC and SO_2 emissions and late 20th century NO_x emissions, coupled with the lack of coherence between ANC and climate, support our conclusion that changes in 20th century ANC were primarily attributed to atmospheric deposition (Figure 2.1, Figure 2.4, and Figure 2.6). We attributed the early 20th century decrease in ANC to acid deposition, which was dominated by sulfate at that time (Table 2.1) and was strongly negatively correlated with ANC (Figure 2.6). SCPs were moderately correlated with sulfate and nitrate deposition (Pla *et al.* 2009; Rose and Juggins 1994). The initial increase in SCPs in Moat and Pear Lakes coincided with increased settlement and energy use during the California gold rush (Williams 1997). We observed the initial decrease in ANC in the early 20th century when SCP concentrations began to accelerate. These trends were consistent with SO_2 emission increases. Sulfate deposition accounted for 69% of acid deposition in 1900, however, the percentage has decreased over time as nitrate deposition has increased (Table 2.1). The nitrate deposition increase was largely attributed to rapid population growth in the

western United States after 1950, the Haber-Bosch process substantially increasing reactive nitrogen in the environment (~ 85 T N yr^{-1} globally), and shifts in fossil fuel types (Galloway and Cowling 2002; Williams 1997).

We attributed the increase in Moat Lake ANC and decrease in SCPs to the success of the CAA. In conjunction with the 1970 CAA, SO_2 emissions began to decline and NO_x emissions plateau (Figure 2.4). NO_x emissions did not begin to decline until 2000 in response to additional regulations included in the 1990 Clean Air Act Amendment which specifically addresses acid deposition (Burns et al. 2011). The CAA has been highly effective in reducing SO_2 emissions and sulfate deposition across the United States (Burns et al. 2011). It has also been effective in reducing NO_x emissions. However, effects on nitrogen deposition are more varied and harder to quantify due to a lack of monitoring data for all nitrogen species and smaller changes in emissions and deposition that are harder to detect (Burns et al. 2011). Studies have shown that the CAA has resulted in improvements in surface water ANC, although most of the focus has been on the northeastern United States (Burns et al. 2011; Kahl et al. 2004; Stoddard et al. 1999).

We observed increasing ANC in measured Emerald Lake chemistry data over the last three decades consistent with the late 20th century increasing trend observed in the Moat Lake sediment record. The increase in Emerald Lake ANC was concurrent with a decrease in lake sulfate concentrations (Clow et al. 2003), suggesting that the Emerald Lake ANC was also responding to the CAA. The observed increase in recent ANC was inconsistent with previous palaeolimnological work by Holmes et al. (1989) and Whiting

et al. (1989) that found Emerald Lake was not affected by acidification, although their methods were not as sensitive as the approach used by Sickman et al. (In press) at Moat Lake. A sediment core will be collected from Emerald Lake in the summer of 2013 and ANC reconstructed with the same methods used at Moat Lake. This will allow for a better comparison of 20th century ANC between the sites.

The critical load that we estimated (Table 2.2) was notably lower compared to other critical load estimates for acid deposition in western mountain regions. Critical loads for the Colorado Front Range lakes were estimated to be between 4.0 to 8.0 kg-N ha^{-1} yr^{-1} for nitrogen deposition (Pardo et al. 2011; Sullivan et al. 2005; Williams and Tonnessen 2000) and 8.4 to 33.3 kg-sulfate ha^{-1} yr^{-1} for sulfate deposition (Sullivan et al. 2005). There was limited information on acidification critical loads for the Sierra Nevada (Baron et al. 2011; Pardo et al. 2011). We did need to consider differences in methodologies when comparing critical load estimates. We computed the critical load as the sum of the acid anions and then converted it to nitrate-nitrogen and sulfate deposition. Our critical load estimate may be higher than some as it included both wet and dry deposition whereas many of the critical load estimates were limited to wet deposition (Williams and Tonnessen 2000). However, it may be lower than others as it did not include ammonium. Ammonium was not included in our calculations because its contribution to acidification is less certain. In addition, our critical load was based on the time period where change in diatom communities and reconstructed ANC was first observed in contrast to a defined ANC concentration (e.g., ANC < 0 μeq L^{-1}). These differences in approaches posed a challenge when quantitatively comparing critical load

estimates. However, because the estimate was so much lower for the Sierra Nevada, we likely can conclude that the acidification critical load for the Sierra Nevada is lower than the previous estimates for the Rocky Mountains. This was consistent with survey data showing that Sierra Nevada lakes are especially sensitive to acid deposition and have some of the lowest ANC values in the United States (Eilers *et al.* 1989).

The recovery of Moat Lake ANC was a positive result that further contributed to the already noted successes of the CAA. However, we must build on these successes in order to continue protecting sensitive high-elevation lakes. Despite the recovery observed in Moat Lake, results from concurrent research we are conducting at a larger spatial scale (n = 42 lakes) show a correlation between present day ANC and SCP concentrations in surface sediments. These results suggest that Sierra Nevada lakes are still being affected by acid deposition (A. M. Heard, unpubl.). In addition, late 20th century deposition data at Emerald Lake exceeds our estimated critical load of 73.9 eq ha^{-1} yr^{-1} (Table 2.1). Burns et al. (2011) found that current emission reductions were not adequate to allow for full recovery of more sensitive ecosystems. The CAA has been most effective at reducing sulfur emissions and deposition (Lehmann et al. 2005; Smith et al. 2011). The effects on NO_x emissions and nitrogen deposition have been less pronounced, especially in the western United States where mobile and agricultural sources are a significant component of total nitrogen deposition. Ammonium and total dissolved nitrogen deposition are increasing in the western United States (Lehmann et al. 2005), which could start to negate the recovery from acidification that we are observing from decreased sulfur dioxide emissions.

The Moat Lake BSi and $\delta^{13}C$ proxies indicated that productivity has increased during the 20th century suggesting that multiple stressors are acting on and changes are occurring in the Moat Lake ecosystem (Figure 2.5). The PCA results suggested that both climate warming and increased nutrient inputs explain increased productivity at Moat Lake. Air temperature and the productivity proxies were strongly correlated. Increases in BSi and $\delta^{13}C$ have been attributed to increased productivity from climate warming (Colman et al. 1995; Hu et al. 2003; Street et al. 2012) and eutrophication (Brenner et al. 1999; Meyers 2003; Wessels et al. 1999). Moat Lake surface water temperatures have been increasing in the later 20th century (Porinchu et al. 2007). NO_x emissions were correlated with BSi and $\delta^{13}C$, although not as strongly as temperature. Bioassay experiments in Moat Lake have demonstrated phytoplankton response to nitrogen additions (A. M. Heard, unpubl.) and sediment core diatom analyses showed 20th century increases in *Fragilaria crotonensis*, a nitrogen sensitive indicator species (Sickman et al. In press). Our research combined with Porinchu et al.'s (2007) surface water temperature reconstruction suggests that aquatic communities in Moat Lake responded to combined effects from acidification, climate change, and eutrophication. Early in the 20th century the primary stressor effecting Sierra Nevada lakes was acid deposition driven by SO_2 emissions. As the century and industrialization progressed NO_x levels increased adding a eutrophication component while simultaneously contributing to acidification. Effects were further complicated by a warming climate, most dramatically in the later 20th century, as warmer temperatures may contribute to the recovery of ANC in lakes via increased weathering rates, while simultaneously enhancing eutrophication effects. There

is a need for further research to understand eutrophication effects and how acidification, eutrophication, and a warming climate are interacting in these ecosystems.

This research highlights the complexities associated with developing critical loads or other criteria (e.g. water chemistry criteria) on landscapes that have been altered well before research and monitoring programs were in place. The critical load at Moat Lake was surpassed in 1920 and the recovery from acid deposition started in 1970. Both of these milestones occurred well before monitoring was initiated at Moat Lake in 2006 and Emerald Lake in 1983, which is well-known for its long-term research and monitoring record. Paleolimnology studies can play an important role in more fully understanding pre- and post-industrial conditions in the absence of long-term monitoring data. It also underscores the importance of continuing to establish long-term monitoring records into the future in order to continue monitoring the effectiveness of environmental policies such as the CAA and tease out effects from multiple stressors including air pollution and climate change.

2.6 Tables and Figures

Table 2.1: Total annual precipitation and deposition at Emerald Lake. The 1900 values were estimated using the hindcast methods and 1985-1999 are direct measurements. The mean and standard deviation in () are for the 1985-1999 time period. Total acid anions were computed as the sum of nitrate and sulfate (eq ha^{-1} yr^{-1}). The percent nitrate and sulfate is the percent that each analyte contributes to the total acid anions.

Water Year	Precip (mm)	Nitrate (eq ha^{-1} yr^{-1})	Sulfate (eq ha^{-1} yr^{-1})	Sum of Acid Anions (eq ha^{-1} yr^{-1})	Nitrate %	Sulfate %
1900	--	10.7	23.8	34.5	31.0	69.0
1985	1156	83.5	50.3	133.9	62.4	37.6
1986	2624	116.9	70.9	187.8	62.3	37.7
1987	959	108.3	64.7	172.9	62.6	37.4
1988	896	89.4	45.8	135.1	66.1	33.9
1989	684	93.1	31.2	124.2	74.9	25.1
1990	727	110.0	43.1	153.1	71.9	28.1
1991	1058	106.6	38.1	144.7	73.7	26.3
1992	787	100.8	41.1	141.9	71.0	29.0
1993	2384	84.8	64.3	149.1	56.9	43.1
1994	935	57.9	25.6	83.5	69.4	30.6
1995	2891	112.1	72.7	184.8	60.7	39.3
1996	1812	81.8	36.3	118.0	69.3	30.7
1997	1862	119.0	65.6	184.5	64.5	35.5
1998	2403	96.1	59.6	155.7	61.7	38.3
1999	1277	119.4	64.0	183.3	65.1	34.9
Mean	**1497 (762.3)**	**98.6 (17.2)**	**51.5 (15.3)**	**150.2 (29.5)**	**66.2 (5.3)**	**33.8 (5.3)**

Table 2.2: Mean critical load (CL) results presented with 90% upper and lower confidence intervals. Mean deposition from 1920-1930 are the hindcasted deposition estimates during the period of initial ANC decrease. The critical load is presented in terms of the sum of acid anions and then converted to nitrate-nitrogen and sulfate deposition based on Emerald Lake deposition chemistry.

	Mean deposition from 1920-1930		Critical Load	Acid anion CL converted to nitrate and sulfate CL using present day nitrate:sulfate deposition ratios			
	Nitrate (eq ha^{-1} yr^{-1})	Sulfate (eq ha^{-1} yr^{-1})	Sum Acid Anions (eq ha^{-1} yr^{-1})	Nitrate (eq ha^{-1} yr^{-1})	Nitrate-Nitrogen (kg ha^{-1} yr^{-1})	Sulfate (eq ha^{-1} yr^{-1})	Sulfate (kg ha^{-1} yr^{-1})
Mean	20.0	54.0	73.9	48.8	0.68	25.1	1.2
Lower	18.4	47.2	65.6	43.3	0.61	22.3	1.1
Upper	21.4	60.8	82.2	54.2	0.76	27.9	1.3

Table 2.3: Maximum SCP concentrations from a selection of lakes in Canada, Chile, Europe, Russia, United Kingdom, and United States. Lakes are listed in increasing order of maximum SCP concentrations. Moat, Emerald, and Pear Lakes are in bold italics

Location	Lake	Max SCP conc (gDM^{-1})	Yr Max	Source
Russia	Lake Baikal	470	1988	Rose et al. 1999
Svalbard	Scurvey	540	--	Rose et al. 1999
Athabasca Oil Sands	SM6	600	1955	Curtis et al. 2010
Athabasca Oil Sands	NE2	1,000	2002	Curtis et al. 2010
Glacier NP	Oldman	1,098	1981	Landers et al. 2008
Norway	Ovre Naedalsvatn	1,300	1990	Rose et al. 1999
Olympic NP	Hoh	1,324	1953	Landers et al. 2008
Sierra Nevada	***Emerald***	***1,520***	***1964***	
Sierra Nevada	***Pear***	***1,821***	***1972***	
Rocky Mt NP	Lone Pine	2,039	1982	Landers et al. 2008
Svalbard	Birgervatnen	2,100	--	Rose et al. 1999
Sierra Nevada	***Moat***	***2,399***	***1984***	
Mt. Rainer	LP #19	3,734	1964	Landers et al. 2008
Russia	Lake Baikal	3,800	1990	Rose et al. 1999
Pyrenees	Laguna Redo	5,900	1987	Rose et al. 1999
Iberian Pen	Laguna Cimera	7,000	1986	Rose et al. 1999
UK/Ireland	Lough Maam	8,800	1981	Rose et al. 1999
Chile	Laguna Chica	9,000	1991	Chironos et al. 2006
UK/Ireland	Lochnagar	30,600	1977	Rose et al. 1999
Tatra Mts	Dlugi Staw	36,000	1993	Rose et al. 1999
Norway	Lille Hovvatn	40,700	--	Rose et al. 1999
Pyrenees	Laguna Aguilo	71,000	1960	Rose et al. 1999
E. Alps	Zornje Krisko	92,000	1994	Rose et al. 1999

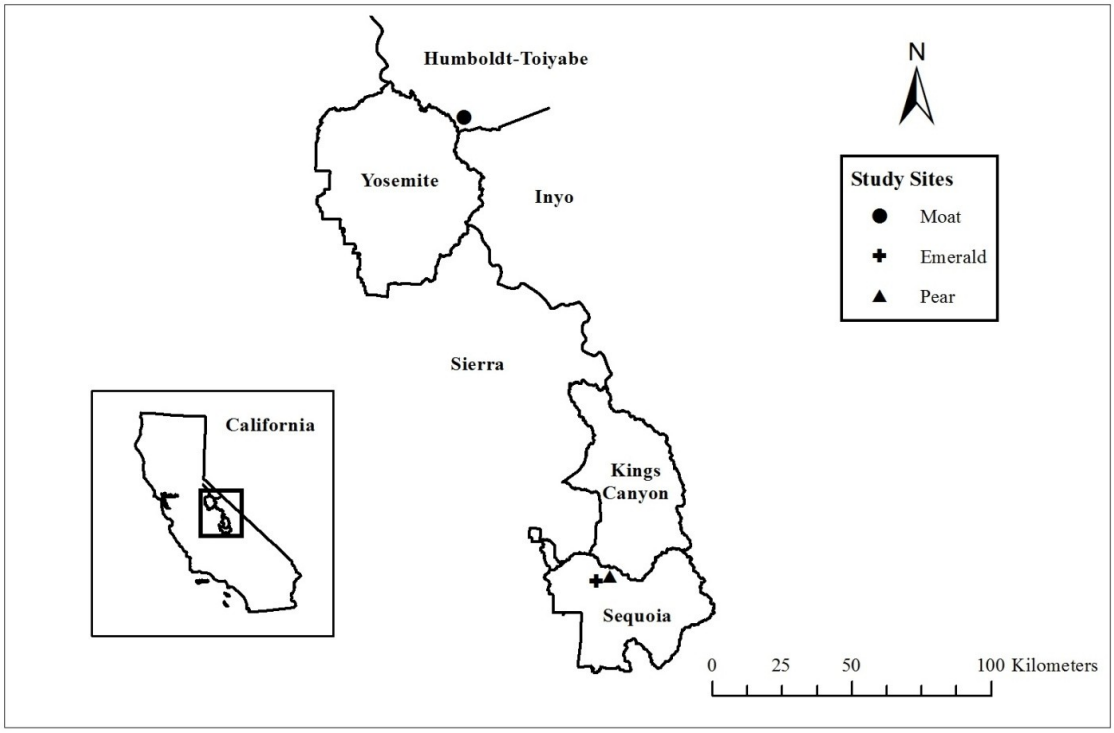

Figure 2.1: Moat, Emerald, and Pear Lake locations in the Sierra Nevada, California.

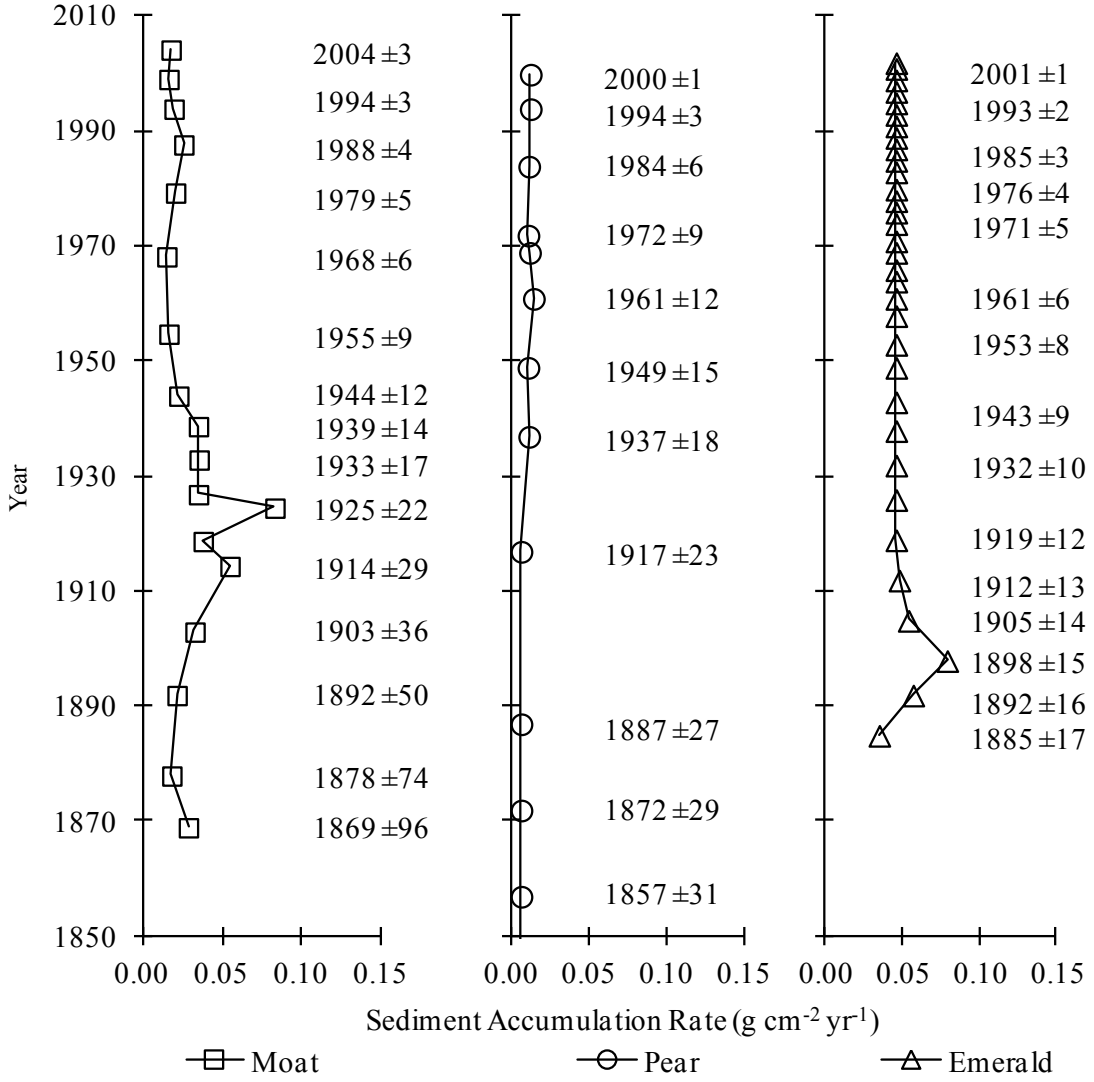

Figure 2: Sediment accumulation rates for Moat, Pear, and Emerald Lakes. ^{210}Pb dates and errors are shown to the right of the depth profiles.

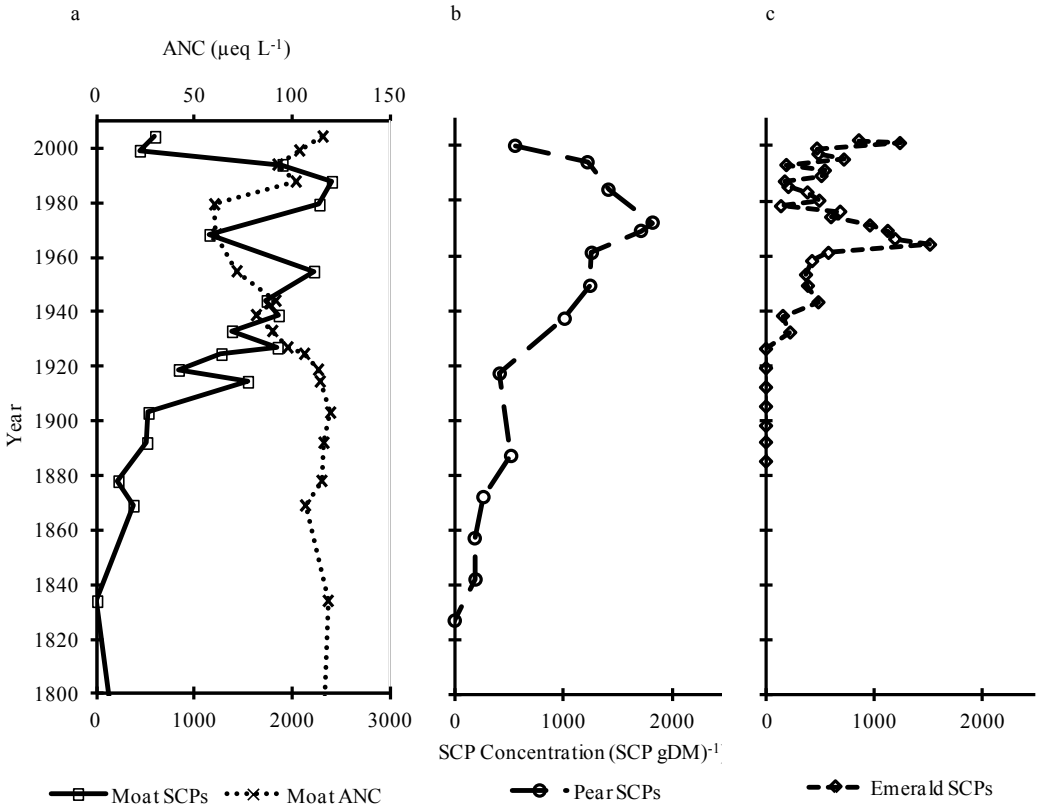

Figure 2.3: a) Moat Lake SCP concentrations and reconstructed ANC, b) Pear Lake SCP concentrations, and c) Emerald Lake SCP concentrations.

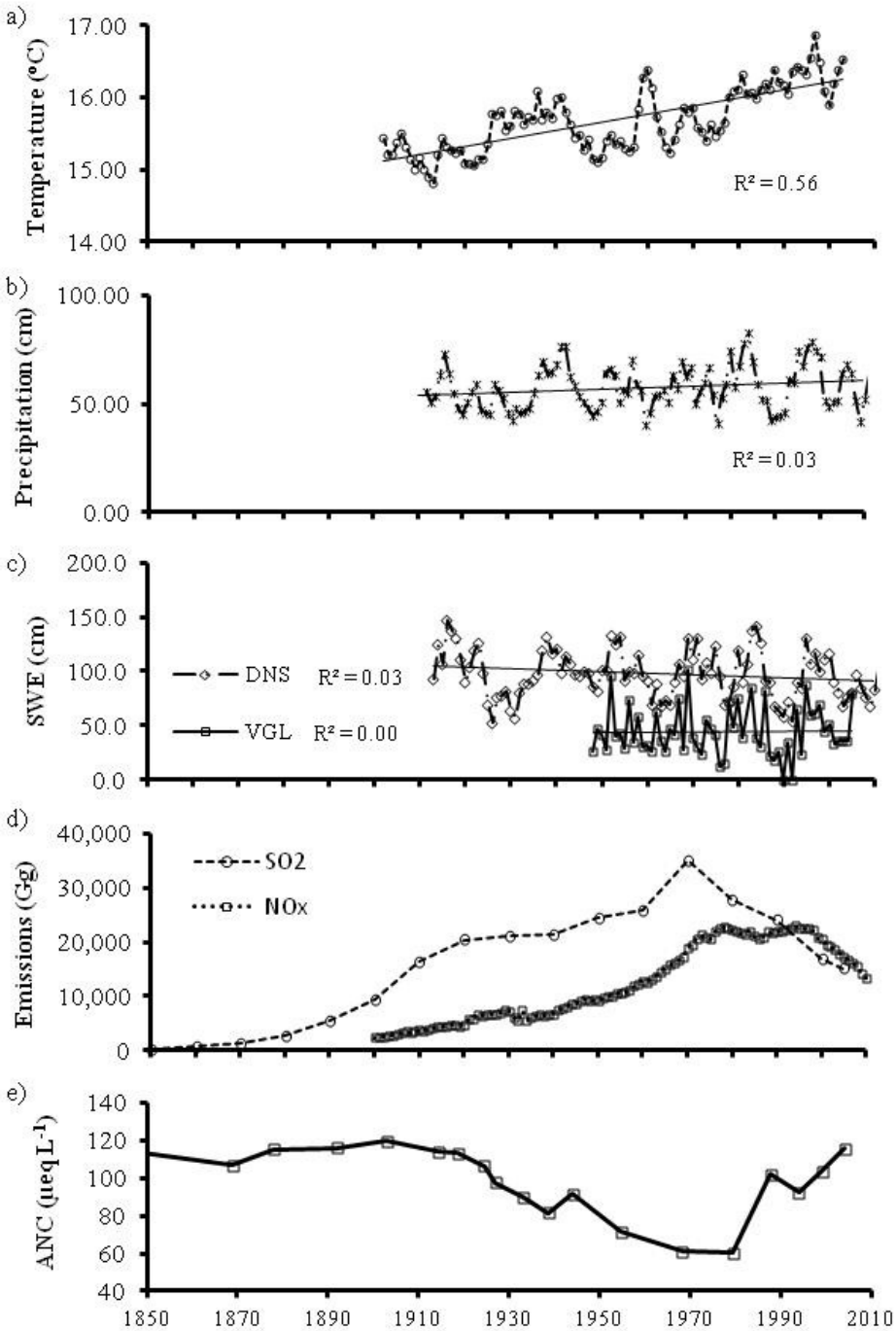

Figure 2.4: Time series graphs for a) California mean annual air temperature presented as the 3-year moving average, b) California mean annual precipitation as the 3-year moving average, c) April 1st SWE at Donner Summit (DNS) and Virginia Lakes (VGL) presented as the 3-year moving averages, d) national NO_x and SO_2 emissions, and e) diatom reconstructed ANC.

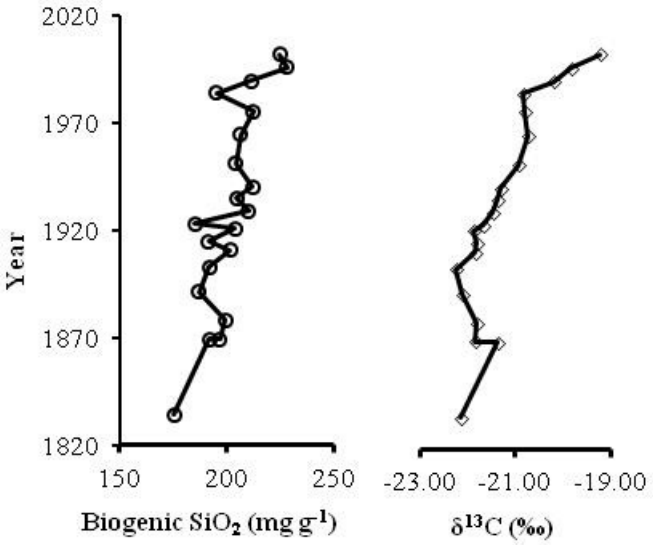

Figure 2.5: BSi and $\delta^{13}C$ profiles for Moat Lake.

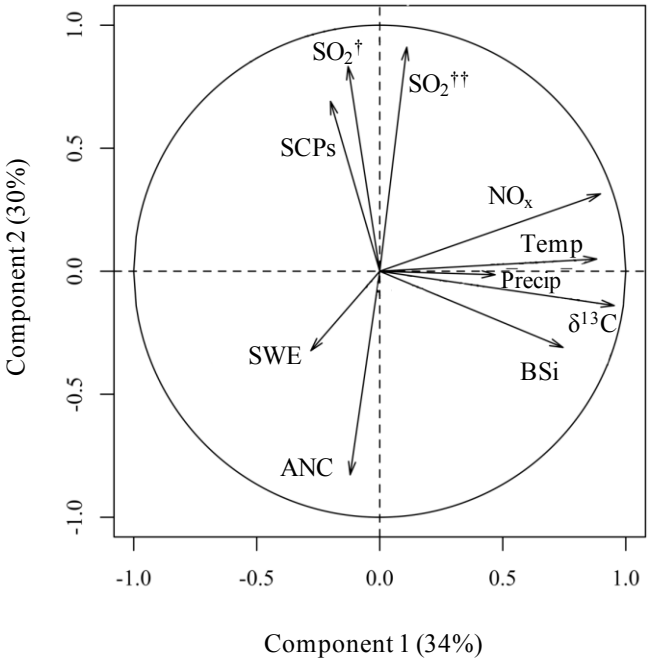

†SO_2 estimates from EPA 2000
†SO_2 estimates from Smith et al. 2011

Figure 2.6: PCA bi-plot for Moat Lake sediment, emissions, and climate variables.

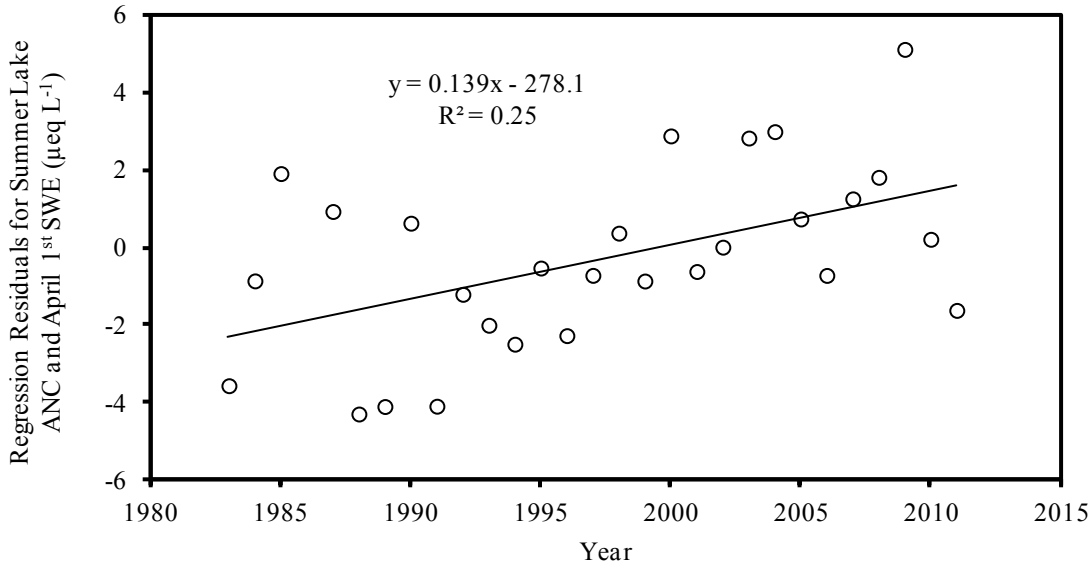

Figure 2.7: Residuals for regression between April 1st SWE and summer ANC graphed over time.

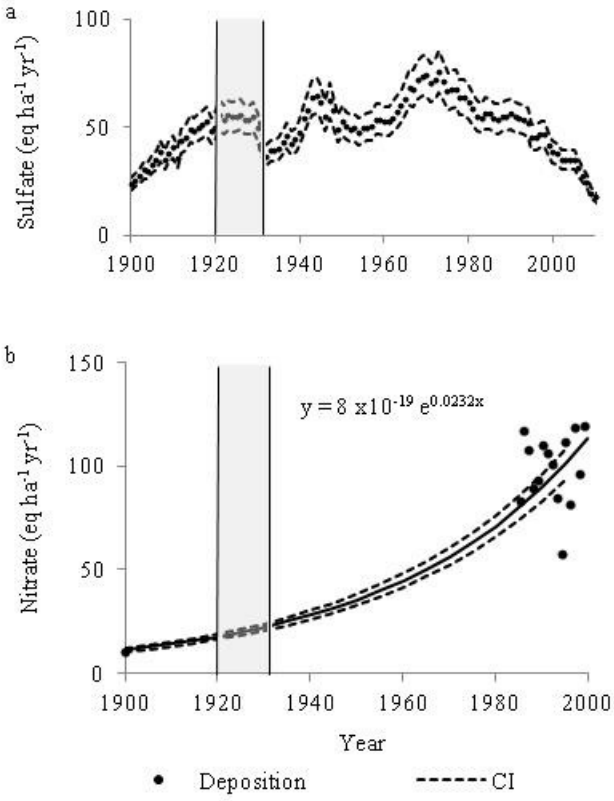

Figure 2.8: Reconstructed acid anion deposition trends for a) sulfate and b) nitrate. The 1920-1930 time periods used to determine the critical load is shaded in gray.

Chapter 3: Landscape Analysis Correlating Atmospheric Deposition and Chemical Indicators of Acidification and Eutrophication to Inform Critical Load Development

3.1 Abstract

We investigated factors contributing to spatial variation in acid and nutrient affected lakes with the objective of linking atmospheric deposition to acidification and eutrophication effects. Indicators of atmospheric deposition (spheroidal carbonaceous particles (SCPs), $\delta^{18}O$ (NO_3^-), and $\delta^{15}N$ (NO_3^-)) and basin characteristics were measured to explain variation in lake acid neutralizing capacity (ANC), pH, nutrient limitation ratios (DIN:TP), and nitrate in the Sierra Nevada, California. SCPs were negatively correlated with ANC, pH, sulfate, and mean slope and were not correlated with nitrate or DIN:TP. $\delta^{18}O$ (NO_3^-) was not significantly correlated with nitrate, DIN:TP, ANC or pH. $\delta^{18}O$ (NO_3^-) was negatively correlated with sulfate and positively correlated with 45-90° aspect and Pleistocene till. $\delta^{15}N$ (NO_3^-) was not significantly correlated with ANC, pH, sulfate, nitrate, or DIN:TP. $\delta^{15}N$ (NO_3^-) was negatively correlated with lake area, shoreline length, mean slope, percent area north facing and greater than 30% slope, 0-45° aspect, non-vegetated area, and percent area with water. $\delta^{15}N$ (NO_3^-) was positively correlated with shore line to lake area ratio, 225-270° aspect, and felsic intrusive bedrock. Following storm events an increase in $\delta^{18}O$ (NO_3^-) and a decrease in $\delta^{15}N$ (NO_3^-) was observed, which may complicate interpretation of spatial results. We concluded that 1) Sierra Nevada lakes are still affected by acid deposition based on the correlation between

SCPs and ANC and pH, 2) spatial SCP and ANC patterns indicate that air patterns and deposition across the Sierra Nevada are complex, and 3) quantifying the relationship between nitrogen deposition and eutrophication across complex mountain landscapes is presently challenging. Calculating critical loads based on acidification is a more robust approach.

3.2 Introduction

Increased rates of atmospheric deposition are altering biogeochemical cycles and ecological processes in remote mountain ecosystems (Fenn *et al.* 2003). The Sierra Nevada Mountains, California are exposed to air pollution that originates from agricultural, urban, and industrial sources in California's Central Valley, the San Francisco Bay Area, and as far away as Asia (Bytnerowicz *et al.* 2002; Vicars and Sickman 2011). Nutrients and acid anions are transported by air currents into the Sierra Nevada where they are deposited as wet and dry deposition. Increased inputs of nutrients and acid anions to oligotrophic high-elevation lakes are contributing to acid neutralizing capacity (ANC) depression, elevated nitrate (NO_3^-) concentrations, shifts in nutrient limitation, and changes in the productivity and structure of biotic communities (Elser *et al.* 2009a; Sickman *et al.* 2003b; Wigington Jr *et al.* 1992).

A need for stricter standards based on measurable ecological effects has been identified as an important step towards the long-term protection of high elevation lakes (National Research Council 2004). One approach is the critical load, which is defined as a quantitative estimate of an input or exposure to a pollutant at which unacceptable

impacts occur to sensitive ecosystem components (Bull 1992). This approach, widely used in Europe for the last few decades (UNECE 1999), is gaining interest and application in the United States (Burns *et al.* 2008; Porter and Johnson 2007). There has been an increase in research to determine critical loads to protect sensitive Wilderness areas, including high-elevation lakes (Pardo *et al.* 2011; Saros *et al.* 2011). Critical loads may be based on ecological change from acidification or eutrophication (Baron *et al.* 2011).

If critical loads are to be an effective tool and incorporated into air quality policy it is important to be able to link atmospheric deposition to chemical and biological lake effects and understand these relationships at landscape scales, the scales at which we protect lakes and apply policy. Sierra Nevada lakes have high spatial variability in ANC and nitrate with lakes ranging from 0 to 499 $\mu eq\ L^{-1}$ ANC and below detectable levels to 36 μM nitrate (J. O. Sickman, unpubl.). There are multiple variables that affect ANC, nitrate concentrations, nutrient ratios, and the potential for a lake to respond to atmospheric deposition inputs. These include nitrogen and sulfur loading from atmospheric deposition and basin characteristics such as catchment topography, vegetation cover, and geology (Berg *et al.* 2005; Clow *et al.* 2010). Nanus et al. (2012) showed that critical loads in the Rocky Mountains vary across the landscape and are sensitive to basin characteristics.

Critical nitrogen loads for Sierra Nevada lakes have been estimated to range from 1.5 to 2.0 kg N $ha^{-1}\ yr^{-1}$ for eutrophication (Baron *et al.* 2011; Saros *et al.* 2011). There is limited information for acidification estimates, however, research we are presenting in a

companion paper suggests it is between 0.61 to 0.76 kg N ha^{-1} yr^{-1} (A. M. Heard unpubl.). These initial estimates would benefit from continued research and efforts to revise them as more data become available (Baron *et al.* 2011). The purpose of our research was to understand factors contributing to spatial variation in acid and nutrient affected lakes to inform critical load development and implementation. We measured indicators of atmospheric deposition (spheroidal carbonaceous particles (SCPs), lake water nitrate $\delta^{18}O$ (NO_3^-), and lake water nitrate $\delta^{15}N$ (NO_3^-)) and basin characteristics to explain variation in lake ANC and nutrient limitation ratios in lakes throughout the central and southern Sierra Nevada mountains. Our research objectives were to 1) determine if ANC, pH, nutrient limitation, nitrate, and sulfate are correlated with atmospheric deposition indicators, 2) determine the extent that basin characteristics explain atmospheric deposition indicator relationships to water chemistry variables, and 3) assess how temporal variation may influence spatial results by conducting intensive temporal $\delta^{18}O$ (NO_3^-) and $\delta^{15}N$ (NO_3^-) sampling at one site.

There are several tools that can be used to measure the extent of anthropogenic atmospheric deposition that is reaching lake waters. SCPs are porous spheroids composed primarily of elemental carbon that are chemically very resistant and well-preserved in lake sediments. They are unambiguous geochemical indicators of anthropogenic atmospheric deposition because they are only produced by industrial combustion of fossil fuels, there are no natural sources. SCPs in surface sediments have been used to investigate atmospheric deposition patterns (Rose and Harlock 1998). Stable isotope measurements of $\delta^{18}O$ (NO_3^-) and $\delta^{15}N$ (NO_3^-) in lake water nitrate can be used to

determine the proportion of nitrate derived from atmospheric deposition. They are used to discern between the two nitrate sources of interest in Sierra Nevada lakes, which are atmospherically derived nitrate from deposition and nitrate that has been stored in and undergone biogeochemical cycling in soils and flushed into receiving waters (Sickman *et al.* 2003a).

3.3 Methods

3.3.1 Study Area

The study area encompasses Yosemite, Sequoia, and Kings Canyon National Parks and adjacent areas on the Humboldt-Toiyabe and Inyo National Forests (Figure 3.1). Yosemite and Sequoia and Kings Canyon contain over 1,200 lakes, most occurring at higher elevations (above 2500 m). The average lake area is between 5 and 6 hectares and lake depth ranges from less than 2 m to well over 30 m.

Temporal $\delta^{18}O$ (NO_3^-) and $\delta^{15}N$ (NO_3^-) sampling was conducted at Emerald Lake, located on the western slope of Sequoia National Park. Emerald Lake (elevation 2800 m) has a maximum depth of 10 m, lake surface area of 2.7 ha, and watershed area of 120 ha. The bedrock geology of the watershed is dominated by granite and granodiorite. Less than 10% of the watershed is vegetated.

3.3.2 Sample Design

We used two data sets for the spatial analysis. The first data set, referred to as the 'diatom data set', consists of sites that were selected as part of a larger study investigating atmospheric deposition effects on lake chemistry and diatom communities with an

emphasis on nitrogen deposition (Sickman et al. In press). Forty-two lakes with known chemistry were selected to capture the full range of lake nitrate concentrations in the region. Sediment and water samples were collected from mid-lake sampling stations at all sites in 2007.

The second data set, referred to as the 'SIEN data set', is part of the National Park Service's, Sierra Nevada Network (SIEN) lake monitoring design (Heard et al. 2012). The SIEN lake monitoring membership design is a generalized random tessellation stratified (GRTS) design that incorporates variable probability sampling. The GRTS design employs a systematic sampling approach along a randomly ordered sequence of location addresses to obtain a spatially balanced probability sample (Stevens and Olsen 2003; 2004). The temporal sampling structure is a serial augmented panel design where sites are either visited annually (n=8) or on an alternating 4-year schedule (n=17 per year). Water samples were collected at the lake outflows. Water chemistry and nutrient ratios were measured at all SIEN sites (n=75; one site could not be samples) and $\delta^{18}O$ (NO_3^-) was measured at a sub-set of sites (n=54).

The intensive temporal sampling was conducted at Emerald Lake on a weekly to monthly frequency. Precipitation data collected by the National Park Service at Lodgepole was used to interpret the time series results.

3.3.3 Sample Collection and Analysis

The diatom and SIEN field methods are described in detail in Sickman et al (Sickman et al. In press) and Heard et al. (2012) respectively, so we only briefly describe them here. The diatom lakes were sampled between late July and early October of 2008

and 2009. Water samples were collected mid-lake at depths of 1 and 7 m using a hand-operated peristaltic pump and silicon tubing. Surface sediment samples were collected using a gravity corer. The top 0-1 cm section of the core was sampled and stored in 60-ml HDPE bottles. SIEN lakes were sampled in August and September of 2008 – 2012. Water samples at the SIEN sites were collected as grab samples from lake outflows.

Diatom and SIEN water samples were analyzed for ANC, pH, dissolved inorganic nitrogen (DIN), total dissolved phosphorus (P), particulate phosphorus (PP), sulfate, and specific conductance. A sub-set of the SIEN water samples were analyzed for $\delta^{18}O$ (NO_3^-) and $\delta^{15}N$ (NO_3^-). Diatom sediment samples were analyzed for SCPs.

Water samples for ANC, pH, and specific conductance analysis were collected unfiltered and stored in 125-ml HDPE bottles. Samples for dissolved inorganic nitrogen, total dissolved phosphorus, and sulfate analysis were field filtered into 125-ml HDPE bottles using 1.0 µm polycarbonate filters. Particulate phosphorus samples were field filtered and collected on 1.0 µm Pall A/E glass fiber filters that were pre-combusted at 500 ^{o}C. Water samples for $\delta^{18}O$ (NO_3^-) and $\delta^{15}N$ (NO_3^-) analysis were concentrated on anion resin columns in the field. Prior to going into the field, resin columns were prepped using an alternating 2M potassium chloride (KCl) and 0.6 M hydrochloric acid (HCl) rinse. pH and ANC were measured with a pH meter and Ross combination electrode using the Gran titration method (Gran 1952). Specific conductance was measured in the lab with a conductivity meter and electrode (cell constant = 1.0). Sulfate and DIN, measured as nitrate, were analyzed on a Dionex ion chromatograph using EPA Method 300.1. Particulate P and total dissolved P were measured using the method described in

Valderrama (1981) followed by EPA Method 365.1. Total phosphorus (TP) was calculated as the sum of PP and dissolved P. Isotope resin columns were stripped with 2M KCl and isotopes were measured using the denitrifier method (Ohte et al. 2004). Blank columns were used to correct for background nitrate contamination in the resin.

SCPs were extracted from sediment sub-samples using a sequential chemical attack to remove unwanted sediment fractions (Rose 1994). Sediment samples were dried, weighed, and placed in 10 ml polypropylene tubes, and tubes were placed in an 80-90 ^{o}C water bath. We sequentially added nitric acid, hydrofluoric acid, and hydrochloric acid to remove organic, siliceous, and carbonate materials, respectively. A known fraction of the remaining suspension was evaporated and mounted on a standard microscope slide. SCPs were then counted at 400x magnification under a light microscope using identification criteria described in Rose (2008) and converted to a concentration of SCPs per gram of dry mass sediment (gDM^{-1}). Reference sediments and blanks were included for quality control and quality assurance (Rose 2008).

3.3.4 Basin Characteristics

Specific conductance from lake samples was included as a integrative indicator of watershed processes. Basin characteristics were quantified for diatom and SIEN lake basins in ArcGIS. 10-m digital elevation model (DEM) and triangulated irregular network (TIN) data were used to determine watershed area, mean elevation, mean slope, and aspect. The USGS National Hydrography Dataset (NHD+) (http://nhd.usgs.gov) was used to determine lake area and shore line length and the National Park Service (NPS) vegetation maps (National Park Service 1998; 2009) (https//irma.nps.gov) were used to

compute the percent area non-vegetated. The NPS geologic resources inventory maps (NPS Geologic Resources Inventory Program 2006; 2013) (https//irma.nps.gov) were used to determine the percent area for the 13 bedrock types present in the study watersheds. In the correlation analysis we omitted types that were present in five or less of the study watersheds. There were seven remaining categories, which included alluvium/mass wasting deposits/lake sediments, felsic intrusive, felsic metamorphic, intermediate intrusive, mafic intrusive, neoglacial/talus/colluvium, and Pleistocene till.

3.3.5 Data Analysis

Summary statistics were computed for the atmospheric deposition indicators (SCPs, $\delta^{18}O$ (NO_3^-), and $\delta^{15}N$ (NO_3^-)) and primary (ANC and DIN:TP) and secondary (pH and nitrate) water chemistry variables. DIN:TP statistics were calculated using methods that incorporate the GRTS design. The mean is calculated as a Horvitz-Thompson estimate (Horvitz and Thompson 1952) and the variance of the mean is calculated using the GRTS neighborhood variance estimator (Stevens and Olsen 2003; 2004). Inclusion probabilities were incorporated into the estimates in order to account for the panel structure where sites were sampled at different time scales (annually and one time). Since $\delta^{18}O$ (NO_3^-) and $\delta^{15}N$ (NO_3^-) were a sub-sample of the full SIEN design, summary statistics were calculated assuming a simple random sample.

Correlation analyses for SCP sediment concentrations, lake water isotopes and chemistry, and basin characteristics were conducted using Kendall's tau ($\alpha = 0.10$). Kendall's tau was selected as it is commonly used for water quality analysis due to its resistance to the effects of outliers and skewness in the data set (Helsel and Hirsch 2002).

3.4 Results

Surface sediment SCP concentrations were measured at 42 sites (diatom data set) throughout the study area and ranged from 0 to 5900 gDM^{-1} with a mean of 760 gDM^{-1} (Table 3.1, Figure 3.2, and Figure 3.3). Lake ANC measurements in the diatom data set ranged from 23.0 to 145 μeq L^{-1} with a mean of 75.6 μeq L^{-1} (Table 3.1, Figure 3.4, and Figure 3.5). Lake pH measurements in the diatom data set ranged from 5.81 to 6.81 with a mean of 6.36. DIN:TP ratios in the diatom data set ranged from below detection to 18 with a mean of 3.3 and nitrate ranged from less than 0.04 to 9.30 μM with a mean of 1.15 μM (Table 3.1). Lake water nitrate $\delta^{18}O$ (NO_3^-) and $\delta^{15}N$ (NO_3^-) (SIEN data set) were measured at 54 sites. $\delta^{18}O$ (NO_3^-) ranged from -1.5 to 54.5‰ with a mean of 14.7‰ and $\delta^{15}N$ (NO_3^-) ranged from -13.8 to 4‰ with a mean of -1.1‰ (Table 3.1). When graphed on the dual isotope plot 2 samples were below the 5‰ soil nitrate estimate and 52 were between soil water and precipitation (Figure 3.6). Soil water and precipitation end-member estimates were from Sickman et al. (2003a) and Homyak (2012). ANC in the SIEN data set ranged from 3.93 to 151 μeq L^{-1} with a mean of 55.3 μeq L^{-1} (Table 3.1). DIN:TP ratios ranged from below detection to 78 with a mean of 6.3 (Table 3.1, Figure 3.7, and Figure 3.8). Nitrate ranged from less than 0.04 to 11.8 μM with a mean of 4.58 μM (Table 3.1).

The Emerald Lake $\delta^{18}O$ (NO_3^-) range was 7.55 to 12.81‰ from June through August with a decreasing trend after July 11, 2011 (Figure 3.9). $\delta^{18}O$ (NO_3^-) September samples increased to 21.24 and 11.90‰ following several precipitation events. $\delta^{15}N$ (NO_3^-) gradually increased from -2.16 to 0.01‰ during the June through August

sampling period. The September samples decreased to -2.97 and -6.65, following the precipitation events.

SCPs were negatively correlated with ANC, pH, sulfate, specific conductance, and mean slope (Table 3.2). SCPs were not significantly correlated with nitrate, DIN:TP, and all basin characteristics except mean slope. ANC was negatively correlated with SCPs, percent area with water cover, and alluvium/mass wasting/lake sediment bedrock type (Table 3.2). ANC was positively correlated with pH, sulfate, specific conductance, watershed area to lake area ratio, mean elevation, UTM_x, and 225-270° aspect. pH was positively correlated with ANC, sulfate, specific conductance, mean elevation, UTM_x, and 225-270° aspect. The SCP-ANC relationship was further investigated by stratifying the data into lakes with low (less than 20 µM) and high (greater than 20 µM) sulfate concentrations. The SCP-ANC correlation for the full data set, no stratification, was tau = -0.22 (p = 0.052) compared to lakes with low sulfate that had a tau of -0.28 (p = 0.028) (Table 3.4 and Figure 3.10). There was not a significant SCP-ANC correlation among the lakes with high sulfate concentrations (p = 0.853).

$\delta^{18}O$ (NO_3^-) was not significantly correlated with nitrate, DIN:TP, ANC or pH (Table 3.3Table 3.2). $\delta^{18}O$ (NO_3^-) was negatively correlated with sulfate and positively correlated with 45-90° aspect and Pleistocene till. $\delta^{15}N$ (NO_3^-) was not significantly correlated with ANC, pH, sulfate, nitrate, or DIN:TP (Table 3.3Table 3.2). $\delta^{15}N$ (NO_3^-) was negatively correlated with lake area, shoreline length, mean slope, percent area north facing and greater than 30% slope, 0-45° aspect, non-vegetated area, and percent area with water. $\delta^{15}N$ (NO_3^-) was positively correlated with shore line to lake area ratio, 225-

270° aspect, and felsic intrusive bedrock. DIN:TP was positively correlated with specific conductance, elevation, mean slope, north facing aspect with greater than 30% slope, UTM_y, $0\text{-}45^o$ aspect, percent watershed area without vegetation, and neoglacial/talus/colluvium. DIN:TP was negatively correlated with UTM_x.

3.5 Discussion

3.5.1 Spheroidal Carbonaceous Particles

The lack of correlation between SCPs and basin characteristics suggests that watershed processes had a minimal effect on SCP concentrations. The only significant correlations were negative correlations with specific conductance and mean slope. This finding was contrary to other studies that have found steeper slopes attributed to increased measures of deposition (e.g. high nitrate and low ANC) as steeper slopes increase runoff of contaminants and nutrients to receiving waters (Clow and Sueker 2000). Other studies have found correlations between SCPs and basin characteristics, primarily elevation, lake area, and lake area to catchment ratio (Fott *et al.* 1998; Rose and Juggins 1994). The specific conductance correlation suggests that watershed processes are affecting SCPs, but without additional watershed correlations it is challenging to explain this correlation. Increased specific conductance can results from higher ionic inputs that may be correlated with higher watershed weathering rates. Higher weathering rates could indicate higher sedimentation rates, which would result in lower SCP concentrations. The negative SCP-specific conductance correlation may also be indicative of a correlation between watersheds with low ionic inputs and sites that receive high amounts of deposition. For example, high-elevation exposed watersheds with little

vegetation may be susceptive to higher deposition estimates and also have lakes that receive minimal ionic inputs. Without additional basin characteristic correlations we are unable to further explain this correlation. We likely observed limited correlations with basin characteristics due to relatively small differences between the characteristics of the study lakes and watersheds. The lack of correlation in our study strengthens the case for using SCPs as an indicator of atmospheric deposition as the data are less complicated by variable watershed and lake processes.

ANC concentrations are affected by multiple basin and lake characteristics (Berg *et al.* 2005; Nanus *et al.* 2009). A positive correlation with watershed area to lake area has been observed previously in Sierra Nevada lakes (Berg *et al.* 2005) and was attributed to shorter transit time for deposition from the catchment to the lake and less weathering inputs resulting in lower buffering capacity. We also observed a correlation with percent water coverage, which was likely reflecting similar processes as catchment to lake area ratio. Consistent with local air pollution patterns that move west to east into the mountains (Bytnerowicz *et al.* 2002), there was a west to east ANC gradient, where lower concentrations were observed in more western lakes. However, contrary to pollution patterns lakes with more westerly facing basins had higher ANC. ANC was negatively correlated with alluvium, mass wasting, and lake sediment bedrock types, in contrast to previous research in Yosemite that found a positive correlation with alluvium deposits due to more developed soils typically associated with alluvium bedrock types (Clow *et al.* 2010). Other studies have found that ANC sensitive lakes were correlated with high percentages of granitic bedrock and less sensitive lakes were often correlated

with calc-silicates and carbonates (Nanus *et al.* 2005). We likely did not see these correlations due to little variation in bedrock type. The majority of the study basins had high percentages of felsic intrusive bedrock (e.g. granites and granodiorites) and, therefore, all had high degrees of sensitivity.

pH was also examined as a secondary measure of acidification. Correlation results supported our ANC results as pH was strongly correlated with ANC ($p < 0.001$). pH was also negatively correlated with SCPs and positively correlated with sulfate and had similar correlations with basin characteristics.

The significant correlation between SCPs and ANC suggests that present day ANC concentrations in Sierra Nevada lakes are also affected by anthropogenic atmospheric deposition. This is further supported by the correlation between SCPs and pH and the ANC and pH. SCPs have been correlated with sulfur emissions (Wik and Renberg 1991), sulfate and nitrate deposition (Rose *et al.* 2001; Rose and Monteith 2005; Wik and Renberg 1991), and trace metals (Rose and Harlock 1998), and in a companion paper (Chapter 2) we presented SCPs correlated with diatom-reconstructed ANC in a lake sediment core (A. M. Heard, unpubl.). However, SCPs in sediments and ANC in lake water samples have not been correlated. This is a useful correlation for Sierra Nevada lakes as there are limited spatial measures of deposition due to the remote and complex mountain terrain, but there are lake chemistry monitoring programs that routinely measure ANC.

The negative correlation between SCPs and sulfate and the positive correlation between ANC, pH, and sulfate suggests that atmospheric deposition was not the

dominant process controlling lake sulfate concentrations. Our results indicated that acid anion lake concentrations are strongly controlled by additional sources, ones not associated with SCPs, and watershed processes. Agricultural and mobile sources are significant sources of N deposition in the Sierra Nevada that do not produce SCPs (Bytnerowicz *et al.* 2002). Additional sources of sulfate include weathering of sulfide-bearing minerals and soil organic matter (Clow *et al.* 1996; Stanko and Fitzgerald 1990). Nitrate and sulfate are both susceptible to extensive biogeochemical cycling within a watershed, which affects their fate and transport to receiving lake waters (Clow *et al.* 1996; Sickman *et al.* 2003a). Further investigation of the SCP-ANC relationship supported this hypothesis. When we stratified the data by low and high sulfate we found no correlation in the high sulfate lakes. At these sites, sulfate and ANC were likely dominated by mineral composition and weathering rates. Omitting the high sulfate lakes where watershed processes are dominant, improved the correlation between SCPs and ANC (Table 3.4).

A visual inspection of the SCP-ANC relationship showed that lakes with SCPs greater than 1000 gDM^{-1} typically had ANC concentrations less than 75 $\mu eq\ L^{-1}$ (Figure 3.10). The one exception was the lake, Upper Gaylor Lake in Yosemite, with an SCP concentration of 1500 gDM^{-1} and ANC concentration of 109 $\mu eq\ L^{-1}$. Upper Gaylor Lake, which was one of the high sulfate lakes (sulfate = 24.6 μM) likely maintained a high ANC despite higher deposition inputs due to the basin's high composition of alluvium, metamorphic, and Pleistocene till bedrock, which are all associated with higher lake ANC (Clow *et al.* 2010). The Upper Gaylor watershed was relatively unique in that it was only

one of two sites in the data set that did not contain felsic intrusive bedrock, the most ANC sensitive and common bedrock type. The 1000 gDM^{-1} value appeared to represent a significant SCP threshold in the Sierra Nevada. The SCP-ANC relationship was considerably more variable (ANC range of 33 to 145 $\mu eq\ L^{-1}$) when SCP's were less than 1000 gDM^{-1}. Lower concentrations had larger standard errors that explained some of the variability, but it may also be due to the effects of basin and in-lake processes that were more pronounced at sites with lower acid deposition inputs. This threshold is similar to the Northern Hemisphere background concentration of 500-1000 gDM^{-1} reported by Rose et al. (1995).

SCPs were also not correlated with DIN:TP ratios, which was consistent with the lack of correlation with nitrate. Thus we were not able to explain nutrient limitation patterns using SCPs.

The correlation of surface sediment SCPs and ANC and pH in recent (2007) water chemistry samples suggests that Sierra Nevada lakes are presently affected by acid deposition. In a companion paper (Chapter 2), we demonstrated that at a single lake on the eastern Sierra Nevada, acid deposition caused a notable decline in ANC concentrations starting in the early 20th century. The trend was reversed in the late 20th century and ANC returned to pre-industrial concentrations by 2005. This recovery was attributed to the effectiveness of the Clean Air Act (1970) and Amendments (1977 and 1990) (CAA). The results we present in this current paper examining a spatially extensive data set showed that many Sierra Nevada lakes have not fully recovered from acidification. It is highly likely, based on sediment profiles that we studied in Moat,

Emerald, and Pear Lakes, that ANC has improved throughout the Sierra Nevada study lakes following implementation of the CAA. However, our spatial results suggest that additional regulatory measures are needed to achieve full recovery at a regional scale. This is consistent with Burns et al.'s (2011) national-scale review that found current emission reductions are not adequate to allow for full recovery of more sensitive ecosystems. Sierra Nevada lakes are considered some of the most sensitive waterbodies in the western United States due to their naturally low ANC and acid buffering capacity (Eilers *et al.* 1989). The CAA has been most effective at reducing sulfur emissions and deposition (Lehmann et al. 2005; Smith et al. 2011). The effects on NO_x emissions and nitrogen deposition have been less pronounced, especially in the western United States where mobile and agricultural sources are a significant component of total nitrogen deposition. Ammonium and total dissolved nitrogen deposition are increasing in the western United States (Lehmann et al. 2005), which could be inhibiting, or even negating, the recovery effects from decreased sulfur dioxide emissions. Ammonium and nitrate wet deposition at Sequoia National Park averaged 1.87 and 3.08 kg ha^{-1} yr^{-1}, respectively, over the last five years (National Atmospheric Deposition Program; http://nadp.sws.uiuc.edu/).

SCP concentrations were highly variable across the landscape and identifying broad-scale patterns was difficult (Figure 3.2 and Figure 3.3). Basin characteristics likely explained some of the spatial variation (Rose and Juggins 1994), but the lack of correlation with basin characteristics showed that the contribution is minimal. There was some evidence of a west to east pollution gradient. ANC was positively correlated with

UTM_x and although, not significant, SCPs were close to being negatively correlated with UTM_x ($p = 0.122$). However, the SCP patterns were much more complex than a longitudinal gradient, leading us to conclude that air pollution and deposition patterns were also complex and acting at smaller watershed scales. This highlights the need for finer-scale measurements and modeling of air patterns and deposition across mountain landscapes to improve our ability to quantify effects of deposition. Present models are not adequate for critical load research at these scales (Tonnesen *et al.* 2007).

3.5.2 Lake Nitrate $\delta^{18}O$ and $\delta^{15}N$

The two main sources of nitrate present in Sierra Nevada lakes were atmospheric and soil nitrate. These sources are most easily distinguished by examining the $\delta^{18}O$ (NO_3^-) on a dual isotope plot as $\delta^{18}O$ (NO_3^-) typically shows more separation than $\delta^{15}N$ (NO_3^-) between sources (Figure 3.6). The majority of the samples (n=52) were between soil nitrate and precipitation nitrate values indicating that nitrate in most lakes was a mix of soil and atmospheric sources. Two samples were below 5‰ and had values within the range of soil nitrate. There were five samples that were greater than 30‰ and had isotopic values more similar to typical precipitation values. Four of these five samples were collected in August of 2012 in days following and during notable thunderstorm activity when a high proportion of precipitation would have run-off into receiving waters. The post-thunderstorm samples were higher than Sierra winter precipitation, which ranges from 25 to 35 ‰ (Sickman *et al.* 2003a) and comparable to the 71 to 78‰ annual precipitation range in the Sierra Nevada and Rocky Mountains (Homyak 2012; Nanus *et al.* 2008). Previous research at three sites in Sequoia National Park found surface water

$\delta^{18}O$ (NO_3^-) ranged from ca. 10 to 20‰ (Sickman *et al.* 2003a). Our $\delta^{18}O$ (NO_3^-) results were similar although exhibited a larger range, probably explained by the larger spatial sample. Nanus et al. (2008) conducted an extensive survey throughout the Rocky Mountains and found $\delta^{18}O$ (NO_3^-) a range from -5.7 to 21.3 ‰. The Sierra Nevada was not quite as low as the Rocky Mountains, with a lowest value of -1.51 ‰. The Sierra Nevada sites had a much higher range, although this might be a result of the timing with the 2012 thunderstorm activity. There was large range of $\delta^{15}N$ (NO_3^-) measurements in precipitation owing to variability in NO_x sources (e.g. power plants, tailpipes, lightning), atmospheric chemical reactions, and deposition type (dry or wet). For example, Sickman et al. (2003a) found more depleted $\delta^{15}N$ (NO_3^-) in surface waters relative to precipitation (i.e. snowpack). Whereas Nanus et al. found $\delta^{15}N$ (NO_3^-) in precipitation was more depleted than lake water. This makes it challenging to compare and draw conclusions using $\delta^{15}N$ (NO_3^-) results. Nitrate $\delta^{15}N$ values in precipitation typically range from to -5 to 10$^{o}/_{oo}$ and in soils from 5 to 10 ‰ (Kendall 1998). Due to the overlap with $\delta^{15}N$ (NO_3^-) values, $\delta^{18}O$ is generally a better measure of atmospheric deposition for Sierra Nevada lakes as there is more separation.

The $\delta^{18}O$ (NO_3^-) time series at Emerald Lake showed a gradual decrease in $\delta^{18}O$ (NO_3^-) (12.81 to 7.55 ‰) following snowmelt in late June/early July through early September (Figure 3.9). The $\delta^{18}O$ (NO_3^-) then spiked in mid-September following several days of precipitation including a significant event (1.73 cm) the day prior to sampling. $\delta^{15}N$ (NO_3^-) was relatively stable through the summer season until it decreased following the September precipitation events. This suggests $\delta^{15}N$ decreases following storm events,

however, we did not observe this in the storm samples from the spatial sample. In contrast to the observed changes following the September storms, we did not observe a response following a 3.81 cm precipitation event in late June. The contribution of water from the storm would be negligible compared to snowmelt runoff during this time and, therefore, the isotope ratios continued to reflect the snowmelt. Late summer and fall thunderstorms may contain more contaminants and nutrients following long periods without precipitation and effects on lake chemistry were found to be more persistent following fall storms (Clow *et al.* 2003). Runoff from the September storms would have also contained nitrogen from dry deposition that had accumulated on vegetation and bedrock surfaces throughout the summer. The last recorded precipitation prior to the September events was in late July.

Examination of the dual isotope plot and time series at Emerald Lake indicated the presence of atmospheric nitrate in Sierra Nevada lakes. However, we were unsuccessful in our attempt to use $\delta^{18}O$ (NO_3^-) and $\delta^{15}N$ (NO_3^-) to explain spatial variation of ANC and nutrient limitation across the landscape. We propose two reasons for the lack of correlation. The first, and primary, is the complexity of the nitrogen cycle leading to high spatial variability. In the case of $\delta^{18}O$ (NO_3^-) there were limited effects from the measured basin characteristics (Table 3.3) and this was consistent with results from the Rocky Mountains (Nanus *et al.* 2008). $\delta^{15}N$ (NO_3^-) correlation results indicated the measure was more affected by basin characteristics. Nitrogen, because it is often a limiting nutrient, is tightly cycled within terrestrial and aquatic ecosystems and subject to mineralization, nitrification, and biotic uptake processes (Schlesinger 1997). On the

terrestrial landscape nitrogen may be taken up and cycled by vegetation and soil microbes. Fifty to seventy percent of the nitrate from snowmelt is derived from soils and talus and undergoes microbial cycling prior to leaching into the lake ecosystem (Sickman *et al.* 2003a). Once in the lake nitrogen cycling within benthic and pelagic plankton communities may occur and alter nitrate concentrations and isotopic composition further. The second explanation we propose for the lack of correlation between $\delta^{18}O$ (NO_3^-), $\delta^{15}N$ (NO_3^-), and lake chemistry variables is the influence of storm events on, primarily, $\delta^{18}O$ (NO_3^-) and to a lesser extent, $\delta^{15}N$ (NO_3^-) as our survey and time series data indicated. We were fortunate to detect high $\delta^{18}O$ (NO_3^-) at sites where we could confirm thunderstorm activity, but this is atypical as it is difficult to monitor and account for thunderstorms due to their high spatial variability. Increased nitrate was also observed in the post-storm samples (data not shown), which could minimize the effects of storm events on the $\delta^{18}O$ (NO_3^-) and nitrate or DIN:TP relationships, if they increased proportionally.

3.5.3 Implications for Critical Loads

We investigated two indicators of atmospheric deposition in order to establish relationships between atmospheric deposition and lake chemistry variables that are indicators of acidification and eutrophication (ANC, pH, sulfate, nitrate, DIN:TP). ANC was the only chemistry variable that was correlated with atmospheric deposition. The SCP-ANC and SCP-pH relationship established an important link between deposition and acidification effects on Sierra Nevada lakes. The lack of correlation with nitrate and DIN:TP indicated it is a greater challenge to correlate atmospheric deposition to

eutrophication effects at landscape scales, likely due to the complexity of the nitrogen cycle. These results led us to conclude that, given current knowledge, acid deposition effects are a more robust approach for quantifying deposition effects for critical load development. Critical load estimates in the Rocky Mountains and northeastern United States are higher for acidification than eutrophication, underscoring a need for lower eutrophication critical load development to protect lakes (Baron *et al.* 2011). Since the Sierra Nevada is one of the most sensitive regions in the western United States with respect to acidification (Eilers *et al.* 1989) and acidification critical load estimates are quite low (0.61 to 0.76 kg N ha^{-1} yr^{-1}) (A. M. Heard unpubl.), it is possible that acidification critical loads will also be effective at protecting Sierra Nevada lakes from eutrophication. Continued regional lake monitoring will be important in assessing the effectiveness of implemented critical load policies.

Despite our concluding emphasis on acidification critical loads, our results also underscore the need for continued research on understanding the complexity of the nitrogen cycle and how nutrient deposition is affecting lake ecosystems at landscape scales. The DIN:TP results indicated a significant latitudinal difference in nutrient limitation (p=0.007) that is not explained by atmospheric deposition indicators (Table 3.3). In Yosemite, 76% of the lakes were N-limited compared to only 36% in Sequoia and Kings Canyon (Figure 3.7 and Figure 3.8). These differences suggest that Sequoia and Kings Canyon may be more sensitive to nitrogen deposition. However, we were unable to explain these differences and attribute them to atmospheric deposition. Additional research on eutrophication in Sierra Nevada lakes is needed, including

improved understanding of the temporal and spatial sensitivity of lakes to atmospheric deposition, finer-scale models of deposition in mountainous regions, synergistic effects with climate change, and development of nutrient thresholds for high-elevation lakes.

3.6 Conclusions

Our investigation of factors contributing to spatial variation in acid and nutrient affected lakes has resulted in several conclusions that inform critical load development. Sierra Nevada lakes are still affected by acid deposition and a need for stricter regulatory standards, such as a critical load approach, is needed for surface waters to fully recovery. Air patterns and deposition across the Sierra Nevada are complex. Finer-scale measurements and modeling across mountain landscapes would improve our ability to quantify effects of deposition. Lastly, quantifying the relationship between nitrogen deposition and eutrophication across complex mountain landscapes is presently challenging leading us to conclude that calculating critical loads based on acidification is a more robust approach.

3.7 Tables and Figures

Table 3.1: Summary statistics for SCPs, $\delta^{18}O$ (NO_3^-), $\delta^{15}N$ (NO_3^-), ANC, DIN:TP, and nitrate in the diatom and SIEN data sets.

	Diatom data set				SIEN data set				
	SCP (gDM^{-1})	ANC ($\mu eq\ L^{-1}$)	DIN:TP	Nitrate (μM)	$\delta^{18}O$ (‰)	$\delta^{15}N$ (‰)	ANC ($\mu eq\ L^{-1}$)	DIN:TP	Nitrate (μM)
Mean	760	75.6	3.3	1.15	14.7	-1.1	55.3	6.3	4.58
SE	156	5.1	0.68	0.269	1.6	0.4	2.3	1.5	1.00
Minimum	0	23.0	0.0	< 0.04	-1.5	-13.8	3.93	0.0	< 0.04
Maximum	5900	145	18	9.30	54.5	4	151	78	11.8
n	42	42	42	42	54	54	101	101	101

Table 3.2: Diatom data set Kendall tau correlation results for atmospheric deposition indicators, lake chemistry variables, and basin characteristics. Significant correlations (α = 0.10) are indicated by bold italics.

	Diatom Data Set					
	SCPs (*n* =42)		ANC (*n* =42)		pH (*n* =42)	
	tau	p-value	tau	p-value	tau	p-value
ANC	***-0.22***	***0.052***	-	-	***0.646***	***< 0.001***
pH	***-0.28***	***0.013***	***0.646***	***< 0.001***	-	-
Sulfate	***-0.24***	***0.031***	***0.32***	***0.003***	***0.367***	***0.001***
Nitrate	-0.11	0.307	-0.02	0.879	0.061	0.580
DIN:TP	-0.10	0.362	-0.07	0.502	-0.009	0.939
Specific Conductance	***-0.30***	***0.007***	***0.79***	***< 0.001***	***0.612***	***< 0.001***
Watershed area	-0.12	0.287	0.09	0.404	0.032	0.778
Lake area	0.05	0.677	-0.03	0.795	-0.019	0.871
Shore line length	0.03	0.784	-0.16	0.143	-0.113	0.298
Watershed area : lake area	-0.16	0.150	***0.20***	***0.067***	0.095	0.386
Shore line : lake area	-0.02	0.835	-0.09	0.429	-0.053	0.633
Elevation - mean	0.03	0.767	***0.24***	***0.028***	***0.186***	***0.087***
Slope - mean	***-0.26***	***0.021***	0.12	0.264	0.242	0.026
North aspect with slope > 30% (% area)	-0.21	0.122	-0.03	0.770	0.074	0.501
Latitude	0.17	0.122	-0.12	0.255	-0.146	0.179
Longitude	-0.17	0.122	***0.34***	***0.001***	***0.335***	***0.002***
Aspect (% area)						
0-45	-0.15	0.170	-0.07	0.523	0.041	0.712
45-90	0.02	0.855	-0.18	0.101	-0.093	0.399
90-135	0.08	0.503	-0.12	0.264	-0.048	0.664
135-180	0.17	0.127	-0.03	0.820	-0.099	0.362
180-225	0.02	0.869	0.13	0.237	0.064	0.558
225-270	-0.08	0.503	***0.25***	***0.022***	***0.214***	***0.048***
270-315	-0.14	0.207	0.14	0.182	0.039	0.729
315-360	-0.10	0.351	0.06	0.566	0.053	0.633
Non-vegetated (% area)	-0.17	0.117	-0.02	0.888	0.074	0.501
Water (% area)	0.18	0.102	***-0.24***	***0.029***	-0.137	0.209
Geology (% area)						
alluvium/mass wasting deposits/lake sediments	0.24	0.270	***-0.38***	***0.070***	-0.287	0.170
felsic intrusive	-0.06	0.612	-0.03	0.816	0.026	0.825
felsic metamorphic	0.11	0.803	-0.36	0.266	-0.278	0.348
intermediate intrusive	-0.24	0.376	-0.33	0.184	0.073	0.815
mafic intrusive	-0.31	0.433	-0.24	0.548	-0.238	0.548
neoglacial/talus/colluvium	-0.03	0.850	0.16	0.260	0.061	0.664
Pleistocene till	0.18	0.370	-0.08	0.729	-0.106	0.620

Table 3.3: SIEN data set Kendall tau correlation results for atmospheric deposition indicators, lake chemistry variables, and basin characteristics. Significant correlations (α = 0.10) are indicated by bold italics.

	SIEN Data Set					
	$\delta^{18}O$		$\delta^{15}N$		DIN:TP	
	tau	p-value	tau	p-value	tau	p-value
ANC	0.11	0.321	0.00	1.000	-0.04	0.516
pH	0.02	0.843	0.01	0.926	0.07	0.533
Sulfate	***-0.19***	***0.084***	0.06	0.600	***0.23***	***0.001***
Nitrate	-0.07	0.423	-0.11	0.255	-	-
DIN:TP	0.16	0.162	-0.14	0.220	-	-
Specific Conductance	0.09	0.441	0.01	0.935	***0.36***	***0.001***
Watershed area	-0.08	0.361	-0.07	0.447	0.04	0.665
Lake area	0.02	0.828	***-0.24***	***0.009***	0.06	0.421
Shore line length	0.01	0.883	***-0.19***	***0.038***	-0.02	0.745
Watershed area : lake area	-0.07	0.421	0.12	0.168	0.04	0.518
Shore line : lake area	0.00	0.969	***0.22***	***0.015***	0.07	0.319
Elevation - mean	-0.11	0.238	-0.10	0.264	***0.37***	***0.000***
Slope - mean	-0.11	0.218	***-0.19***	***0.032***	***0.38***	***0.000***
North aspect with slope > 30% (% area)	-0.03	0.716	***-0.18***	***0.050***	***0.21***	***0.009***
Latitude	0.04	0.641	0.11	0.232	***-0.22***	***0.007***
Longitude	-0.11	0.238	-0.09	0.322	***0.28***	***0.001***
Aspect (% area)						
0-45	0.14	0.130	***-0.24***	***0.009***	***0.25***	***0.002***
45-90	***0.16***	***0.079***	-0.04	0.650	0.13	0.105
90-135	-0.01	0.893	-0.13	0.147	-0.05	0.537
135-180	-0.05	0.596	-0.03	0.764	-0.07	0.360
180-225	-0.06	0.536	0.10	0.281	-0.02	0.797
225-270	-0.04	0.646	***0.16***	***0.074***	-0.02	0.768
270-315	0.00	0.995	0.12	0.182	-0.11	0.162
315-360	-0.09	0.335	-0.04	0.632	0.04	0.606
Non-vegetated (% area)	-0.10	0.269	***-0.17***	***0.055***	***0.41***	***0.000***
Water (% area)	0.02	0.818	***-0.22***	***0.013***	0.00	0.993
Geology (% area)						
alluvium/mass wasting deposits/lake sediments	0.10	0.522	-0.23	0.149	-0.04	0.777
felsic intrusive	-0.01	0.898	***0.15***	***0.094***	-0.07	0.338
felsic metamorphic	0.14	0.848	0.41	0.339	0.36	0.158
intermediate intrusive	0.20	0.411	-0.31	0.184	0.07	0.682
mafic intrusive	-0.26	0.454	0.04	1.000	0.06	0.820
neoglacial/talus/colluvium	0.07	0.670	-0.16	0.304	***0.20***	***0.052***
Pleistocene till	***0.31***	***0.070***	0.22	0.199	-0.04	0.768

Table 3.4: SCP-ANC Kendall tau correlation results comparing the correlation for all data to data stratified by low and high sulfate concentrations. Significant correlations (α = 0.10) are indicated by bold italics.

	SCP - All data		SCP - Sulfate < 20 μM		SCP - Sulfate > 20 μM	
	tau	p-value	tau	p-value	tau	p-value
ANC	***-0.22***	***0.052***	***-0.28***	***0.028***	-0.07	0.853

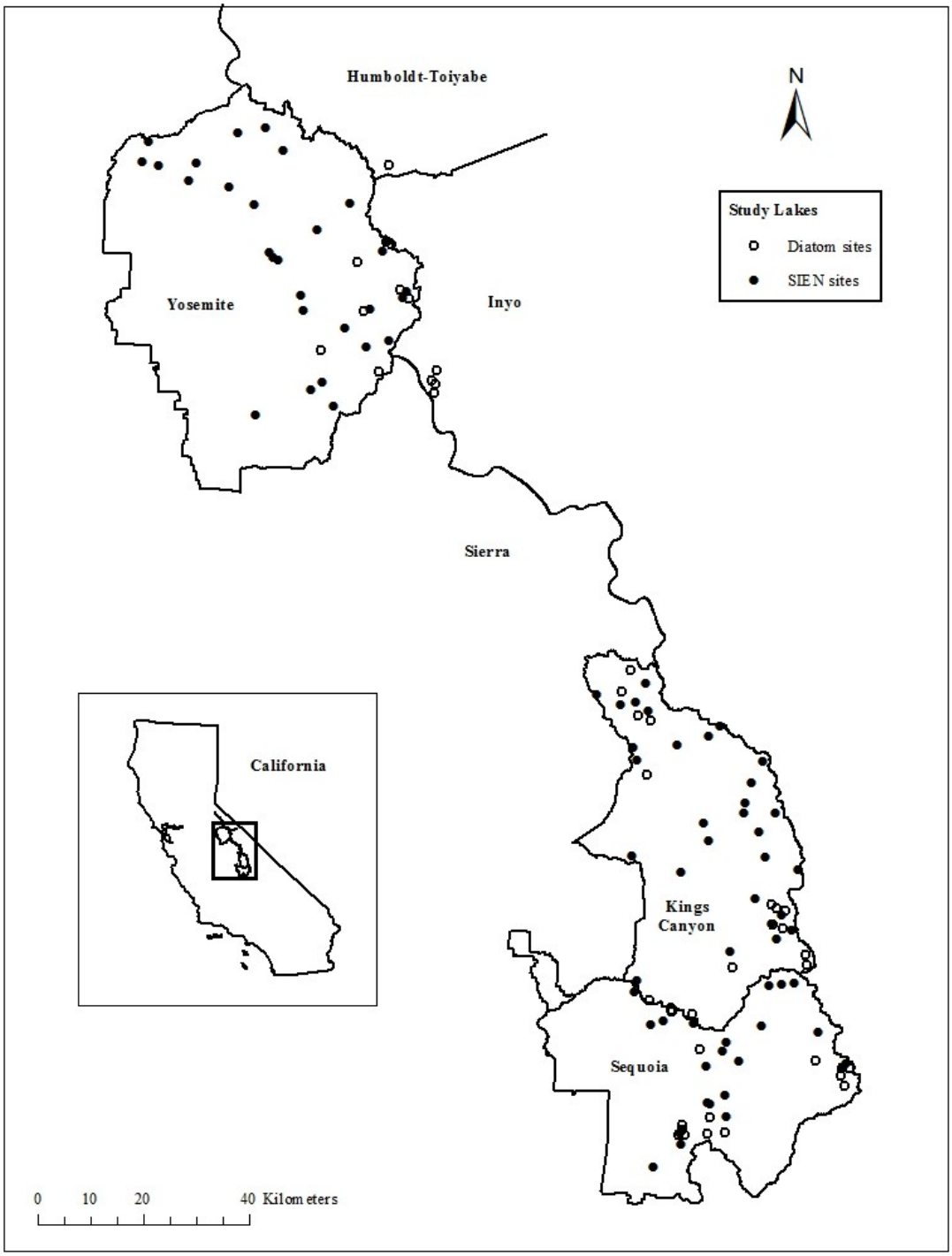

Figure 3.1: Diatom and SIEN lake sites. The study area, located in the Sierra Nevada, California, USA, includes Yosemite, Kings Canyon and Sequoia National Parks and Humboldt-Toiyabe and Inyo National Forests.

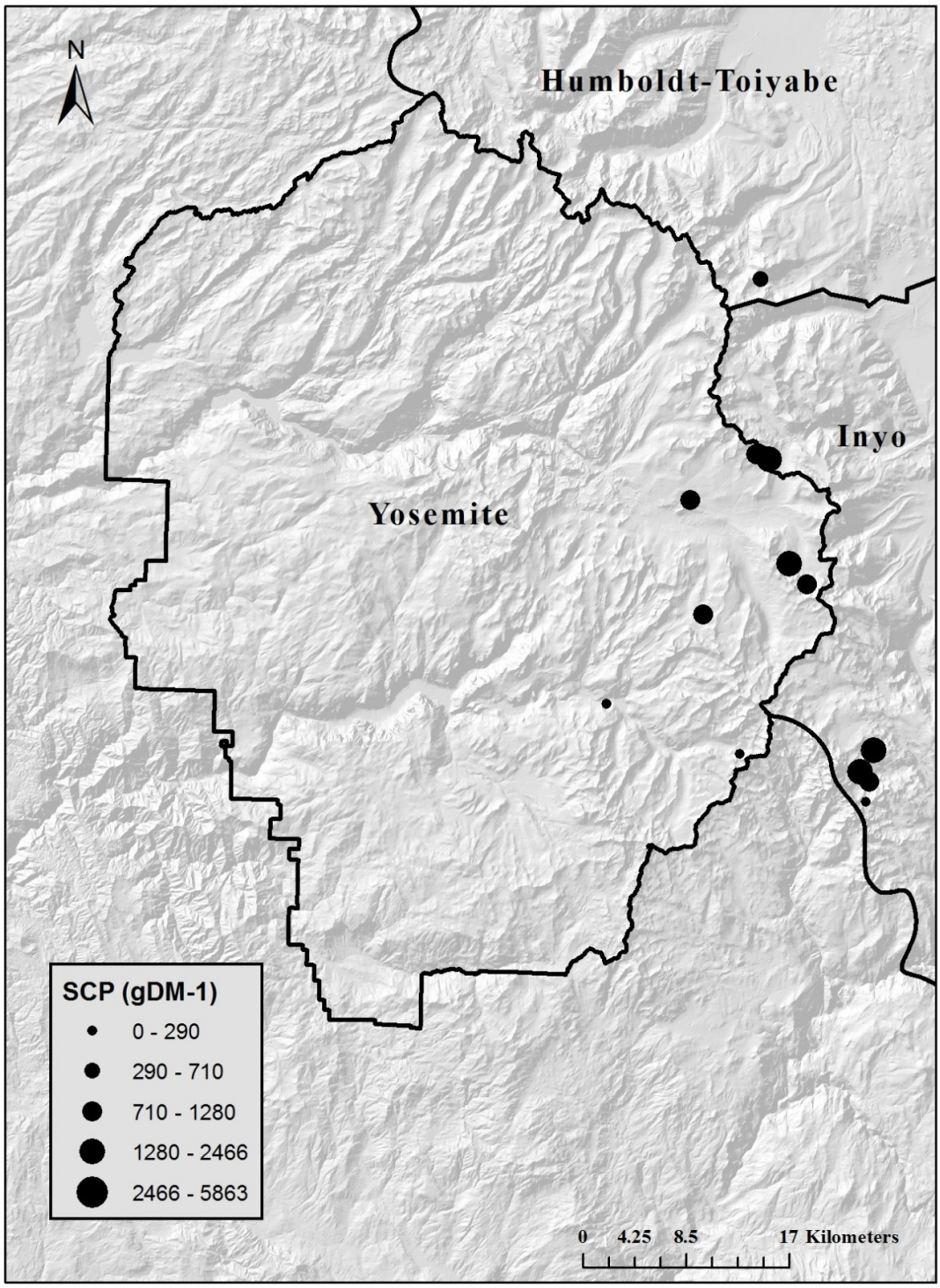

Figure 3.2: SCP concentrations in Yosemite National Park, and Humboldt-Toiyabe and Inyo National Forests.

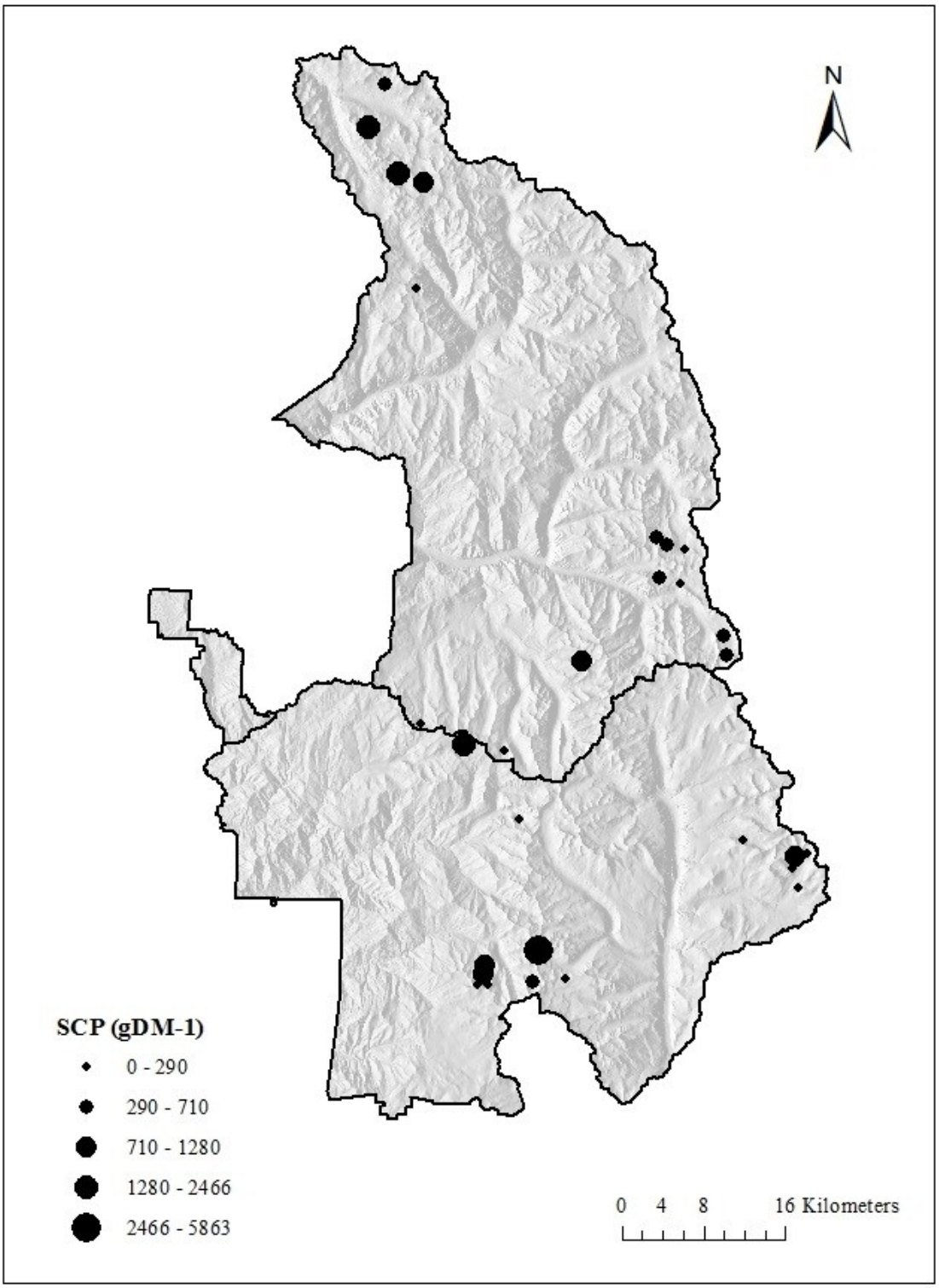

Figure 3.3: SCP concentrations in Sequoia and Kings Canyon National Parks

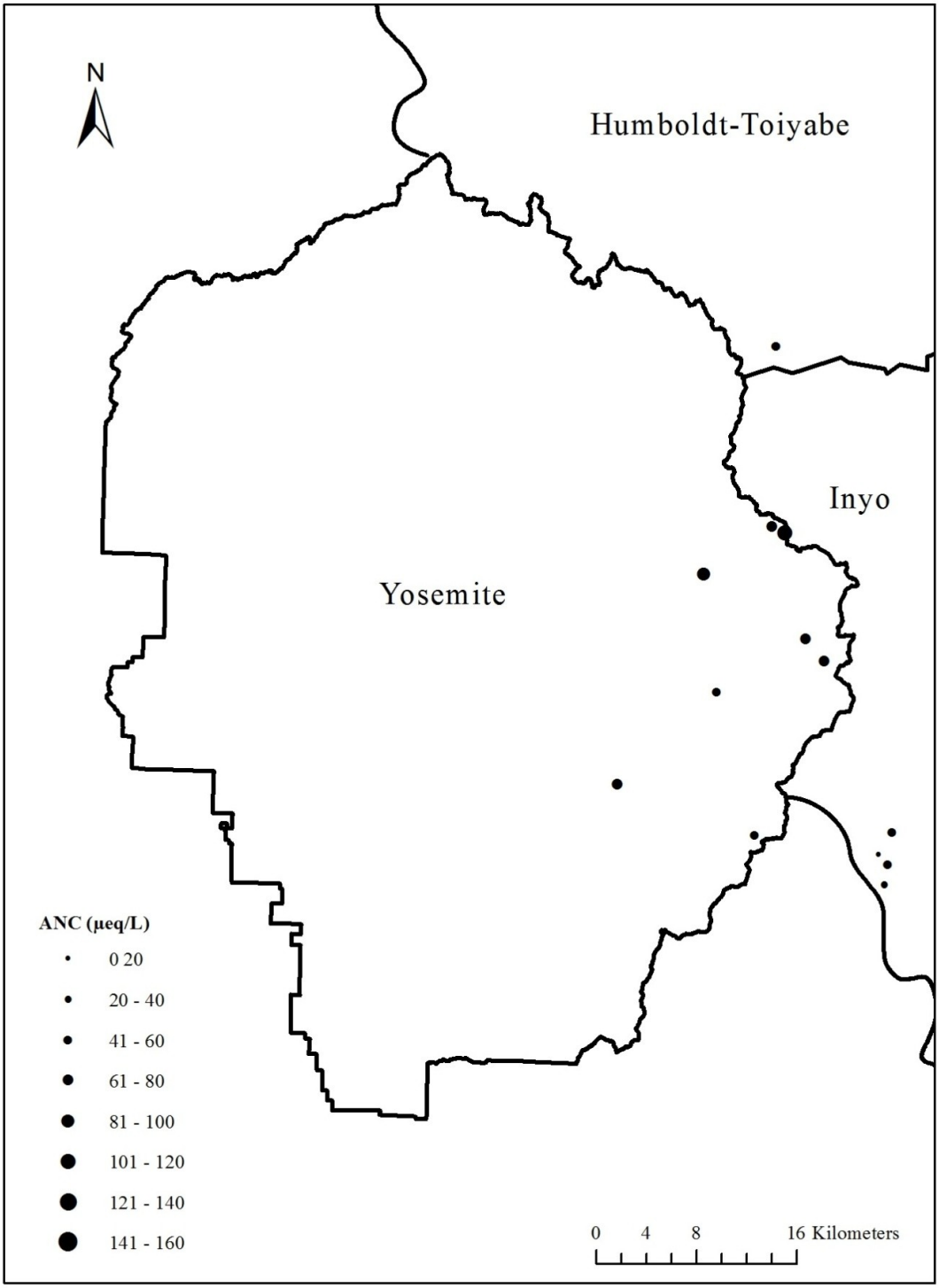

Figure 3.4: ANC concentrations in Yosemite National Park, Humboldt-Toiyabe National Forest, and Inyo National Forest (diatom data set).

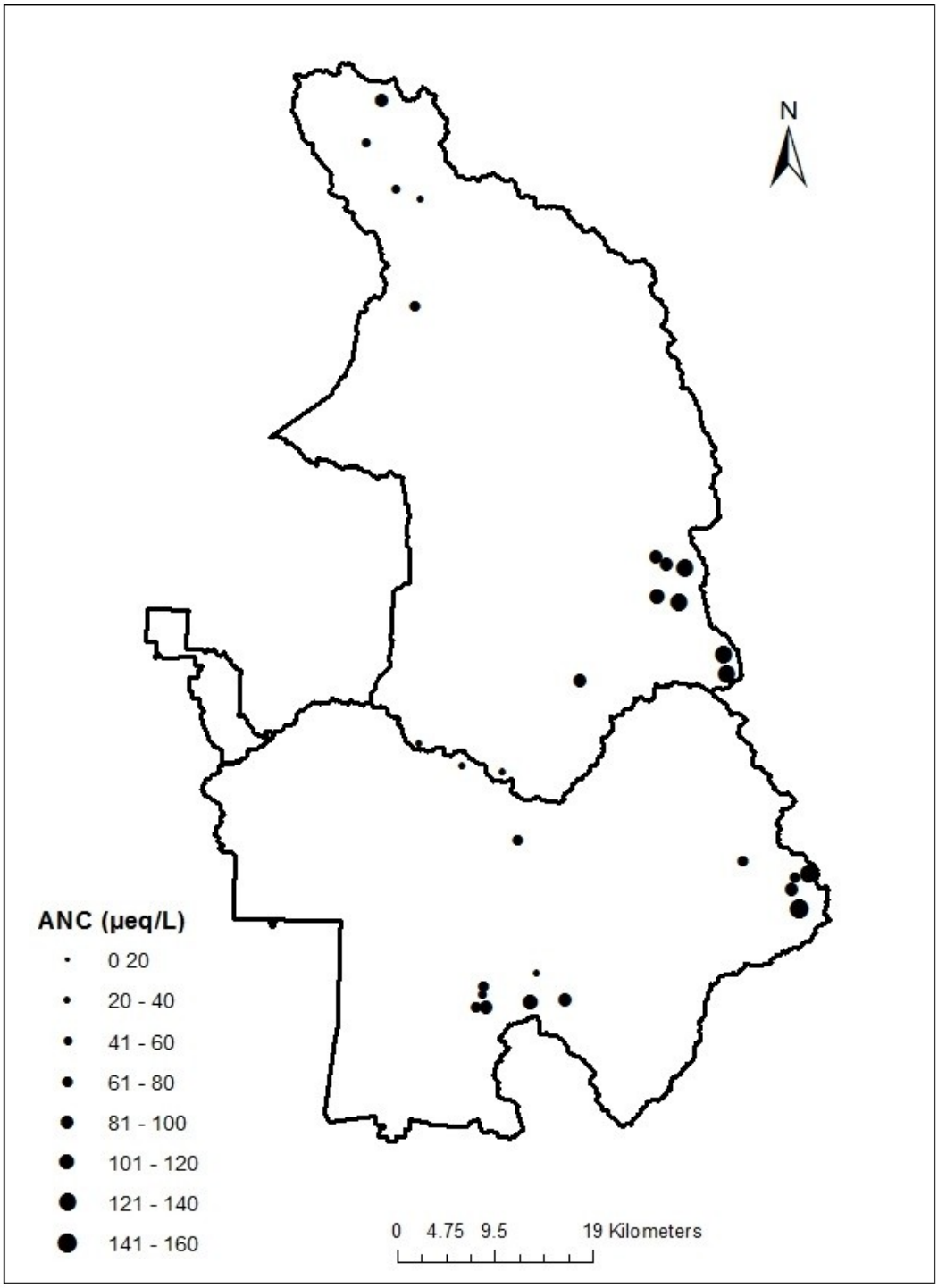

Figure 3.5: ANC concentrations in Sequoia and Kings Canyon National Parks (diatom data set).

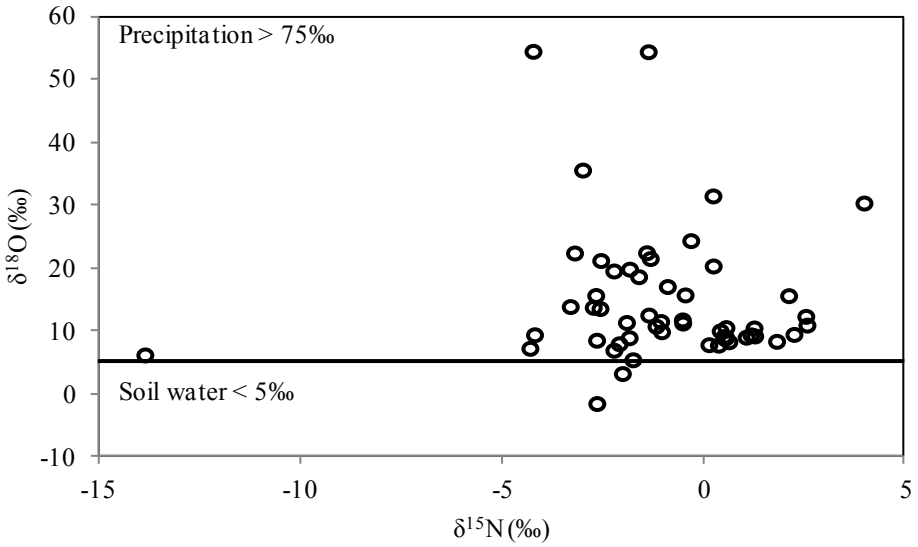

Figure 3.6: Dual isotope plot for lake water nitrate samples collected at SIEN sites. Lines and text indicate precipitation and soil water nitrate values.

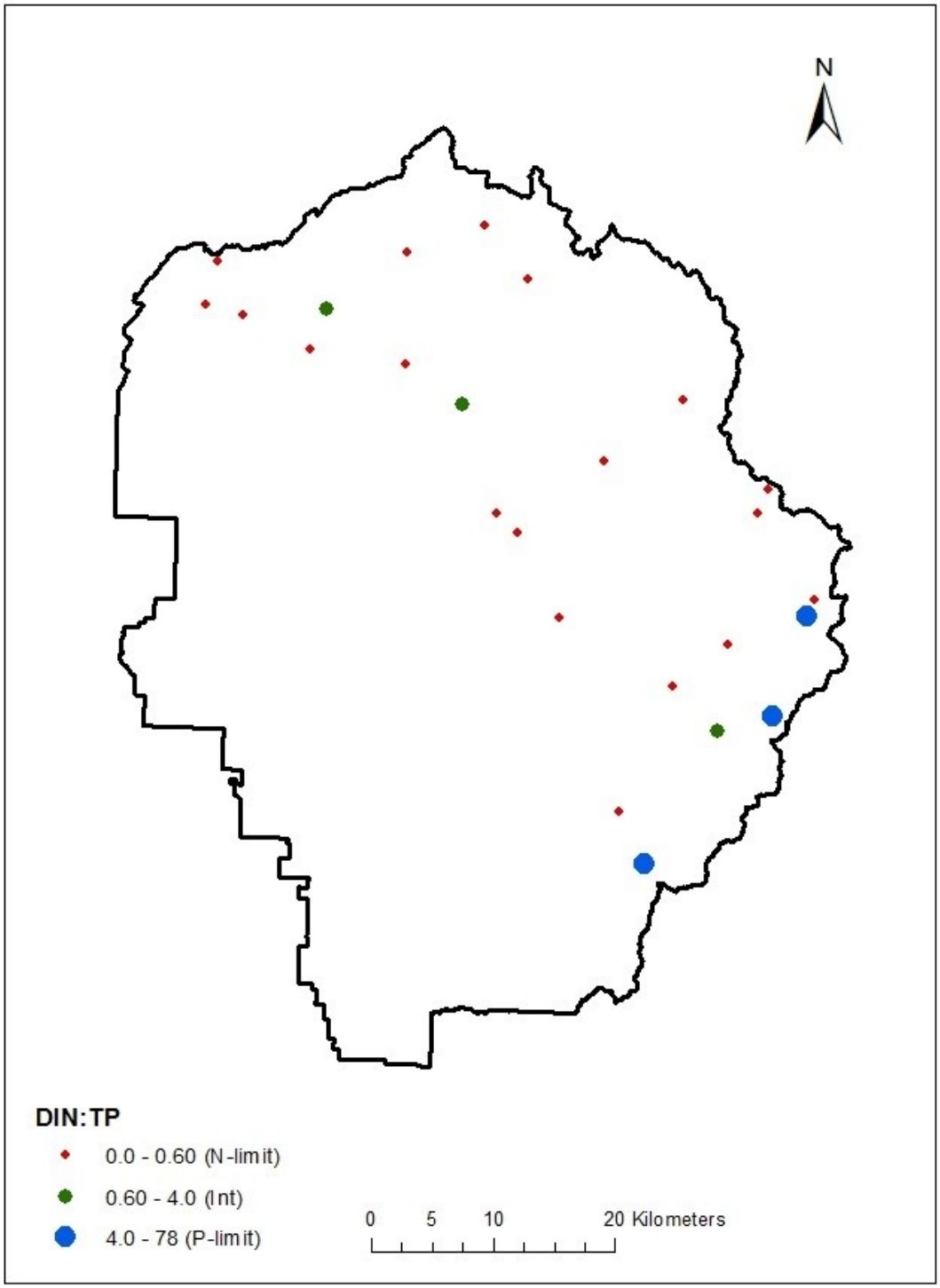

Figure 3.7: DIN:TP nutrient ratios for Yosemite National Park. 0.0 - 0.60 indicates N-limitation, 0.60 - 4.0 indicates intermediate limitation (Int), and greater than 4.0 indicates P-limitation.

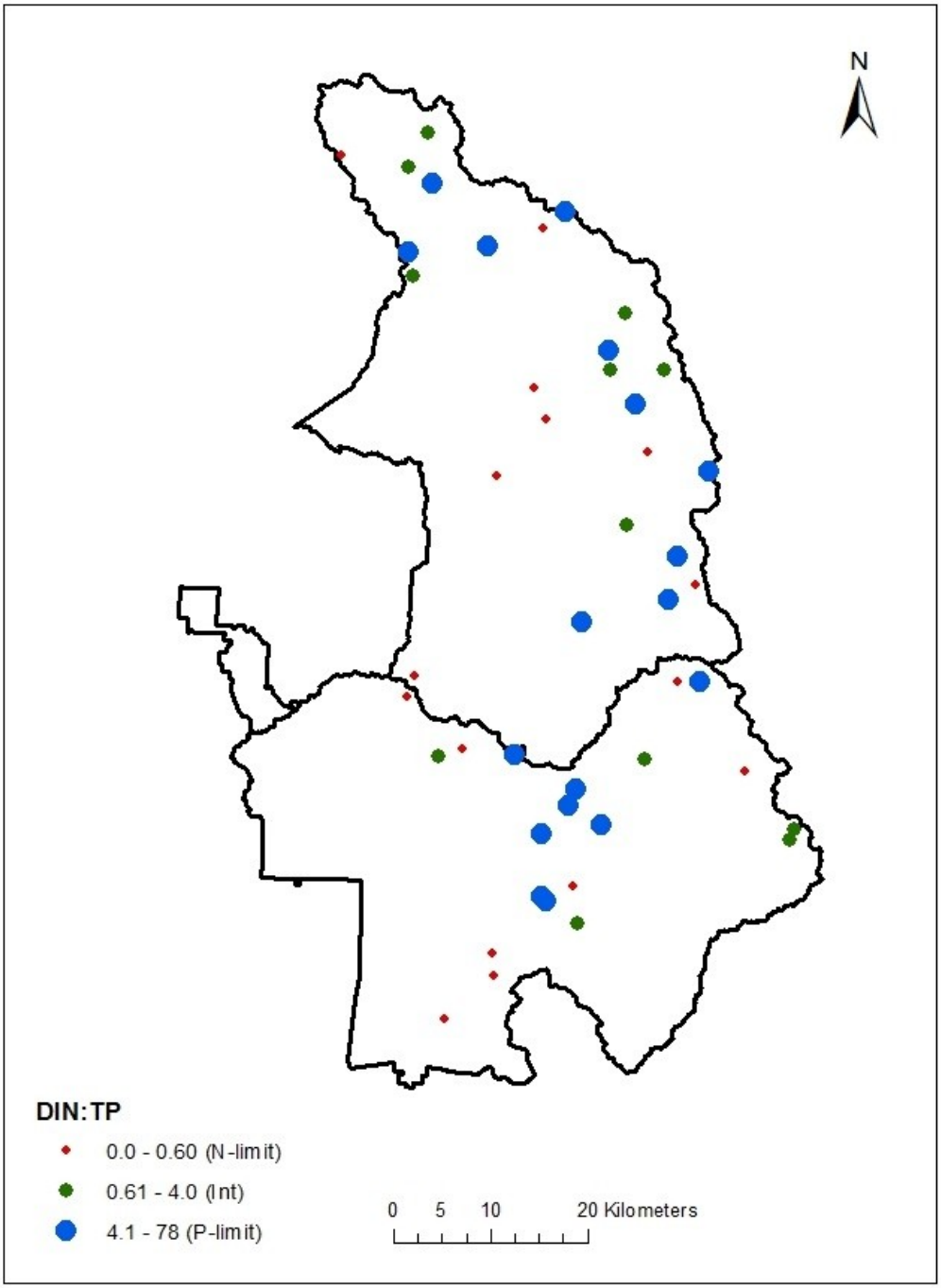

Figure 3.8: DIN:TP nutrient ratios for Yosemite National Park. 0.0 - 0.60 indicates N-limitation, 0.60 - 4.0 indicates intermediate limitation (Int), and greater than 4.0 indicates P-limitation.

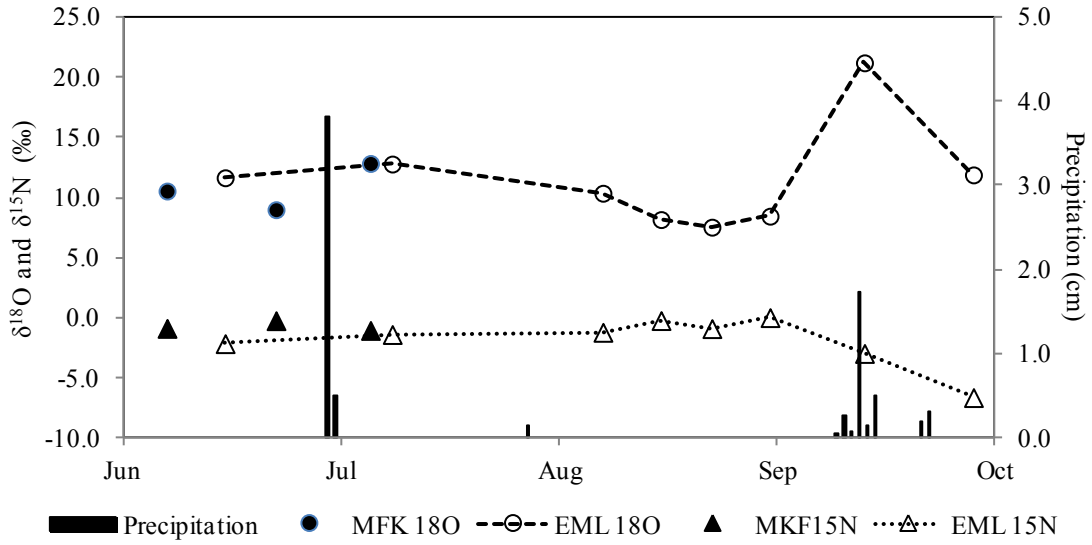

Figure 3.9: $\delta^{18}O$ (NO_3^-) and $\delta^{15}N$ (NO_3^-) time series during the summer and fall of 2011 at Emerald Lake (EML) and Marble Fork of the Kaweah (MFK), just downstream of EML. Precipitation data are from the Lodgepole meteorological station.

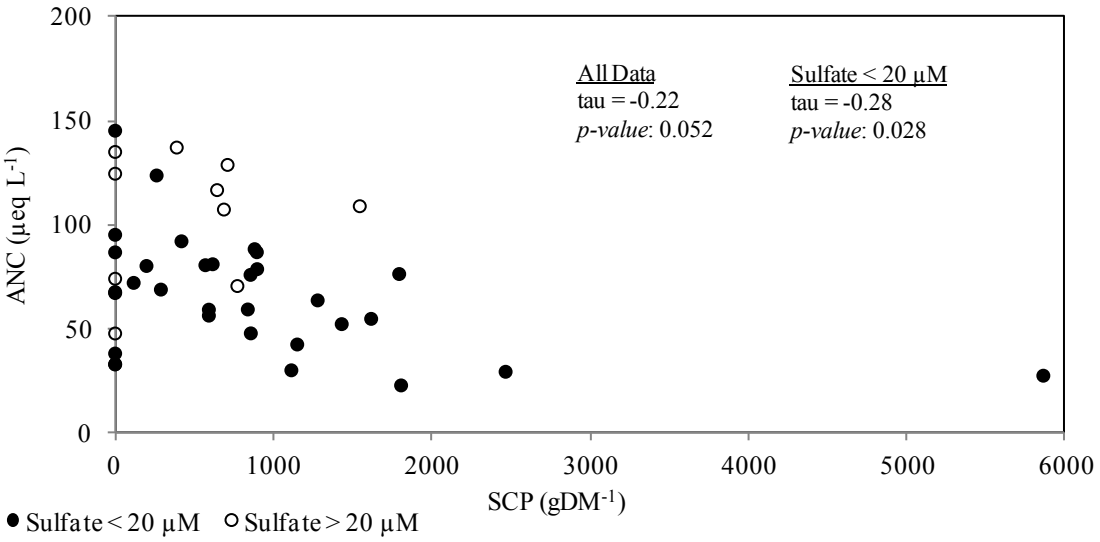

Figure 3.10: ANC vs. SCP concentration for study region. Correlation results are presented for all lakes (open and closed circles) and for lakes with sulfate less than 20 µM (closed circles).

Chapter 4: Nutrient Criteria Development and Application to Sierra Nevada Lakes

4.1 Abstract

Increased nitrogen (N) and phosphorous (P) inputs to oligotrophic high-elevation lakes are contributing to long-term eutrophication, changes in nutrient cycles, and shifts in phytoplankton communities. Present water quality standards do not adequately protect sensitive mountain lake ecosystems from atmospheric deposition. The development of quantitative nutrient criteria based on measurable ecological effects specific to high-elevation lakes is an important step in long-term protection of these ecosystems. We conducted in situ bioassay experiments and modeled the response of phytoplankton to nutrient additions using algal growth models with the purpose of developing nutrient criteria. Phytoplankton responded to nutrient additions (N and N + P) in 5 out of 7 of the experiments conducted in N-limited lakes and to P additions in one P-limited lake experiment. Phytoplankton in the P-limited lake did not respond to N additions. Results were modeled using Michaelis-Menten, Monod, and four parameter logistics function dose response curves and used to calculate effective doses for phytoplankton growth (i.e. nutrient criteria). The 10, 50, and 90% low range effective dose estimates for nitrate were 0.33, 1.0, and 3.1 μM, respectively and the 10, 50, and 90% high range effective dose estimates for nitrate were 0.89, 4.0, and 18 μM, respectively. The 10, 50, and 90% effective doses for phosphate ranged from 0.03 - 0.45, 0.24 - 1.1, and 2.0 - 2.5 μM phosphate, respectively. We compared high and low estimates of nitrogen criteria to

nitrate survey data to assess the status of Sierra Nevada lakes. Survey data were collected from 75 lakes from 2008-2011. Mean nitrate concentration was 4.58 µM and ranged from less than 0.04 to 11.8 µM. The 10% effective dose was exceeded by 28% of lakes using the high nutrient criteria and 37 % using the low nutrient criteria. The 50% effective dose was exceeded by 18% of lakes (high criteria) and 29% (low criteria). The 90 % effective dose was exceeded by 0.0 % of lakes (high criteria) and 21% (low criteria).

4.2 Introduction

Atmospheric nitrogen (N) deposition is altering biogeochemical cycles and ecological processes in Sierra Nevada mountain ecosystems (Fenn *et al.* 2003). The Sierra Nevada Mountains are exposed to air pollution that originates from agricultural, urban, and industrial sources in California's Central Valley, the San Francisco Bay Area, and as far away as Asia (Bytnerowicz *et al.* 2002; Vicars and Sickman 2011). Nutrients are transported by air currents into the mountains where they are deposited as wet and dry deposition. High elevation lakes in the Sierra Nevada are particularly sensitive to change from atmospheric deposition because they are oligotrophic, have a low buffering capacity and occur in predominantly granitic basins with relatively little soil and vegetation (Clow *et al.* 2010).

In contrast to the traditionally accepted paradigm that phosphorus (P) is the limiting nutrient in freshwater lake ecosystems (Schindler 1974), there is increasing evidence that many oligotrophic lakes in the northern hemisphere were once nitrogen limited and shifted to phosphorus limitation as a result of increased anthropogenic N

deposition (Bergström and Jansson 2006; Goldman 1988). A high proportion of lakes in the Sierra Nevada are presently N-limited, although nutrient limitation varies across the landscape (Chapter 3, Figure 3.7 and Figure 3.8). Therefore, increased nitrogen inputs will continue to have regional scale effects on phytoplankton growth and lake productivity.

Increased nitrogen and phosphorous inputs to oligotrophic high-elevation lakes are contributing to long-term eutrophication, changes in nutrient cycles, and shifts in phytoplankton communities (Elser *et al.* 2009a; Goldman *et al.* 1993; Nydick *et al.* 2004; Sickman *et al.* 2003b). Phytoplankton blooms reduce lake clarity and threaten the exceptionally clear blue lakes that define the high-Sierra landscape (Goldman 1988). Cascading effects of N enrichment through the food web may be observed as it is hypothesized that phytoplankton species that thrive in P-limited lakes are poorer food quality for zooplankton (Elser *et al.* 2009a). Nydick et al. (2004) observed a decrease in zooplankton species following N enrichment, although further research is needed.

Land management agencies are tasked with the job of protecting these sensitive and highly valued ecosystems. This is especially challenging in the 21st century when stressors of high concern (i.e. air pollution and climate change) often originate outside of protected boundaries and affect resources at landscape scales. The establishment of water quality standards based on measurable ecological effects specific to these ecosystems is an important step in their long-term protection. Nutrient water quality criteria may be compared directly to water survey and monitoring data and may be used to develop critical loads (Nanus *et al.* 2012).

Presently, the criteria available to compare Sierra Nevada waters against are state water quality standards. The study region is under the jurisdiction of Regional Water Quality Control Boards 5 (Central Valley) and 6 (Lahontan). Standards are described in Water Quality Control Plans, which have been developed for the Tulare Lake Basin, Sacramento-San Joaquin River Basins, and Lahontan Region: North and South Basins. Current nutrient guidance is generally the same across the basins and falls under the objective for 'Biostimulatory Substances' (California Regional Water Quality Control Board - Central Valley Region 1995; 1998; California Regional Water Quality Control Board - Lahontan Region 1994). The concentrations of nitrogen and phosphorus that cause impairment or ecological change vary widely, much more so than other water quality criteria (e.g., dissolved oxygen, metals). This poses a challenge for developing numeric criteria for large regions. The Environmental Protection Agency (EPA), in the last decade, has been providing guidance to states to develop numeric criteria, given these challenges (Gibson *et al.* 2000). The State of California is in the process of evaluating several approaches with the goal of establishing numeric nutrient objectives for inland surface waters (State Water Resources Control Board and California Environmental Protection Agency 2011). The State's recommended approach is using nutrient numeric endpoints (NNE), which incorporates chemical and biological indicators and is based on the ecological response of a waterbody to nutrient inputs (Creager *et al.* 2006). Current and historic Sierra Nevada lake monitoring programs and periodic surveys are focused on water chemistry indicators and lack biological response data (Berg 2006; Eilers *et al.* 1989; Heard *et al.* 2012), therefore, nutrient concentration based criteria are of benefit to

these programs and land managers. In addition, the State's efforts are focused on developing criteria linked to beneficial uses and not focused on ecological change specific to Sierra Nevada lakes. There is a need for quantitative nutrient criteria specific to Sierra Nevada lake ecosystems (Creager *et al.* 2006).

The purpose of this study was to develop nutrient criteria (phosphorus and nitrogen) for high-elevation lakes in the Sierra Nevada and apply these criteria to lake chemistry survey data. The comparison to survey data of potentially nutrient-affected lakes allowed us to assess regional effects of atmospheric deposition. Sierra Nevada land managers will continue to use the criteria to evaluate lake ecosystem status and trends as part of ongoing monitoring programs.

One approach for developing criteria are bioassay experiments where the response of phytoplankton is measured across a gradient of nutrient concentrations. There are several algal growth models that may be used to model the response and calculate criteria. Michaelis-Menten (M-M) was the first model used to describe algal nutrient uptake (Dugdale 1967):

$$V = V_{max} * (S/(K_s+S)$$

where V = uptake, V_{max} = maximum uptake, S = substrate (or nutrient) concentration, and K_s = concentration that yields half the maximum rate. Prior to its use in algal ecology, M-M was developed to describe enzyme catalyzed reactions, specifically relating the reaction rate to the concentration of the substrate. The curve is a rectangular hyperbola function.

The M-M model works well for nutrient uptake, but not as well for growth because uptake and growth in algae are often not tightly coupled. Algae can rapidly take up and store nutrients more rapidly than they deploy them. The Monod equation was proposed to better model algal growth relative to extracellular nutrient concentrations (Monod 1950). The mathematical expression and curve shape are analogous to M-M:

$$\mu = \mu_{max} * (S/(K_{\mu}+S)$$

where μ = specific growth rate, μ_{max} = max specific growth rate, S= substrate (or nutrient) concentration, and K_{μ} = ½ saturation concentration for growth limiting nutrient.

In pharmokinetics and ecotoxicology, dose response curves are a widely accepted approach to modeling Michaelis-Menten type relationships (Bindslev 2008; Ritz 2010). The advantage of dose response models is the ability to calculate effective doses (i.e. criteria), especially in low concentration ranges. Dose response curves, although not commonly used in algal studies, are based on the traditional Michaelis-Menten (M-M) and Monod models. Dose response curves are modeled using a 4-parameter logistics function:

$$f(x) = c + [(d-c)/(1+exp^{(b*(Ln\ x-Ln\ e)})]$$

where b is the relative slope around e, c is the lower response limit, d is the upper response limit, and e is the 50% effective dose (ED50) – the dose producing a response between c and d. The result is a sigmoidal curve that is statistically easier to analyze as opposed to the square hyperbolic curve. The ED50, e, is related to K_s and K_{μ} in M-M and Monod equations and the upper response limit, d, is related to V_{max} and μ_{max}.

Effective doses can be calculated from the curve (e.g., 10, 50, 90% doses). These doses can be used to characterize the biological response in several ways: 1) they indicate the initial threshold response level (10% dose), 2) they indicate the level where rapid changes are likely to occur (50% dose) and 3) they determine the saturating level of nutrients (90% dose). Albertin (2009) and Pinowska et al. (2007) used this approach to determine effective doses for *Lyngbya wollei*, a macroalgae, in Florida springs. Their results were used to by the state of Florida to establish nutrient criteria for *Lyngbya wollei*.

The objectives of this study were to 1) conduct in situ bioassay experiments and model the response of phytoplankton to nutrient additions using algal growth models (Michaelis-Menten, Monod, and dose response curves), 2) use dose response curves to calculate the 10, 50 and 90% effective doses for nitrogen and phosphorus, 3) assess the status of Sierra Nevada lakes by conducting a spatially extensive lake water chemistry survey and calculating the proportion of lakes that exceed the 10, 50 and 90% effective doses for nitrogen. Our focus was on N enrichment experiments in N-limited lakes. However, we conducted one experiment in a P-limited lake to test if N additions will elicit a growth response under P-limitation and to obtain initial criteria estimates for P.

4.3 Methods

We conducted bioassay experiments using 200-L limnocorrals and 10-L cubitainers. The limnocorral experiments were conducted in July, August, and September

of 2009. Results were used to develop the experimental design of the cubitainer experiments, which were conducted in September 2011.

4.3.1 Limnocorral Experiments

4.3.1.1 Site Descriptions

The study sites are two sub-alpine lakes located in the Sierra Nevada, California, United States of America (Figure 4.1). Moat Lake (elevation 3224 m) is a N-limited lake located on the eastern slope of the Sierra Nevada 12.5 km west-northwest of Mono Lake on Toiyabe National Forest. The lake has a maximum depth of 7 m, lake surface area of 2.8 ha, and watershed area of 59.1 ha. A majority of the watershed is comprised of the western flank of Dunderberg Peak (elevation 3772 m), a rock and scree-covered slope with a mean angle of 35°. The bedrock geology of the watershed is dominated by metasedimentary rocks including quartzite and argillite. Thirteen percent of the watershed is vegetated. Hamilton Lake (elevation 2510 m) is a P-limited lake located on the western slope of the Sierra Nevada in Sequoia National Park. Hamilton Lake has a maximum depth of 29 m, lake surface area of 16 ha, and watershed area of 540 ha. The bedrock geology of the watershed is dominated by granite and diorite. Twenty-nine percent of the watershed is vegetated.

4.3.1.2 Experimental Design

The nutrient additions were conducted in situ at Moat and Hamilton Lakes using limnocorrals, constructed using polyethylene bags that were pulled over a PVC pipe skeleton to give them structure in the water. Sixteen corrals were deployed at each lake

and each filled with approximately 200 L of lake water. Once the corrals were filled, the water inside was not permitted to mix with lake water. A gradient of nutrient concentrations (N or P, depending on the experiment) were added to 14 of the corrals. Two corrals were controls.

The experiment was conducted twice at each site (Table 4.1). At Moat Lake, nitrogen (as KNO_3 and $NaNO_3$), the limiting nutrient, was added during both experiments. At Hamilton Lake, phosphorus (as K_2HPO_4), the limiting nutrient, was added during the first experiment. During the second experiment at Hamilton, nitrogen, the non-limiting nutrient was added. The number of days the experiments were run varied and ranged from 13 to 24 days. The nutrient gradient ranged from 0-35 µmol/L and 0-50 µmol/L for N and 0-10 µmol/L for P.

Samples were collected from each corral and the lake immediately following nutrient additions to obtain the initial spiked concentrations and background phytoplankton levels. The corrals and lakes were then sampled approximately every seven days. Samples were field filtered and then analyzed in the lab for nitrate (EPA Method 300.1), phosphate (EPA Method 365.5), chlorophyll a (fluorometric determination (Wetzel and Likens 2000)) , particulate N and carbon (C) (EPA Method 440.0), particulate P (Valderrama (1981) followed by EPA Method 365.5), and sodium (Na^+) and potassium (K^+) (EPA Method 200.7).

4.3.2 Cubitainer Experiments

4.3.2.1 Site Descriptions

Cubitainer experiments were conducted at Moat Lake and three additional N-limited, sub-alpine, lakes located on the western slope of Sequoia National Park (Figure 4.1). Emerald Lake (elevation 2800 m) has a maximum depth of 10 m, lake surface area of 2.7 ha, and watershed area of 120 ha. The bedrock geology of the watershed is dominated by granite and granodiorite. Less than 10% of the watershed is vegetated. Aster Lake (elevation 2774 m) has a maximum depth of 8 m, lake surface area of 1.6 ha, and watershed area of 177 ha. The bedrock geology of the watershed is dominated by granodiorite and granite. Forty-five percent of the watershed is vegetated. Topaz Lake (elevation 3219 m) has a maximum depth of 5 m, lake surface area of 5 ha, and watershed area of 152 ha. The bedrock geology of the watershed is dominated by granodiorite. Thirty percent of the watershed is vegetated.

4.3.2.2 Experimental Design

The cubitainer experiments were also conducted in situ, but at a smaller scale (i.e. 10 L mesocosms instead of 200 L). We deployed 16 10-liter cubitainers for each experiment, consistent with the limnocorral design. The cubitainers were contained in 1.5 x 1.5 m PVC corrals fitted with floatation devices that were deployed onto the lake. Mesh screening, used to filter UV light, covered the corrals.

Cubitainers were filled with lake water that was filtered through a 64 micron net to exclude large grazers. At Emerald, Aster, and Topaz, nitrogen concentration gradients, between 0 and ~ 15 μM, were added to 14 of the corrals and two were left as controls

(Table 4.1). Two experiments, Moat and Emerald-P, received both N and P additions. The same N gradient was added as in the other experiments and in addition, P was added at a constant level (1.5 μM) to all cubitainers so the experiment did not quickly become P limited. Experiments were run for seven days. Water samples were collected from each cubitainer and the lake immediately following nutrient additions to obtain the initial spiked concentrations. Chlorophyll a was measured in situ using a Turner Designs' CYCLOPS-7 Submersible Fluorometer to determine the initial phytoplankton levels. The cubitainers and lake were sampled approximately every other day for chlorophyll a. Water and particulate fraction samples were collected from each cubitainer at the end of the experiment. Samples were analyzed for nitrate, particulate N, C and P, and total dissolved phosphorus (TDP) using the methods described in section 4.3.1.2. The fluorometer was calibrated against extractable chlorophyll a samples which were analyzed using methods described in Wetzel and Likens (2000).

4.3.3 Survey Data

4.3.3.1 Site Descriptions

The study area encompasses Yosemite, Sequoia, and Kings Canyon National Parks (Figure 4.1). Yosemite and Sequoia and Kings Canyon contain over 1,200 lakes, most occurring at higher elevations (above 2500 m). The average lake area is between 5 and 6 hectares and lake depth ranges from less than 2 m to well over 30 m. Samples were collected at 75 lakes across the parks (Figure 4.1).

4.3.3.2 Sample Design

Nitrate survey data were collected as part of the National Park Service's lake

monitoring program (Heard *et al.* 2012). The lakes survey membership design is a generalized random tessellation stratified (GRTS) design that incorporates variable probability sampling. The GRTS design employs a systematic sampling approach along a randomly ordered sequence of location addresses to obtain a spatially balanced probability sample (Stevens and Olsen 2003; 2004). The temporal sampling structure is a serial augmented panel design where sites are visited annually (n=8) and on an alternating 4-year schedule (n=17 per year).

Water samples were collected as grab samples at the lake outflows in August and September of 2008 to 2011. Samples were field filtered into 125-ml HDPE bottles using 1.0 µm polycarbonate filters and analyzed for nitrate in the laboratory on a Dionex ion chromatograph using EPA Method 300.1.

4.3.4 Data Analysis

We analyzed sodium and potassium concentrations (the cations that were added with the nitrate and phosphate additions) to determine if any of the limnocorrals leaked during the experiment. Cubitainers were visually inspected for leaks. Any mesocosms with significant leakage were excluded from the analysis.

We modeled the relationship between nutrient concentrations and phytoplankton response using M-M, Monod, and four-parameter logistics function dose-response curves. Maximum uptake rates (V_{max}), growth rates (μ_{max}), and ½ saturation concentrations ($K_{s/\mu}$) were calculated for M-M and Monod models and 10, 50, and 90% effective doses were calculated for the logistics models. Modeling was conducted using the 'drc' add-on package (Ritz and Streibig 2005) in the R environment (R Development

Core Team 2011). The initial nitrate and phosphate concentrations measured in the mesocosms were used as the nutrient concentration gradient. In the cubitainer experiments, if an initial concentration was below detectable levels we used the calculated concentration.

Chlorophyll a, particulate C, particulate N, and particulate P concentrations, and uptake of nitrate and phosphate from the limnocorral experiments were analyzed using the logistics function to determine the best measure of phytoplankton growth. We assessed the results of these different measures to determine which were best suited for the dose-response analysis. We also assessed the most suitable time period. Assessments were determined by examining the fit of the data to the logistics function (i.e. a low residual error for the function and low error for the effective dose estimates), assessing if the effective dose estimates were realistic, and visual examination of the modeled dose response curves. The variable(s) and time period that best fit the models were used in the cubitainer experiments and to for the final nutrient criteria calculations.

In order to obtain final nutrient criteria estimates that can be applied to survey data, the effective dose results were grouped by high and low results. Results in each group were averaged to obtain a final range of low and high nutrient criteria estimates.

Descriptive statistics were computed for the nitrate survey data using methods described in Heard et al. (2012) so we only briefly describe them here. The mean is calculated as a Horvitz-Thompson estimate (Horvitz and Thompson 1952) and the variance of the mean is calculated using the GRTS neighborhood variance estimator (Stevens and Olsen 2003; 2004). Inclusion probabilities were incorporated into the

estimates in order to account for the panel structure where sites were sampled at different time scales (annually and one time). Censored data were accounted for using the robust maximum likelihood estimation (MLE) approach recommended by Helsel (2005). The 10, 50, and 90% effective doses, high and low estimates, were applied to the survey data to determine the proportion of lakes exceeding criteria in Sequoia, Kings, Canyon, and Yosemite National Parks. To estimate the proportion of the population exceeding a threshold *c*, for variable Y (e.g., nitrate) we computed an indicator variable X_c , such that:

$$X_c = \begin{cases} 1, & \text{if } Y > c \\ 0, & \text{if } Y \leq c \end{cases}.$$

The proportion was estimated as the mean and standard error (SE) of X_c using the GRTS estimator (Stevens and Olsen 2003; 2004). Analyses were conducted in the R workspace (R Development Core Team 2011).

4.4 Results

4.4.1 Chemistry and Chlorophyll a

Nitrate and phosphate results indicated the desired nutrient gradients were achieved for each experiment (Figure 4.2 and Figure 4.3). Concentration gradients for nitrogen in the limnocorral experiments ranged from below detection to 38 µM for Moat-July, from 0 to 48 µM for Moat-September, and from 10 to 58 µM for Hamilton-September. The phosphorus gradient in the Hamilton-July experiment ranged from 0.03 to 6.68 µM. Concentration gradients for nitrogen in the cubitainer experiments ranged from 0 to 13 µM for Moat, 0 to 16 µM for Topaz, 0 to 12 µM for Emerald-P, 0 to 13 µM

for Emerald, and 0 to 13 μM for Topaz. A decline in nitrate, and phosphate for Hamilton-July, was observed over the experiment time period at the four limnocorral sites. A similar trend was observed in the cubitainer experiments at Moat and Emerald-P. Little or no change in nitrate over the seven day experiments was observed at Topaz, Emerald, and Aster.

Sodium and potassium results indicated that two limnocorral bags may have leaked (Figure 4.4). We excluded corrals 7 and 13 in the Hamilton-September experiment from the analysis. The large decrease in potassium in corral 7 was consistent with the large decrease in nitrate and suggested that this bag mixed with lake water. In corral 13 the initial nitrate and potassium concentrations were inconsistent, potassium was higher than nitrate and higher than the expected spiked concentration. No leaks were observed in the cubitainers.

Chlorophyll a concentrations increased in the July and September Moat experiments and the Hamilton-July experiment, where the inferred limiting nutrient was added (Figure 4.5). There was no response in the Hamilton nitrogen addition experiment in September, when the inferred non-limiting nutrient was added. The first sampling period on ~ day seven yielded the best results for the N addition experiments (i.e. a chlorophyll a gradient that follows the nutrient gradient) therefore, we report primarily on day seven results. Chlorophyll a concentrations at day 14 or later became more variable and less consistent with the initial nutrient gradient. The second sampling period, day 14, yielded the best results for the P addition experiment at Hamilton. On day seven in the Moat-July experiment, chlorophyll a concentrations increased from less than 2.0 μg L^{-1} in

the lake and controls to a maximum concentration of 5.4 μg L^{-1} in the 13.4 μM corral. Chlorophyll a then drops to 3.5 – 4.4 μg L^{-1} in the higher concentration corrals. In the Moat-September experiment overall chlorophyll a concentrations were lower, ranging from less than 0.5 to 2.1 μg L^{-1}, however, a gradient was still observed. On day 14 in the Hamilton-July experiment concentrations increased from less than 0.1 to a maximum of 5.4 μg L^{-1} in the 5.1 μM limnocorral. In the Hamilton-September experiment chlorophyll a concentrations were relatively consistent across the gradient. In the cubitainer experiments, increasing gradients of chlorophyll a were observed in Moat, Topaz, and Emerald-P (Figure 4.6). Moat increased from less than 3 to 4.6 μg L^{-1}, although concentrations varied across the gradient. Chlorophyll a at Topaz increased from 0.2 to 1.1 μg L^{-1} and at Emerald P increased from 0.58 to 1.1 μg L^{-1}. Emerald and Aster had little variation in chlorophyll a along the gradient, although a subtle bi-model response was observed (Figure 4.6). Emerald chlorophyll a concentrations ranged from 0.48 to 0.78 μg L^{-1} and Aster ranged from 0.16 to 0.23 μg L^{-1}.

Phosphate concentrations showed little variation across the nitrogen gradient in the Moat-July, Moat-September, and Hamilton-September experiments (Figure 4.7). Phosphate concentrations also changed little from days 1 to 14, although some increases were observed in the September experiments. In the Hamilton-July experiment trends in nitrate were observed across the gradient on days seven and 14. On day 14 nitrate had decreased from 13.3 μM to 0.8 in the 1.3 μM limnocorral. Concentrations stabilized and remained low in the higher concentration limnocorrals (1.6-6.7 μM P). TDP concentrations were consistently low (less than 0.23 μM) across the nitrogen gradient and

through time in the Topaz, Emerald, and Aster experiments (Figure 4.8). TDP concentrations were also less than 0.23 μM in the control cubitainers at Moat Lake and Emerald-P. TDP at Moat ranged from 1.19 to 1.50 μM in the first eight spiked cubitainers and 0.76 to 1.3 μM in the last six cubitainers. TDP concentrations decreased an average of 0.175 μM between days one and seven. TDP in the spiked cubitainers at Emerald-P ranged from 1.22 to 1.71 μM. TDP concentrations decreased an average of 0.074 μM between days one and seven.

DIN:TP ratios at Moat on day one ranged from 0.0 to 3.9 and on day seven from 0.0 to 4.6 (Figure 4.9). Ratios decreased during the seven day time period in all cubitainers except the highest N concentration cubitainer where DIN:TP increased and the lowest concentrations where the ratios remained 0.0. DIN:TP ratios at Topaz on day one ranged from 0.0 to 24.1 and on day seven from 0.0 to 19.0. Ratios decreased during the seven day time period in all cubitainers except the 2.7 μM cubitainer where DIN:TP increased and the lower concentrations where the ratios remained 0.0 (Figure 4.9). DIN:TP ratios at Emerald-P on day one ranged from 0.0 to 2.1 and on day seven from 0.0 to 2.6. Ratios decreased during the seven day time period in all cubitainers except in the lower concentrations where the ratios remained 0.0 (Figure 4.9). DIN:TP ratios at Emerald on day one ranged from 0.0 to 28 and on day seven from 0.0 to 22. Ratios decreased during the seven day time period in all cubitainers except in the first cubitainer where the concentration remained 0.0 and the 0.6 μM cubitainer where DIN:TP slightly increased (Figure 4.9). DIN:TP ratios at Aster on day one ranged from 0.0 to 19 and on

day seven from 0.0 to 27. Ratios decreased in four cubitainers, increased in eight cubitainers, and remained unchanged in two cubitainers (Figure 4.9).

4.4.2 Modeling

In the limnocorral experiments, we were able to model phytoplankton response using a four-parameter logistics function for the three experiments that exhibited a response. The logistics function did not work for every measure and the best measures varied between sites (Table 4.2). The best measure to use for the phytoplankton growth response in the Moat nitrogen addition experiments was chlorophyll a from sampling day 6. The best measure in the Hamilton phosphorus addition experiment was particulate phosphorus and phosphorus uptake from sampling day 14. There were a high proportion of nutrient doses that were above the 50% thresholds, especially in the Moat-July experiment which had the highest response of all the experiments. The results were more variable at these very high doses. We found in the Moat-July experiment that it was best to limit the analysis to low to mid range doses (the first 8 corrals).

The Moat-July Monod model μ_{max} and K_{μ} were 0.30 (SE, 0.04) μg L^{-1} day^{-1} chlorophyll a and 0.56 (SE, 0.37) μM nitrate, respectively. The logistics function 10, 50, and 90% effective doses were 0.44 (SE, 0.60), 1.1 (SE, 0.67), and 2.6 (SE, 2.2) μM nitrate, respectively (Figure 4.10).The Moat-September Monod model μ_{max} and K_{μ} were 0.17 (SE, 0.04) μg L^{-1} day^{-1} chlorophyll a and 3.7 (SE, 4.7) μM nitrate, respectively. The logistics function 10, 50, and 90% effective doses were 0.89 (SE, 3.9), 4.0 (SE, 7.5), and 18 (SE, 28) μM nitrate, respectively (Figure 4.11).The Hamilton-July Michaelis-Menten model, using P uptake as a response variable, results were a V_{max} and K_s of 0.06 (SE,

0.02) μM P/day and 1.0 (SE, 1.1) μM phosphate, respectively. The logistics function 10, 50, and 90% effective doses were 0.45 (SE, 0.67), 1.1 (SE, 0.69), and 2.5 (SE, 2.2) μM phosphate, respectively (Figure 4.12).The Hamilton-July Monod model, using PP as the response variable, results were a μ_{max} and K_{μ} of 0.04 (SE, 0.003) μg L^{-1} day^{-1} PP and 0.23 (SE, 0.16) μM phosphate, respectively. The logistics function 10, 50, and 90% effective doses were 0.03 (SE, 0.07), 0.24 (SE, 0.24), and 2.0 (SE, 202) μM phosphate, respectively (Figure 4.13).

The Moat cubitainer experiment Monod model μ_{max} and K_{μ} were 0.43 (SE, 0.08) μg L^{-1} day^{-1} chlorophyll a and 0.43 (SE, 0.55) μM nitrate, respectively. The logistics function 10, 50, and 90% effective doses were 0.23 (SE, 0.44), 67 (SE, 0.69), and 2.0 (SE, .17) μM nitrate, respectively (Figure 4.14).The Emerald-P cubitainer experiment Monod model μ_{max} and K_{μ} were 0.06 (SE, 0.02) μg L^{-1} day^{-1} chlorophyll a and 1.5 (SE, 1.2) μM nitrate, respectively. The logistics function 10, 50, and 90% effective doses were 0.32 (SE, 0.34), 1.2 (SE, 0.84), and 4.7 (SE, 6.3) μM nitrate, respectively (Figure 4.15). Monod parameters and effective doses were not computed for Topaz and Aster because the data did not fit the traditional rectangular hyperbola M-M function or sigmoidal dose response curve and the modeling yielded unrealistic parameters (e.g. infinite effective dose estimate). Emerald (without the P additions) was not modeled due to lack of chlorophyll a response.

Criteria estimates were computed using the effective dose results from the Moat July and September limnocorral, Moat cubitainer, and Emerald-P cubitainer experiments. The Moat-September effective doses determined the 10, 50, and 90% high range criteria

estimates of 0.89, 4.0, and 18 μM N, respectively (Table 4.3). The results for Moat-July limnocorral, Moat cubitainer, and Emerald-P cubitainer experiments were averaged to determine a low range criteria estimate. The 10, 50, and 90% low criteria estimates were 0.33, 1.0, and 3.1 μM N, respectively.

4.4.3 Application of Criteria to Survey Data

Survey data were collected from 75 lakes from 2008-2011. Mean nitrate concentration was 4.58 (SE, 1.00) μM (n = 101) and ranged from less than 0.04 to 11.8 μM (Table 4.4). The 10% effective dose was exceeded by 28 (SE, 7.6) % of lakes in Sequoia, Kings Canyon, and Yosemite National Parks using the high estimate criteria and 37 (SE, 8.0) % using the low nutrient criteria. The 50% effective dose was exceeded by 18 (SE, 7.0) % of lakes using the high estimate and 29 (SE, 7.6) % using the low estimate. The 90 % effective dose was exceeded by 0.0 % of lakes using the high estimate and 21 (SE, 7.6) % using the low estimate.

4.5 Discussion

4.5.1 Response to Nutrient Additions

In the N-limited lakes we measured gradient growth responses following addition of N in 5 out of 7 of the experiments. We measured a growth response in both of the experiments where N + P was added. At all the sites where chlorophyll a increased we also observed a decline in nitrate as the experiment progressed. In our first experiments at Moat Lake using the limnocorrals the experiment had a wide nitrogen gradient (~ 0 - 50 μM) and an extended sampling period (2-3 weeks) in order to ensure we captured the 10,

50 and 90% effective doses. The high variability of chlorophyll a data at the higher end of the range and after the first week of the experiment indicated that the experiments worked best at lower concentrations and shorter time periods. The modeling data, discussed in more detail below, also indicated that the effective doses were in the lower nitrogen ranges. We used these results to inform the design of the cubitainer experiments where we limited the N range from ~ 0 to 15 μM, only ran the experiment for seven days, and monitored chlorophyll a more frequently by collecting in situ measurements.

Addition of P to the nitrogen gradient experiments was successful as it minimized the mesocosms from rapidly becoming P-limited. DIN:TP ratios indicate that only one cubitainer became P-limited during the experiment and it was the highest N addition at Moat. TDP decreases were observed between the beginning and end of the N + P addition experiments, but P concentrations remained relatively high throughout all cubitainers (greater than 0.75 μM). The Emerald and Aster experiments where P was not added elicited minimal to no measurable growth. However, examination of the decrease in nitrate and DIN:TP ratios between days one and seven in some of the Emerald cubitainers suggested that additional nitrogen was taken up by phytoplankton (Figure 4.3 and Figure 4.9). DIN:TP ratios indicated that at the start of the experiment all cubitainers above 2.0 μM nitrate (10 of 16 cubitainers) were P-limited and this would explain the limited phytoplankton response. However, by day seven, the decrease in DIN:TP indicated that only 4 of 15 cubitainers were P-limited, 3 were N-limited and the remaining were intermediate. Small increases in algal growth have been observed when the non-limiting nutrient is added (Francoeur 2001). In Emerald, there may have been subtle increases in

phytoplankton growth that might not be detectable with the chlorophyll a methods we used or it might not be detectable along a gradient as a subtle phytoplankton response to a non-limiting nutrient may be less sensitive to the initial concentration. Phytoplankton may also take up and store N in the cells faster than they deploy it (Pedersen and Borum 1996) or the decline may be explained by nitrate taken up by bacteria (Nelson and Carlson 2011). Aster did not appear to respond at all to nutrient additions. There was no change in nitrogen between days one and seven and DIN:TP changed, but the response was variable (Figure 4.3 and Figure 4.9). Aster cubitainers were P-limited above 4.5 µM nitrate. Interestingly, Topaz, the other cubitainer experiment where only N was added, did respond to the N additions. The largest chlorophyll a increase (0.23 to 0.63 µg L^{-1}) along the gradient was between the controls and the lowest N addition, 0.1 µM (Figure 4.6). N was still the limiting nutrient in the first 4-5 cubitainers (Figure 4.9). Topaz may have been able to better respond to the N additions because TDP concentrations in the lake were slightly higher than Aster or Emerald (Figure 4.8). Average initial TDP in the Topaz cubitainers was 0.129 µM compared to 0.057 µM in the Emerald cubitainers and 0.093 µM in the Aster cubitainers. A response was also observed in Topaz at higher N concentrations, where DIN:TP ratios suggested P-limitation. Phytoplankton may have utilized P stored in their cells. The higher TDP concentrations may have afforded them this luxury P storage that may be more limited in Emerald or Topaz.

Adding the inferred non-limiting nutrient in the Hamilton-September experiment did not elicit a growth response. Albertin et al. (2009) found *Lyngbya wollei*, a macroalga common in Florida springs, responded to additions of nitrate under apparent phosphorus

limiting conditions. The ability to continue taking up nitrogen and growing under apparent P depleted conditions was largely attributed to the algae's ability to store P in its cells. We did observe uptake of nitrate during the experiment. Similar to Emerald, these results may be explained by method sensitivity, uptake and storage of N in cells (Pedersen and Borum 1996), or uptake by bacteria (Nelson and Carlson 2011). The July experiment where P was added did elicit a growth response and a decrease in P was observed throughout the experiment. Our results confirmed that the phytoplankton in Hamilton Lake were growing under true P-limiting conditions. Nutrient ratios, such as DIN:TP, are often used to predict nutrient limitations (Bergström 2010; Morris and Lewis 1988). However, nutrient limitation ultimately is determined in the field or laboratory using fertilization experiments (Vitousek 2004).

There was evidence that nutrients were taken up quite rapidly and initial growth observed shortly after the nutrients were added. The initial TDP concentrations in the Moat cubitainer experiment were notably lower in the higher nitrate concentration cubitainers (Figure 4.8). The second line of evidence was the variability in initial chlorophyll a readings between limnocorrals and the lower chlorophyll a concentrations in the lake sample (Figure 4.5). Phytoplankton can rapidly take up nutrients and increase growth rates on time scales less than a day (D'Elia *et al.* 1986; Rigler 1956). Our methods were to spike a few mesocosms at a time and minimize the time between nutrient additions and sampling, however, it was not possible to completely control the timing in the field. This may have had some effect on the accuracy of the growth rates, but had

minimal effect on the modeling and effective dose calculations as these were based on the relative changes on a given day.

4.5.2 Modeling

Four of the seven experimental results in the N-limited lakes fit the Monod and logistics function curves when using chlorophyll a as the indicator of growth. We compared our ED50 results from the dose response curve to the more traditional Monod half-saturation constant, K_μ. Moat-July had the largest discrepancy with a difference of 0.54 μM (K_μ of 0.56 μM and ED50 of 1.1 μM). Moat-September estimates were closer, differing by 0.30 and with a K_μ of 3.7 μM and ED50 of 4.0 μM. The Moat cubitainer experiment differed by 0.24 μM with a K_μ of 0.43 μM and ED50 of 0.67 μM. The Emerald-P estimates differed by 0.32 μM with a K_μ of 0.1.5 μM and ED50 of 0.1.2 μM. The differences ranged from 0.24 to 0.54 μM, suggesting that we got good agreement between the two modeling approaches with the possible exception of the Moat-July experiment. Moat-July had a large data gap in the area of the curve where there was the most change.

The limnocorral results indicated effective doses vary by season and were higher in the fall. The 50% dose from the Moat-July experiment was 1.1 μM nitrate, compared to 4.0 μM nitrate from the Moat-September experiment. A higher nitrogen threshold in the late season might be explained by the presence of other growth limiting factors such as water temperature and incoming solar radiation (Williamson *et al.* 2010). Chlorophyll a was higher overall during the July experiments, suggesting the early season was more productive in Moat Lake. Phosphate concentrations did not differ between the

experiments (Figure 4.7). Concentrations were consistently below 0.050 μM in the lake and the corrals, but never went below detectable levels.

The cubitainer experiments were conducted in the fall season to further refine fall nitrogen criteria estimates. However, the effective dose estimates for the Moat and Emerald cubitainers were more similar to the Moat-July limnocorral experiments. The cubitainer experiments were conducted during a year (2011) with a late snowpack where Emerald lake was still ice-covered in early July. Weekly monitoring of nutrient limitation using nutrient addition experiments in Emerald Lake during the summer of 2011 indicated that Emerald switched from a P-limited lake to an N-limited lake just 1-2 weeks prior to our bioassay experiments (T. Martin, unpublished data). Emerald Lake was initially P-limited during the early snowmelt time period due to increased nitrogen released from the snowpack. As snowmelt flows and the nitrogen source decreased and biotic uptake in the lake increased, the lake was just switching nutrient limitation. This may explain the lower effective doses and similarity to the 2009 July experiments. Therefore, when averaging the results of the experiment to calculate the final effective doses, we grouped the Moat-July experiment with the Moat and Emerald cubitainer experiments to establish a 'low criteria estimate'. The Moat-September experiment was used as the 'high criteria estimate'. This was not a perfect grouping as the September cubitainer experiments would also be limited by seasonal factors such as air temperature and duration of day. However, snowpack dynamics and hydrology are such dominant drivers of watershed and lake ecosystem biogeochemical cycling that grouping by

hydrologic influence was the better approach (Meixner and Bales 2003). The similar results in criteria estimates supported this decision.

Two of the experiments were conducted under elevated P concentrations that do not necessarily reflect typical lake nutrient status. We found this was a better approach when the objective was to develop a nitrogen gradient response curve as P-limitation will limit the range of the gradient. Lake P concentrations vary spatially and temporally and eutrophication from increased P-deposition is also of concern (Sickman *et al.* 2003b) . The N criteria developed under non-limiting P will protect lakes from eutrophication with any level of P. It does need to be recognized that it is a conservative criteria, with respect to lake conservation, for lakes with low P. The lake may become depleted in P and growth limited before the nitrogen criteria level is reached.

Our criteria were higher than criteria previously estimated for high-elevation lakes in the Rocky Mountains. Nanus et al. (2012) determined a maximum growth threshold (i.e. ED90) at 0.5 μM and Arnett et al. (2012) determined K_μ (ED50) and max growth (ED90) thresholds of 0.18 and 0.36 μM, respectively. These thresholds were based on the response of the N-sensitive diatom species *Asterionella formosa*. Michel et al. (2006) modeled the response of four diatom species in situ and determined that K_μ ranged from 0.0003 to 0.041 μM. Estimates varied by species and light levels. Our experiments may have yielded higher thresholds because the estimates were based on a community response as opposed to single species. Our criteria were more similar to Theobald et al.'s (2010) reference condition estimate of 1.6 μM, which was determined by comparing lake nitrate concentrations to a deposition gradient.

We established initial criteria estimates for P using the results from the Hamilton-July experiment. In the P-limited experiment, P uptake and PP were better indicators of response than chlorophyll a with respect to growth modeling results. Comparison of K_μ to ED50 showed that the estimates were very close. Using P-uptake as a response indicator, K_μ and ED50 differed by 0.1 μM with a K_μ of 1.0 μM and ED50 of 1.1 μM. Using PP as a response indicator, K_μ and ED50 differed by 0.01 μM with a K_μ of 0.23 μM and ED50 of 0.24 μM. Our initial modeling results were promising and we recommend continuing to refine criteria for P-limited lakes. Seventy-six percent of the lakes in Sequoia and Kings Canyon National Parks were P-limited and effects of P deposition on N and P-limited lakes is also of high concern within the study region (Sickman *et al.* 2003b; Vicars and Sickman 2011).

There were a few limitations to the modeling results and criteria estimates that should be considered when applying criteria. These data were highly variable and would benefit from repeated experiments that cover the range of temporal conditions (e.g. high and low snowpack years). Standard errors around the M-M, Monod, and logistics function parameters were high. High variability is typically observed in M-M and Monod model parameters due to the low concentrations at which the Kμ and ED50 occur (Grover 1989). Preparation and measurement methods do not offer the resolution needed in the typical K_μ concentration range. We used chlorophyll a as an indicator of growth for the N-limited experiments. However, phytoplankton responding to nutrient increases may alter their chlorophyll quotas instead of increasing biomass (Elser *et al.* 2009b). Despite this limitation chlorophyll a is commonly used as an indicator of phytoplankton growth

(Elser *et al.* 2007). Phytoplankton biomass is affected by grazing, however, effects on the experimental results were likely minimal as the short time period of the experiments would not have allowed for zooplankton populations to respond (Carter 1974; Schwartz 1984).

4.5.3 Application of Criteria

We compared high and low estimates of nutrient criteria to nitrate monitoring data to assess the status of lakes within Yosemite, Sequoia, and Kings Canyon National Parks. A regional assessment of lakes in the Rocky Mountains that used criteria similar to our low criteria estimates determined that 1.1 to 21% of lakes exceeded nitrate thresholds (Nanus *et al.* 2012). This was lower than our Sierra Nevada estimates that range from 21-37% exceeding low criteria. Specifically the Rocky Mountain study found that 21± 8% of lakes exceeded a 0.5μM threshold, 4.3±1% exceeded a 1.0 threshold, and 1.1 ± 0.2% exceeded a 2 μM threshold. Their percent exceedance results were more similar to the range we calculated, 0 to 28%, using the high criteria. These results suggest that a greater proportion of lakes in the Sierra Nevada were affected by nitrogen deposition.

The limitations discussed in section 4.5.2 need to be considered when applying criteria to survey and monitoring data. Individual criteria estimates have high errors, however, presenting a range can be a more robust approach (Baron *et al.* 2011; Nanus *et al.* 2012). Our criteria estimates were reasonable and consistent when compared with previous studies (Michel *et al.* 2006; Nanus *et al.* 2012; Theobald *et al.* 2010). The complexity of nutrient limitation and its sensitivity to change should also be considered when comparing survey data to criteria. Nutrient limitations change over time, especially

when N and P concentrations are low and the ratios of actual concentration to phytoplankton requirements are similar (Sterner 2008). For example, long-term research at Emerald Lake showed a shift from P-limitation in the 1980s to N-limitation during the 1990s and back to P-limitation in the 2000s (Nelson and Carlson 2011; Sickman *et al.* 2003b). Recent literature suggests that pre-industrial nutrient status of Emerald Lake would have likely been N-limited (Bergström and Jansson 2006). However, despite extensive research in the nutrient limitation field there is still much debate and many aspects that remain poorly understood (Smith and Schindler 2009; Sterner 2008). As discussed in Chapter 2, Sierra Nevada lakes were first affected by atmospheric deposition in the early 20th century, decades before monitoring programs were established. Our understanding of the natural balance of nutrients in these ecosystems is complicated by a lack of historic nutrient data and an understanding of how nutrient limitation varied across the pre-industrial landscape.

Despite the challenges, the initial development of these criteria and continued refinement is of direct benefit toward the protection of Sierra Nevada lakes as it establishes a range that can be used in conjunction with lake monitoring programs to assess the status of sensitive high-elevation lakes, incorporated in resource condition assessments and planning efforts by land management agencies, and used to communicate the status of lakes to the public and policymakers (Heard *et al.* 2012; Theobald *et al.* 2010). The nutrient criteria may also be used to determine and apply critical loads to the Sierra Nevada using a similar approach taken by Nanus et al. (2012).

4.6 Tables and Figures

Table 4.1: Descriptions of each experiment including the type of mesocosm used, nutrient(s) added, inferred limiting nutrient of the lake, and the dates the experiment was run.

Experiment Name	Mesocosm Type	Nutrient Added	Limiting Nutrient†	Dates
Moat-July	limnocorrals	N	N	7/22/09 - 8/14/09
Moat-September	limnocorrals	N	N	9/9/09 - 9/22/09
Hamilton-July	limnocorrals	P	P	7/23/09 - 8/4/09
Hamilton-September	limnocorrals	N	P	9/16/09 - 9/28/09
Moat	cubitainers	N+P	N	9/10/11 - 9/16/11
Topaz	cubitainers	N	N	8/31/11 - 9/7/11
Emerald	cubitainers	N	N	8/30/11 - 9/6/11
Emerald-P	cubitainers	N+P	N	8/30/11 - 9/6/11
Aster	cubitainers	N	N	8/31/11 - 9/7/11

† Inferred limiting nutrient determined by DIN:TP ratios prior to experiment

Table 4.2: Logistics function modeling results. Bold font indicates the measures that fit the logistics function and were used for criteria estimates.

	Experiment	Measure	Fit to Logistics Func.	Residual SE
Limnocorrals	Moat - July (day 6)	**Chl a**	**Yes**	**0.092**
		Particulate N	Yes	1.6
		Particulate C	No	
		Nitrate Uptake	No	
	Moat - Sept (day 6)	**Chl a**	**Yes**	**0.063**
		Particulate N	No	
		Particulate C	No	
		Nitrate Uptake	No	
	Hamilton - July (day 12)	Chl a	No	
		Particulate P	**Yes**	**0.0060**
		Particulate C	No	
		Phosphate Uptake	**Yes**	**0.022**
Cubitainers	Moat - Sept (day 3)	**Chl a**	**Yes**	**0.17**
	Topaz - Sept (day 7)	**Chl a**	No	
	Emerald - Sept	Chl a	*	*
	Emerald-P - Sept (day 6)	**Chl a**	**Yes**	**0.019**
	Aster -Sept	Chl a	No	

* Data were not run due to lack of observed growth

Table 4.3: High and low criteria estimates and summary of effective dose results used to calculate criteria estimates.

Experiment	10% Dose µM N	50% Dose µM N	90% Dose µM N
Moat-July: limnocorrals	0.44	1.1	2.6
Moat-Sept: limnocorrals	0.89	4.0	18
Moat: cubitainers	0.23	0.67	2.0
Emerald - cubitainers	0.32	1.2	4.7
High critieria estimate†	0.89	4.0	18
Low criteria estimate††	0.33	1.0	3.1

† Moat-September limnocorral results

†† Average of Moat-July limnocorrals, Moat cubitainers, and Emerald-P cubitainers

Table 4.4: Percent of lakes in Sequoia, Kings Canyon, and Yosemite that exceed high and low criteria estimates.

	10% Dose µM N	% Exceeded	50% Dose µM N	% Exceeded	90% Dose µM N	% Exceeded
High	0.89	28 (7.6)	4.0	18 (7.0)	18	0
Low	0.33	37 (8.0)	1.0	29 (7.6)	3.1	21 (7.6)

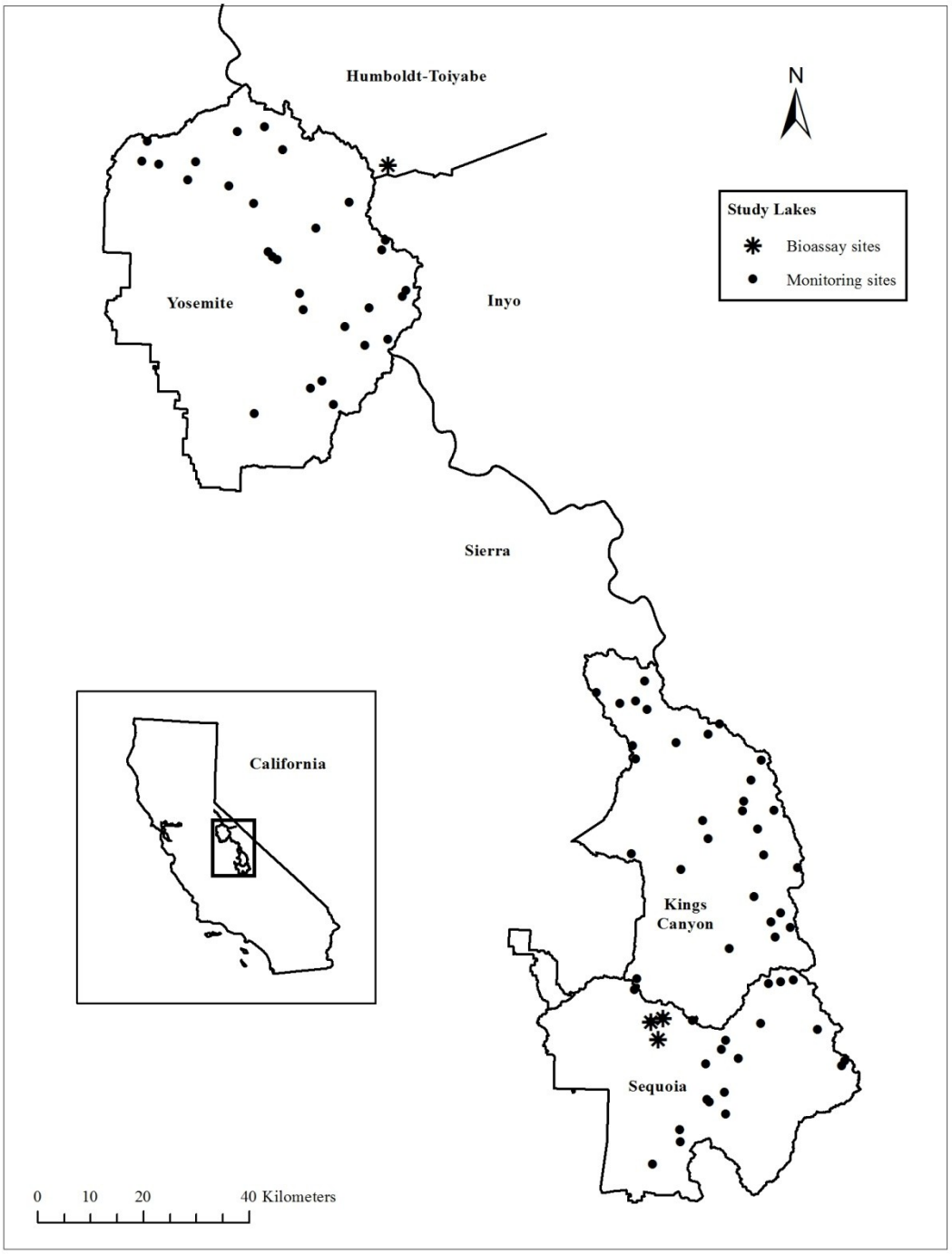

Figure 4.1: Sierra Nevada study area, including bioassay experiment sites in Humboldt-Toiyabe National Forest and Sequoia National Park and nutrient monitoring sites throughout Yosemite, Kings Canyon, and Sequoia National Parks.

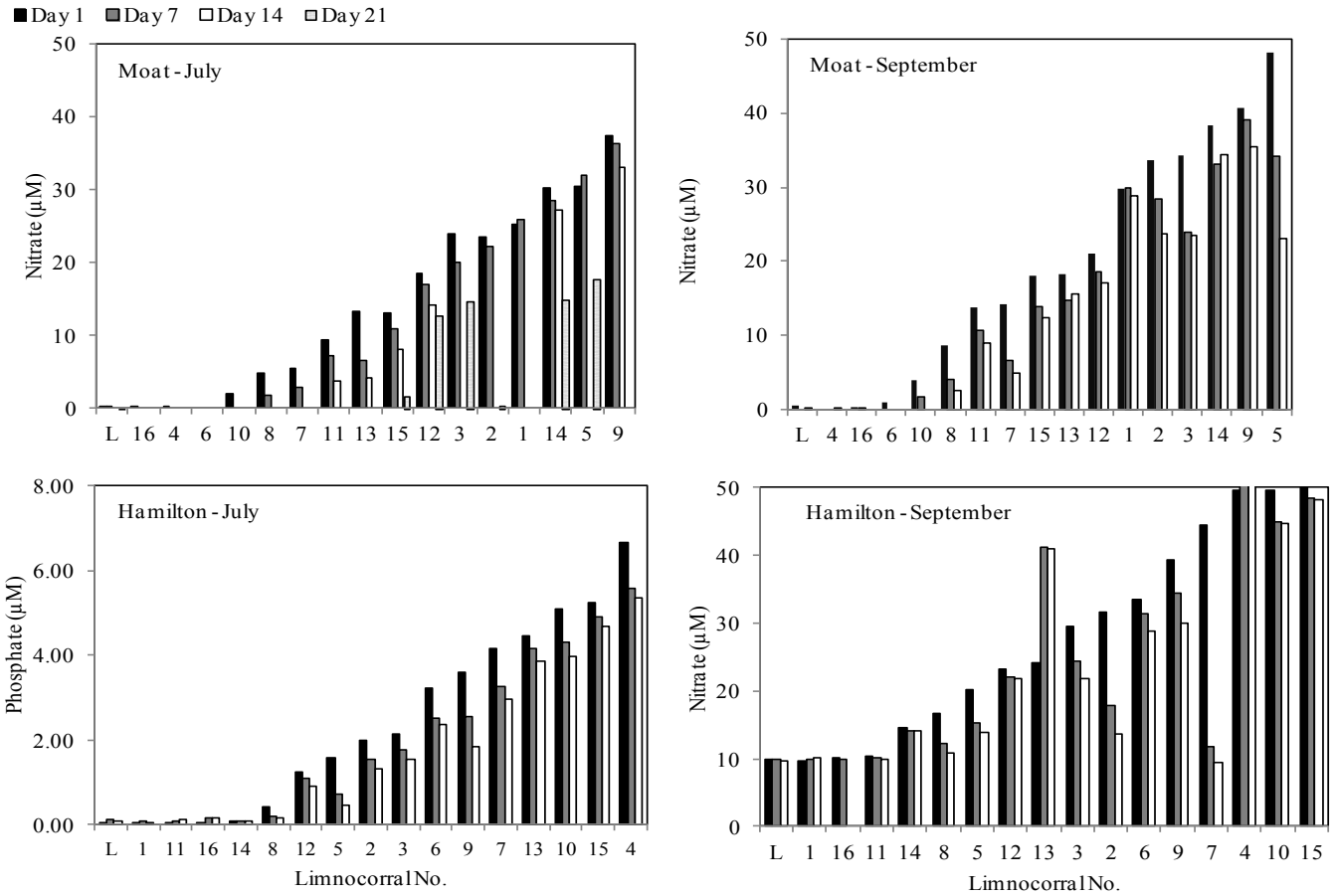

Figure 4.2: Nutrient gradients for Moat and Hamilton limnocorral experiments in July and September. Nitrogen was added to the Moat-July, Moat-September, and Hamilton-September experiments. Phosphorus was added to the Hamilton-July experiment. 'L' refers to the lake sample.

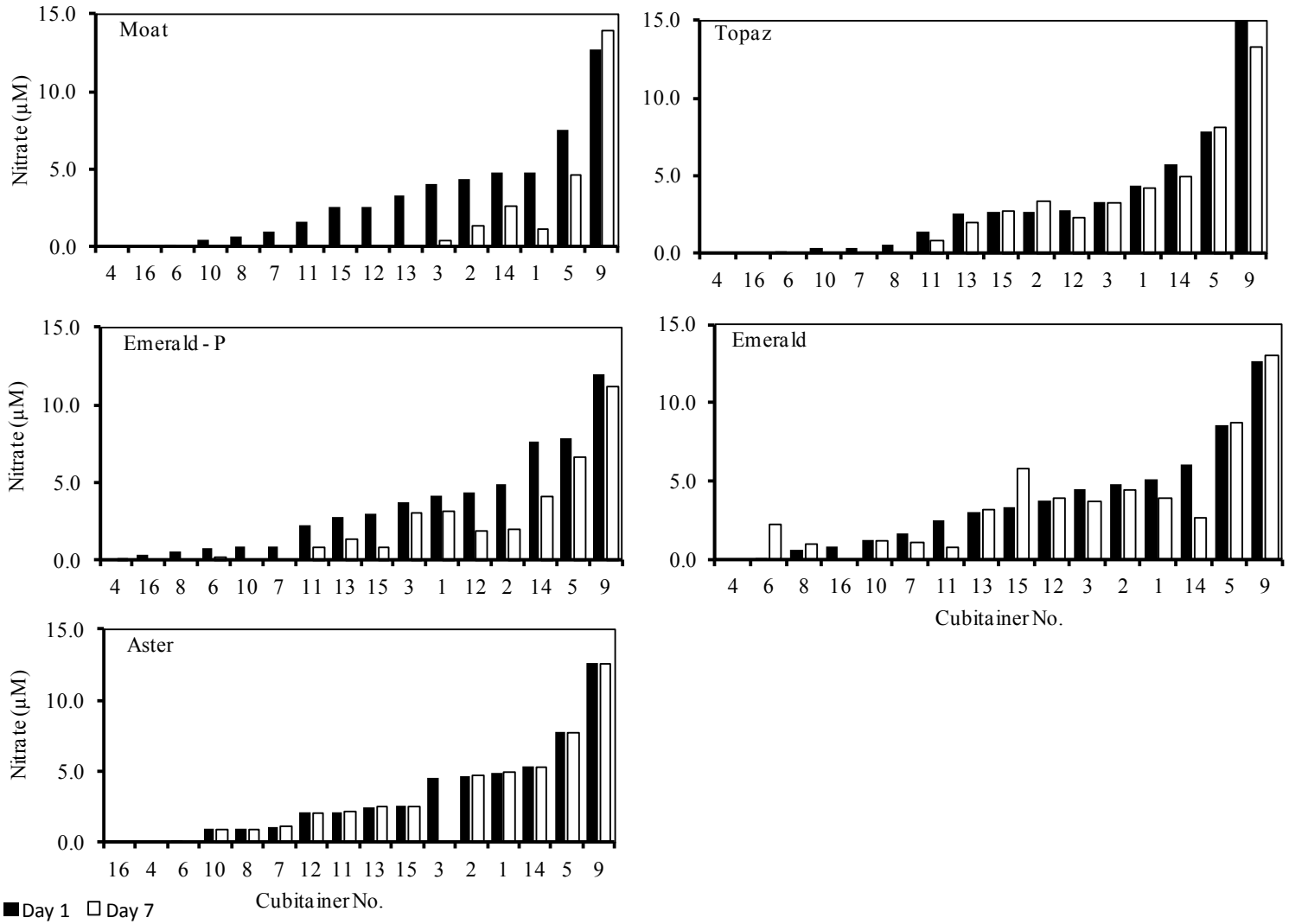

Figure 4.3: Nitrate gradients for Moat, Topaz, Emerald-P, Emerald, and Aster cubitainer experiments.

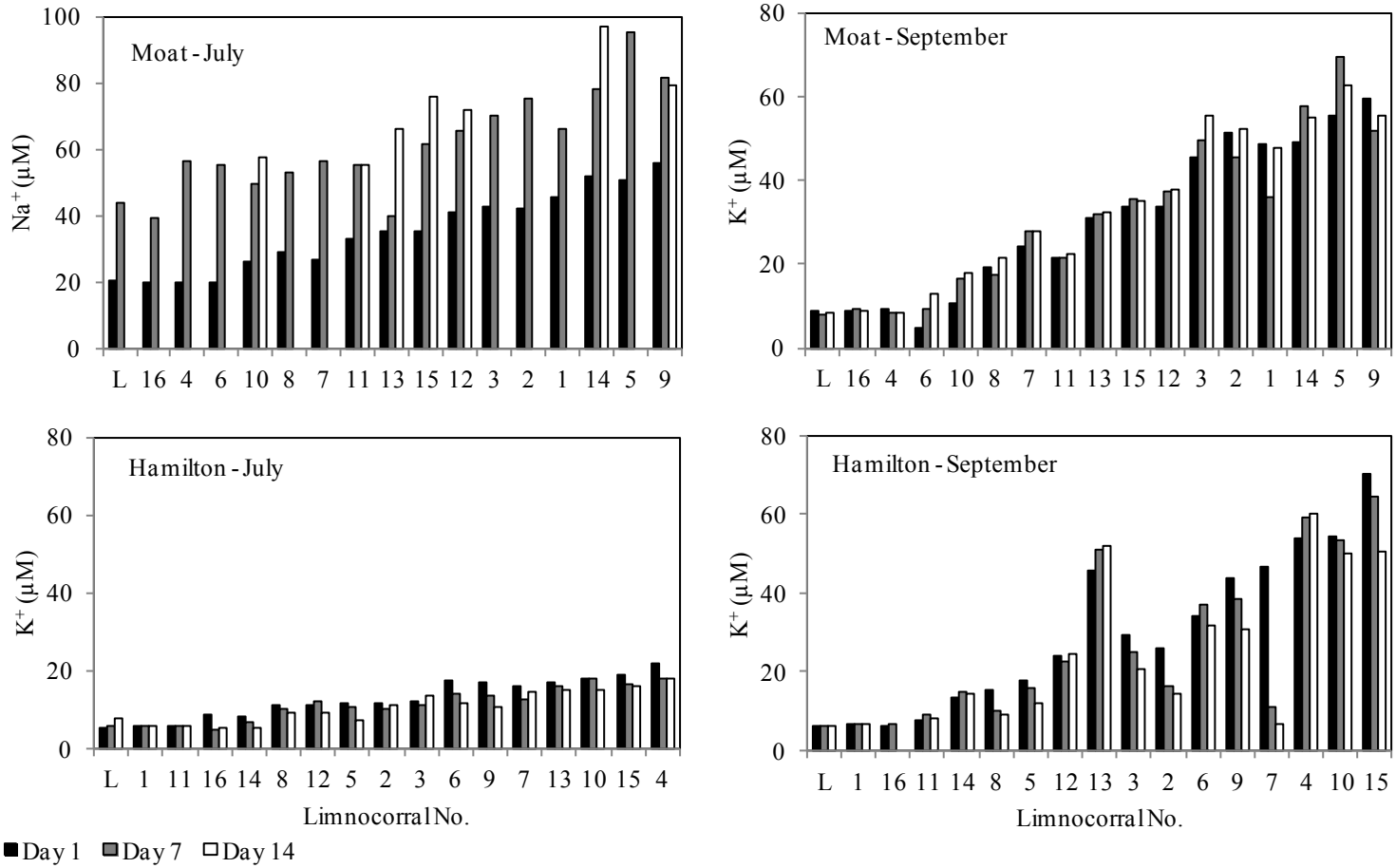

Figure 4.4: Cation (Na^+ or K^+) gradients for the Moat and Hamilton limnocorral experiments. Changes in cation concentrations were used to determine if limnocorrals leaked. 'L' refers to the lake sample.

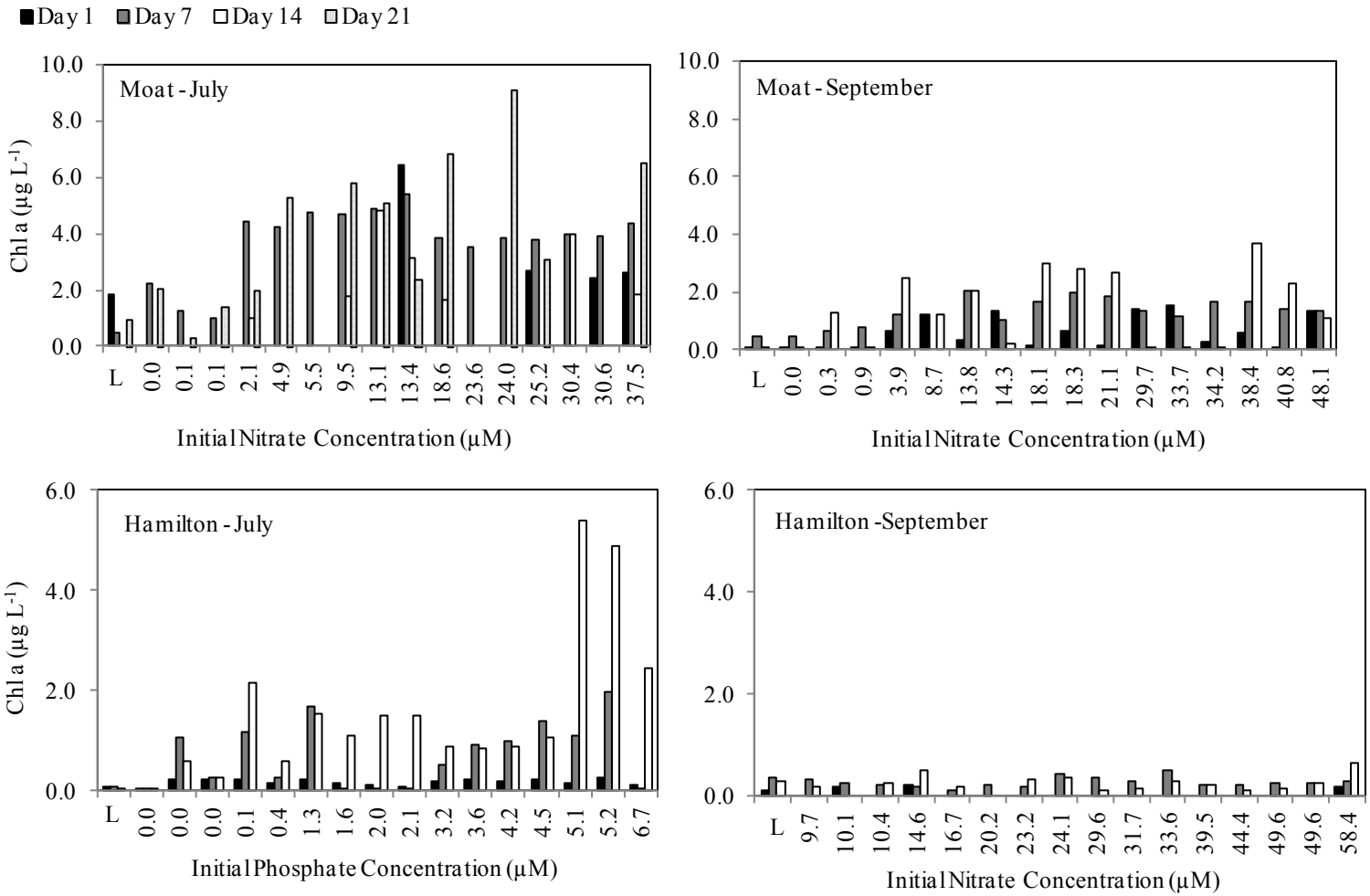

Figure 4.5: Chlorophyll a concentrations for Moat and Hamilton limnocorral experiments. 'L' refers to the lake sample.

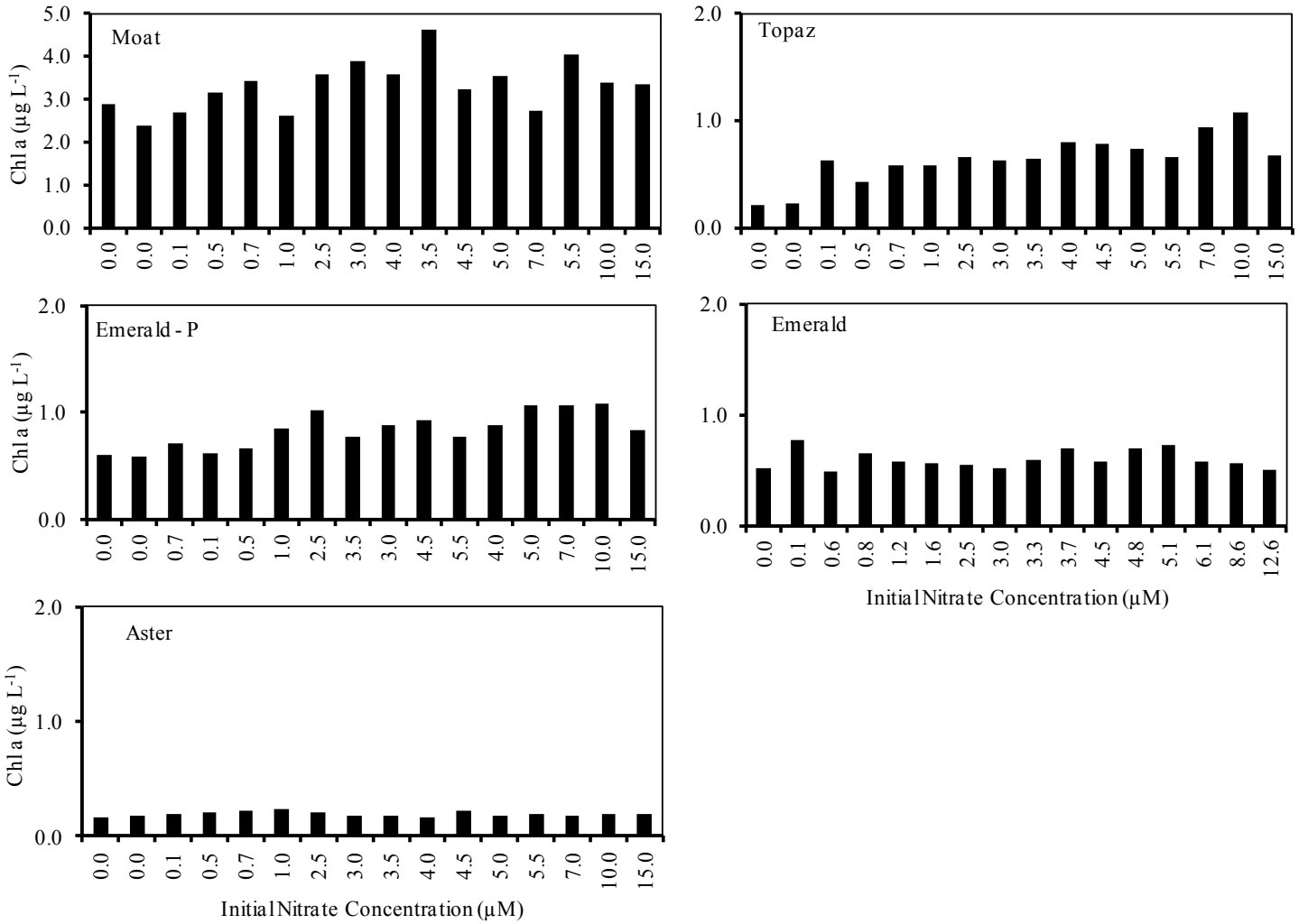

Figure 4.6: Chlorophyll a concentrations for Moat, Topaz, Emerald-P, Emerald, and Aster cubitainer experiments.

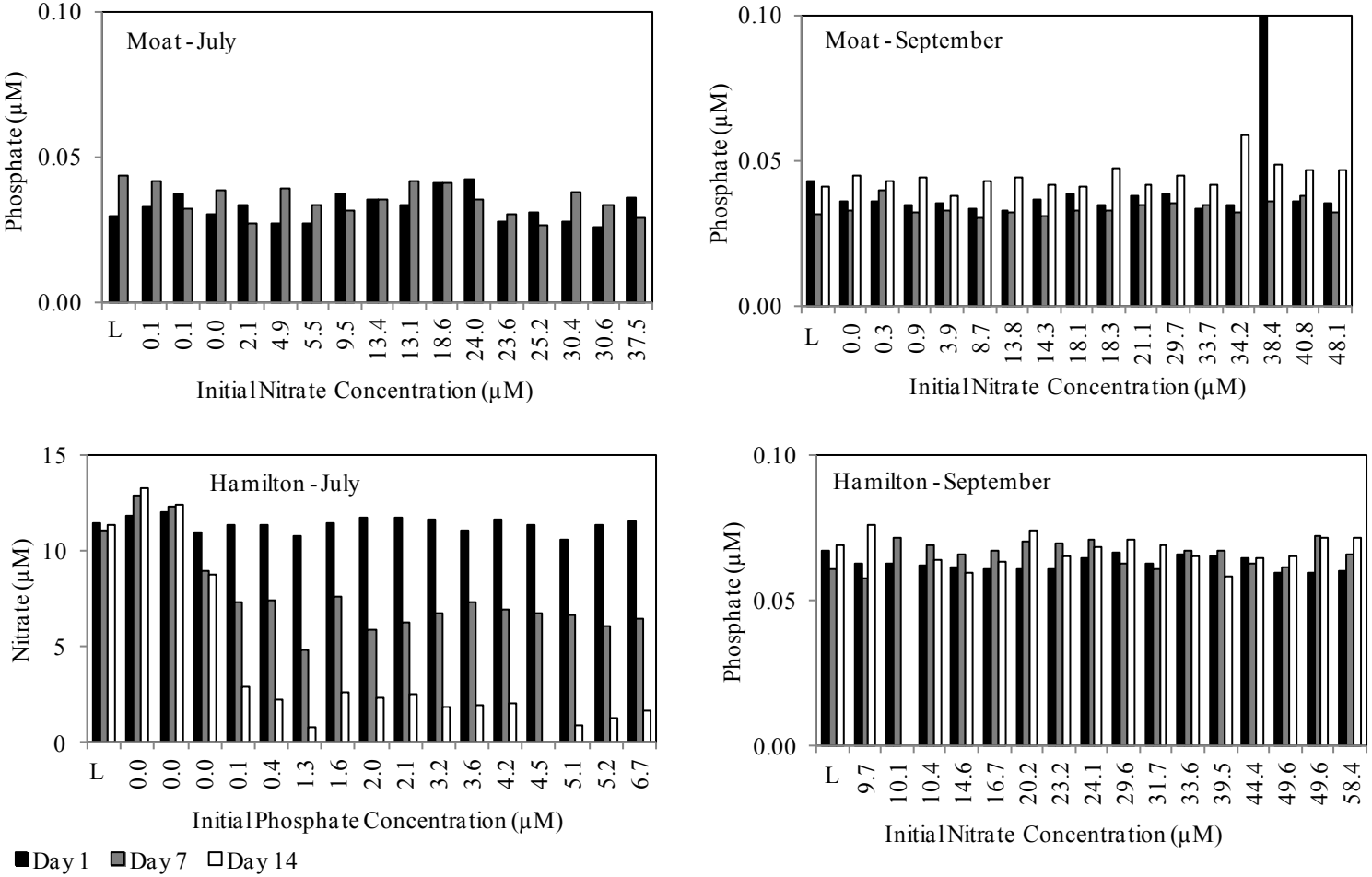

Figure 4.7: Phosphate gradients for the sites where N was added (Moat-July and September, Hamilton-September) and the nitrate gradient at Hamilton-July where P was added. 'L' refers to the lake sample.

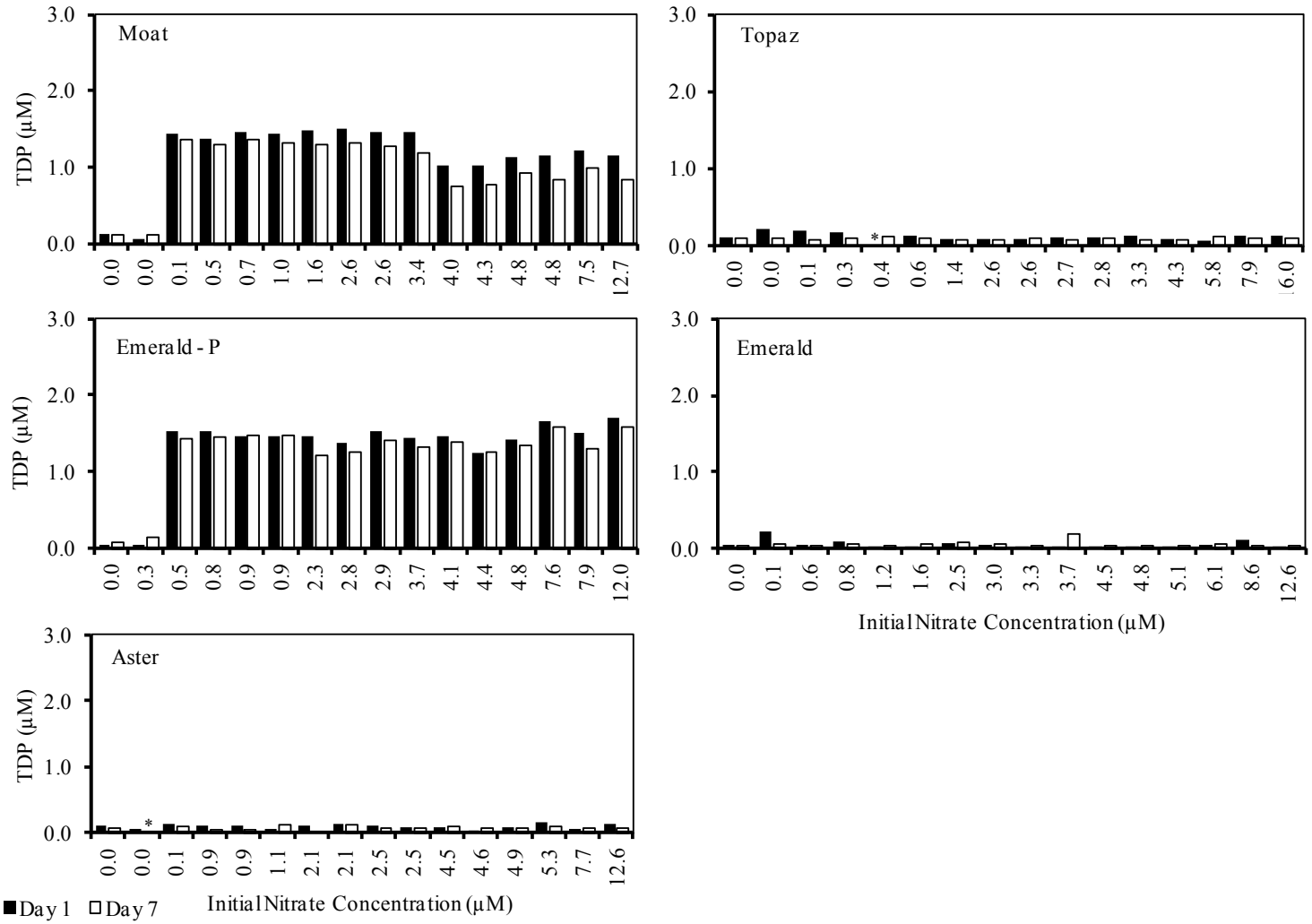

Figure 4.8: TDP gradients for the cubitainer experiments. The TDP concentrations at Moat and Emerald-P were experimentally elevated at a constant level across cubitainers. * indicates missing data.

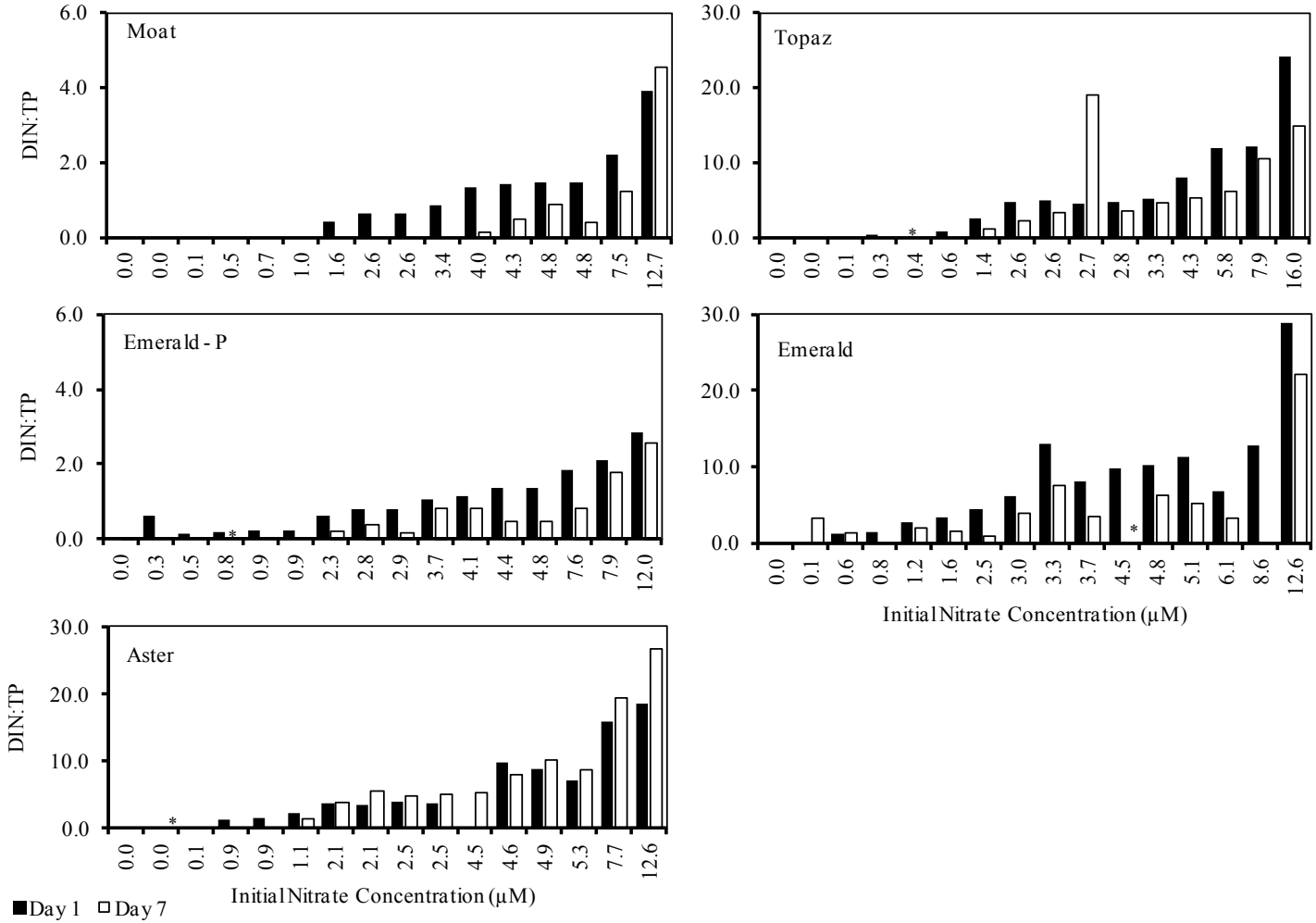

Figure 4.9: Nutrient ratio, DIN:TP, gradients for the cubitainer experiments. A ratio of 0-0.6 indicates N-limitation, 0.6-4.0 indicates intermediate limitation, and greater than 4.0 indicates P-limitation. * indicates missing data.

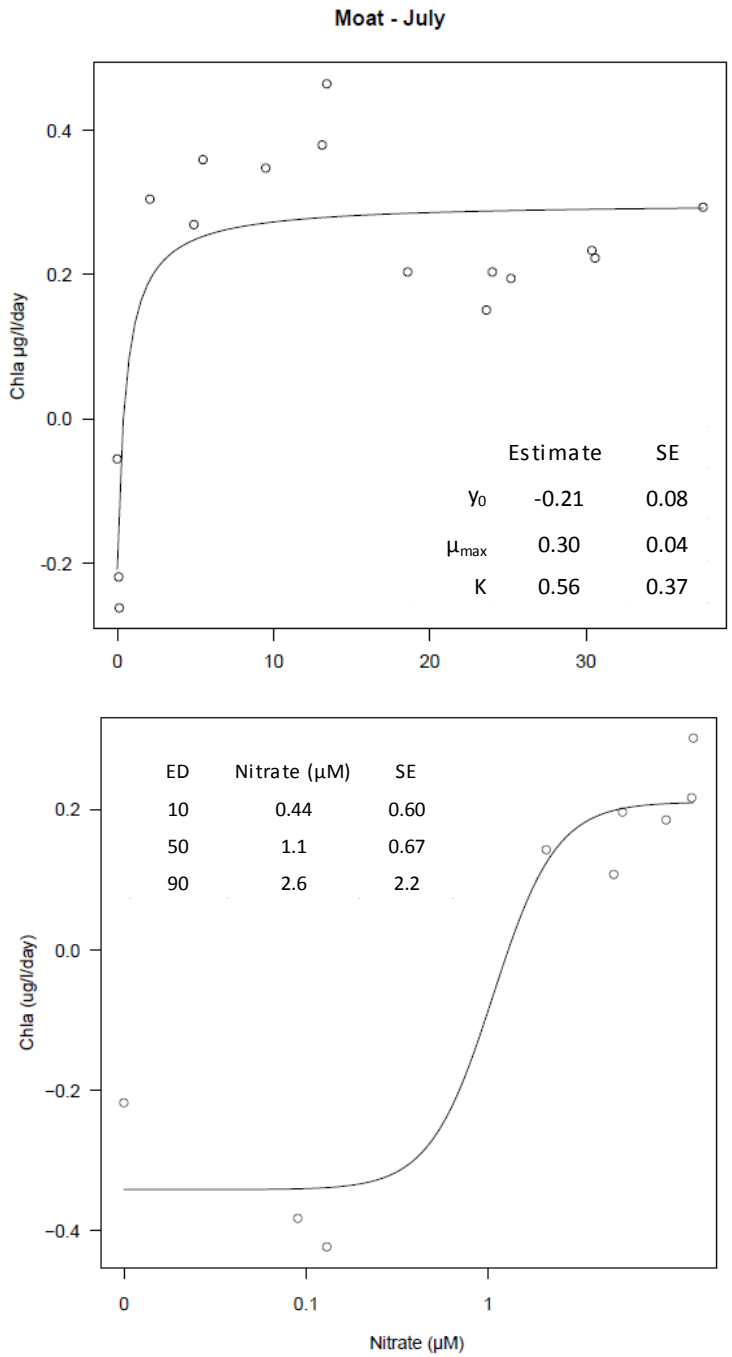

Figure 4.10: Monod (top) and dose response (bottom) curves for the Moat-July limnocorral experiment.

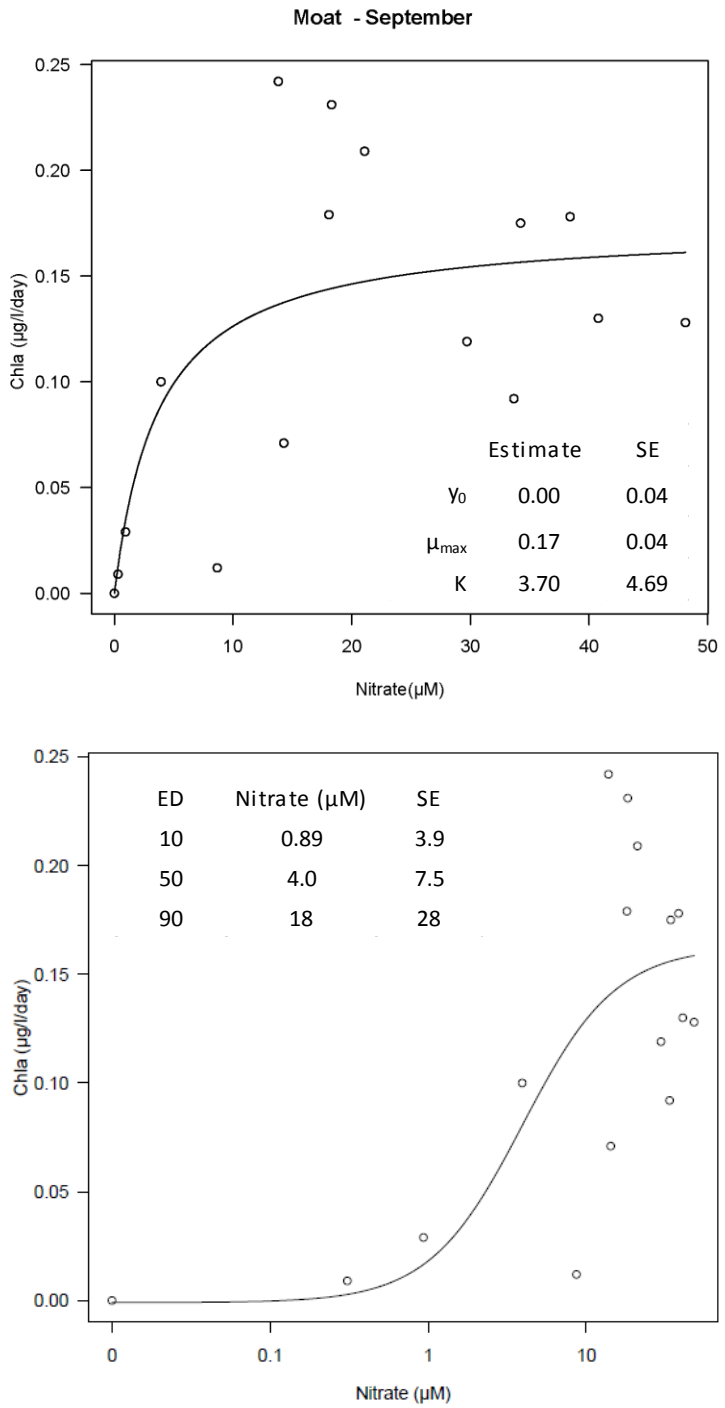

Figure 4.11: Monod (top) and dose response (bottom) curves for the Moat-September limnocorral experiment.

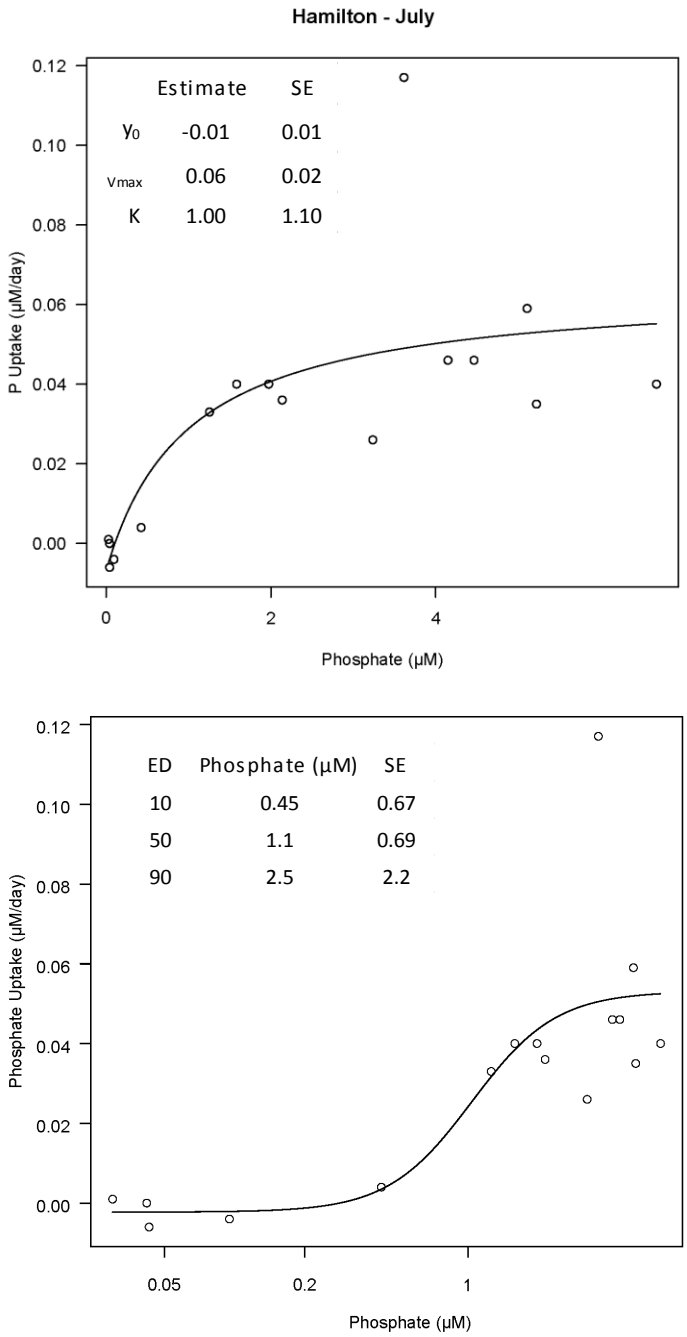

Figure 4.12: M-M (top) and dose response (bottom) curves for the Hamilton-July limnocorral experiment using phosphate uptake as an indicator of growth.

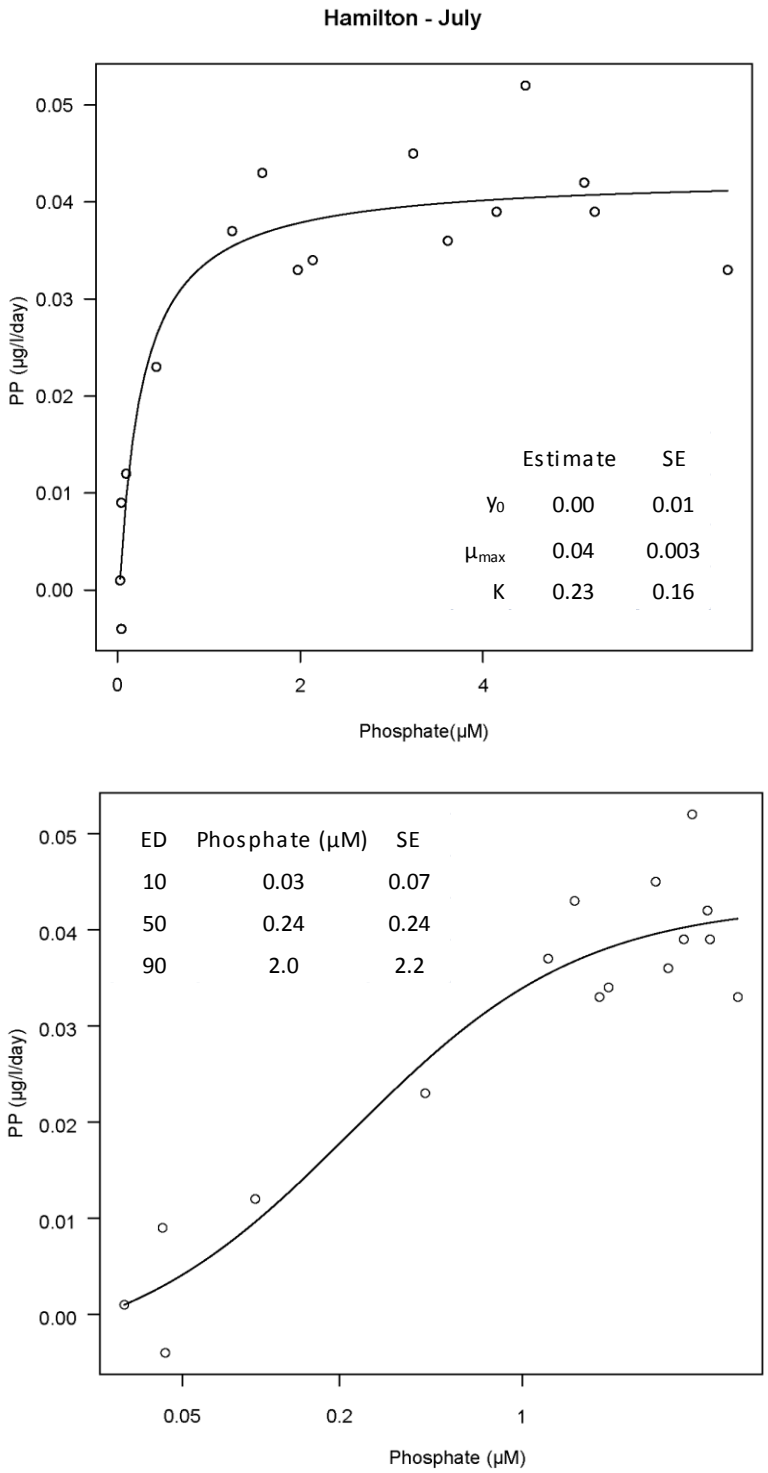

Figure 4.13: Monod (top) and dose response (bottom) curves for the Hamilton-July limnocorral experiment using particulate phosphorus as an indicator of growth.

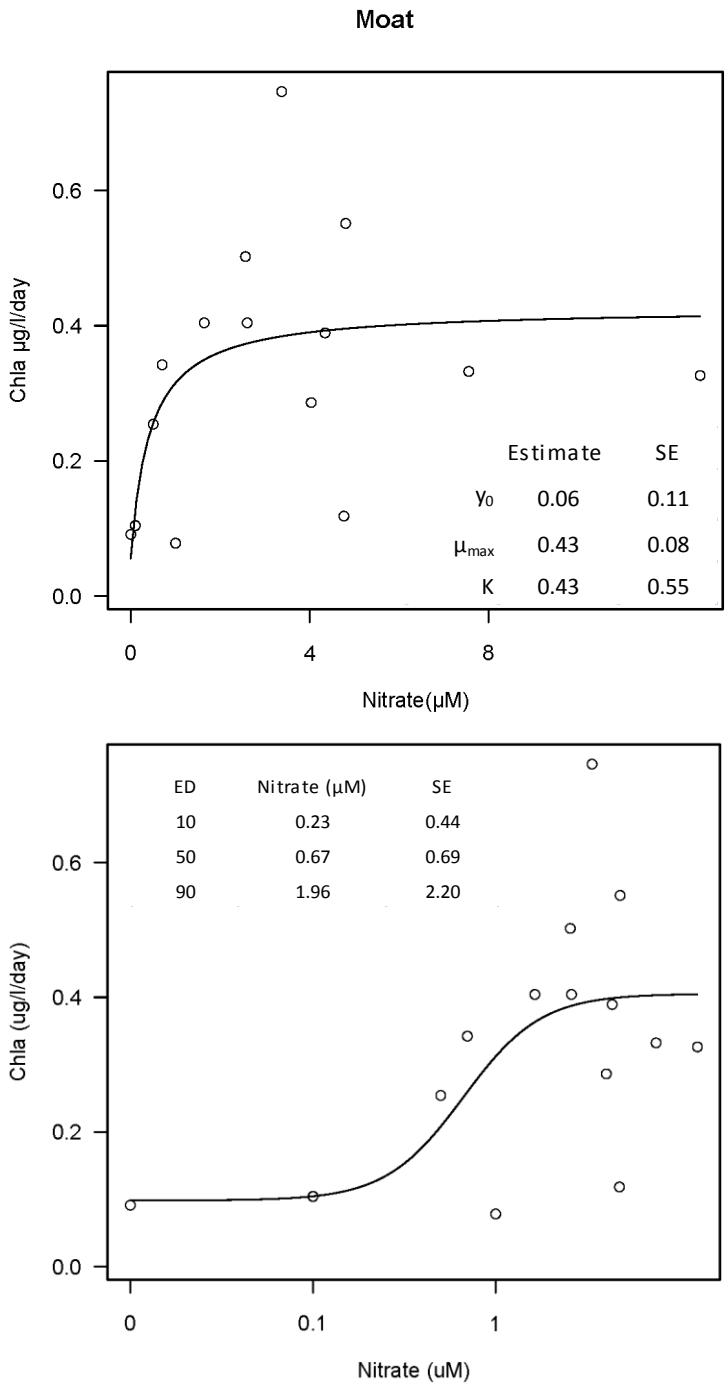

Figure 4.14: Monod (top) and dose response (bottom) curves for the Moat cubitainer experiment.

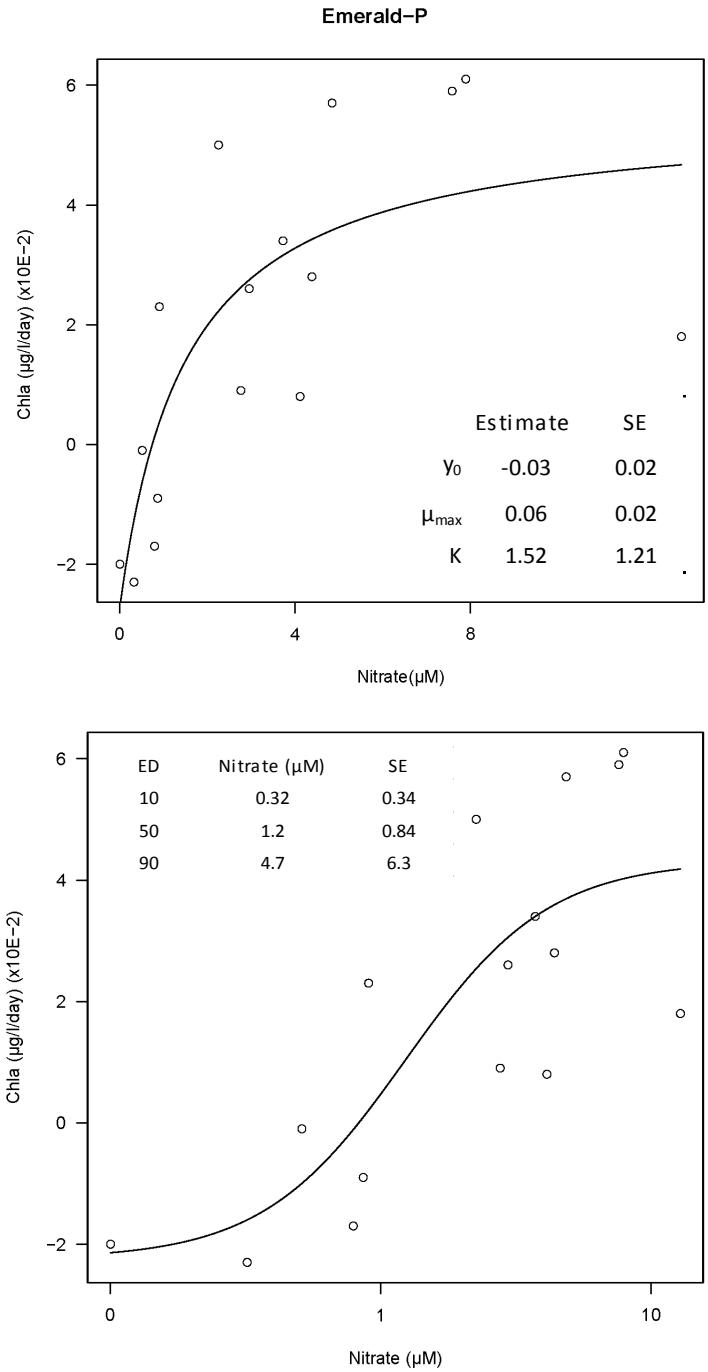

Figure 4.15: Monod (top) and dose response (bottom) curves for the Emerald-P cubitainer experiment.

Chapter 5: Conclusion

In this dissertation I set out to gain a greater understanding of how global change is affecting mountain lakes and how this information can be used to inform environmental policy to protect sensitive aquatic ecosystems. My goals were to link atmospheric deposition with acidification and eutrophication effects, develop critical loads and nutrient criteria, and use this information to assess the status and trends of Sierra Nevada lakes.

I started by investigating the extent that atmospheric deposition and climate explain 20th century trends in lake acidification and eutrophication with the objectives to assess effectiveness of existing environmental policy and to inform future policy by developing a critical load for acidification. Investigation of multiple proxies and direct measurements of deposition, ANC, climate, and eutrophication indicated that early 20th century lake ANC decline in Moat Lake is attributed to atmospheric deposition and the subsequent recovery in the late 20th century is attributed to the success of the Clean Air Act and Amendments (CAAA). The trends observed in Moat Lake are supported by three decades of chemistry data from Emerald Lake. Emerald Lake ANC has a positive temporal trend concurrent with a decline in sulfate concentrations, suggesting that Emerald ANC is also responding to the CAAA. This was a significant finding as most of the focus on the evaluation and attributed successes of the CAAA have been in the northeastern United States (Burns et al. 2011; Kahl et al. 2004; Stoddard et al. 1999). Although atmospheric deposition was the dominant driver of ANC in the 20th century,

our results also indicated that aquatic communities were responding to combined effects of acidification, climate change, and eutrophication. There is a need for further research to understand eutrophication effects and how acidification, eutrophication, and a warming climate are interacting in these ecosystems.

The recovery of Moat Lake ANC was a positive result that further contributes to the already noted successes of the CAAA. However, when I looked more broadly across the landscape I found that many Sierra Nevada lakes are still affected by acid deposition. This was demonstrated by the correlation between present day ANC in water samples and SCP concentrations in surface sediments. These results highlighted the need for stricter regulatory standards and were consistent with national-scale reviews that found current emission reductions were not adequate to allow for full recovery of more sensitive ecosystems (Burns *et al.* 2011).

The critical load is an approach that can define the stricter standards and enable recovery of sensitive ecosystems. However, if critical loads are to be an effective tool and incorporated into air quality policy it is important to link atmospheric deposition to chemical lake effects and understand these relationships at a landscape scale, the scale at which policy is applied. I measured indicators of atmospheric deposition and basin characteristics to explain variation in lake ANC and nutrient limitation across the Sierra Nevada landscape. The results indicated a correlation with atmospheric deposition and ANC, however, did not indicate a relationship with eutrophication indicators and atmospheric deposition. I concluded that quantifying the relationship between nitrogen deposition and eutrophication across complex mountain landscapes is presently

challenging and that calculating critical loads based on acidification is a more robust approach. In Chapter 2, I estimated an acidification critical load for acid anions of 73.9 eq ha^{-1} yr^{-1}, which translates to 0.68 kg-N ha^{-1} yr^{-1} and 1.2 kg-SO_4 ha^{-1} yr^{-1}. We also concluded that air patterns and deposition across the Sierra Nevada are complex as indicated by spatial SCP patterns. Finer-scale measurements and modeling across mountain landscapes would improve our ability to quantify effects of deposition and improve critical load estimates.

Despite the concluding emphasis on acidification critical loads, the results also underscore the need for continued research on understanding the complexity of the nitrogen cycle and how nutrient deposition is affecting lake ecosystems. In the final chapter, I investigate the response of phytoplankton to nutrient enrichment gradient and used the results to develop a range of nutrient criteria for nitrate and phosphate. Low range nutrient criteria estimates for nitrate were 0.33 μM (10% effective dose (ED)), 1.0 μM (50% ED), and 3.1 μM (90% ED). High range nutrient criteria estimates for nitrate were 0.89 μM (10% ED), 4.0 μM (50% ED), and 18 μM (90% ED). Phosphate criteria ranged from 0.03 - 0.45 μM (10% ED), 0.24 - 1.1 μM (50% ED), and 2.0 - 2.5 μM (90% ED). I applied the nitrogen criteria to a population of lakes to assess the status of Sierra Nevada lakes and found that the 10% effective dose was exceeded by 28% of lakes using the high nutrient criteria and 37 % using the low nutrient criteria, the 50% effective dose was exceeded by 18% of lakes (high criteria) and 29% (low criteria), and the 90% effective dose was exceeded by 0.0 % of lakes (high criteria) and 21% (low criteria). The nutrient criteria will be used in conjunction with lake monitoring programs to assess the

status of sensitive high-elevation lakes, to inform resource condition assessments and planning efforts by land management agencies, to develop critical loads, and to communicate the status of lakes to the public and policymakers (Heard *et al.* 2012; Nanus *et al.* 2012; Theobald *et al.* 2010).

Chapter 6: References

Albertin, A. R. 2009. Nutrient dynamics in Florida springs and relationships to algal blooms. PhD Dissertation, 159 pp, University of Florida, Gainesville.

Arnett, H., J. Saros, and M. Alisa Mast. 2012. A caveat regarding diatom-inferred nitrogen concentrations in oligotrophic lakes. Journal of Paleolimnology 47(2): 277-291.

Baron, J. S. 2006. Hindcasting nitrogen deposition to determine an ecological critical load. Ecological Applications 16(2): 433-439.

Baron, J. S., C. T. Driscoll, J. L. Stoddard, and E. E. Richer. 2011. Empirical critical loads of atmospheric nitrogen deposition for nutrient enrichment and acidification of sensitive US lakes. BioScience 61 (8): 602-613.

Berg, N. H., A. Gallegos, T. Dell, J. Frazier, T. Procter, J. Sickman, S. Grant, T. Blett, and M. Arbaugh. 2005. A screening procedure for identifying acid-sensitive lakes from catchment characteristics. Environmental Monitoring and Assessment 105: 285-307.

Berg, N. H. 2006. Water quality review Sierra Nevada 2005 Lake Monitoring. 28 pp, PSW Research Station, USDA Forest Service, Albany, CA.

Bergström, A.-K. 2010. The use of TN:TP and DIN:TP ratios as indicators for phytoplankton nutrient limitation in oligotrophic lakes affected by N deposition. Aquatic Sciences 72: 277-281.

Bergström, A. K., and M. Jansson. 2006. Atmospheric nitrogen deposition has caused nitrogen enrichment and eutrophication of lakes in the northern hemisphere. Global Change Biology 12(4): 635-643.

Bindslev, N. 2008. Drug-acceptor interactions - Modeling theoretical tools to test and evaluate experimental equilibrium effects. Co-Action Publishing Sweden.

Bonfils, C. l., B. D. Santer, D. W. Pierce, H. G. Hidalgo, G. Bala, T. Das, T. P. Barnett, D. R. Cayan, C. Doutriaux, A. W. Wood, A. Mirin, and T. Nozawa. 2008. Detection and attribution of temperature changes in the mountainous western United States. Journal of Climate 21(23): 6404-6424.

Brenner, M., T. Whitmore, J. Curtis, D. Hodell, and C. Schelske. 1999. Stable isotope (δ13C and δ15N) signatures of sedimented organic matter as indicators of historic lake trophic state. Journal of Paleolimnology 22(2): 205-221.

Bull, K. R. 1992. An introduction to critical loads. Environmental Pollution 77(2-3): 173-176.

Burns, D. A., T. Blett, R. Haeuber, and L. H. Pardo. 2008. Critical loads as a policy tool for protecting ecosystems from the effects of air pollutants. Frontiers in Ecology and the Environment 6(3): 156-159.

Burns, D. A., J. A. Lynch, B. J. Cosby, M. E. Fenn, J. S. Baron, and U.S. Environmental Protection Agency Clean Markets Division. 2011. National Acid Precipitation Assessment Program report to Congress 2011: An integrated assessment. 114 pp, National Science and Technology Council, Washington, DC.

Bytnerowicz, A., M. Tausz, R. Alanso, D. Jones, R. Johnson, and N. Grulke. 2002. Summer-time distribution of air pollutants in Sequoia National Park, California. Envionmental Pollution 118: 187-203.

California Regional Water Quality Control Board - Central Valley Region. 1995. Water quality control plan for the Tulare Lake Basin. 65 pp, California Regional Water Quality Control Board - Central Valley Region, Sacramento, CA.

California Regional Water Quality Control Board - Central Valley Region. 1998. The water quality control plan (basin plan) for the California Regional Water Quality Control Board, Central Valley Region. 80 pp, California Regional Water Quality Control Board - Central Valley Region, Sacramento, CA.

California Regional Water Quality Control Board - Lahontan Region. 1994. Water quality control plan for the Lahonton Region, North and South basins. 590 pp,

California Regional Water Quality Control Board - Lahontan Region, South Lake Tahoe, CA.

Carter, J. C. H. 1974. Life cycles of three limnetic Copepods in a beaver pond. Journal of the Fisheries Research Board of Canada 31(4): 421-434.

Cayan, D. R., S. A. Kammerdiener, M. D. Dettinger, J. M. Caprio, and D. H. Peterson. 2001. Changes in the onset of spring in the western United States. Bulletin of the American Meteorological Society 82: 399-415.

Chirinos, L., N. L. Rose, R. Urrutia, P. Munoz, F. Torrejon, L. Torres, F. Cruces, A. Araneda, and C. Zaror. 2006. Environmental evidence of fossil fuel pollution in Laguna Chica de San Pedro lake sediments (Central Chile). Environmental Pollution 141(2): 247-256.

Clow, D. W., M. A. Mast, and D. H. Campbell. 1996. Controls on surface water chemistry in the upper Merced River basin, Yosemite National Park, California. Hydrological Processes 10(5): 727-746.

Clow, D. W., and J. K. Sueker. 2000. Relations between basin characteristics and stream water chemistry in alpine/subalpine basins in Rocky Mountain National Park, Colorado. Water Resources Research 36(1): 49-61.

Clow, D. W., J. O. Sickman, R. G. Striegl, D. P. Krabbenhoft, J. G. Elliott, M. Dornblaser, D. A. Roth, and D. H. Campbell. 2003. Changes in the chemistry of lakes and precipitation in high-elevation national parks in the western United States, 1985-1999. Water Resources Research 39(6): 1171.

Clow, D. W., L. Nanus, and B. Huggett. 2010. Use of regression-based models to map sensitivity of aquatic resources to atmospheric deposition in Yosemite National Park, USA. Water Resour. Res. 46(9): W09529.

Coats, R., J. Perez-Losada, G. Schladow, R. Richards, and C. Goldman. 2006. The warming of Lake Tahoe. Climatic Change 76(1-2): 121-148.

Colman, S. M., J. A. Peck, E. B. Karabanov, S. J. Carter, J. P. Bradbury, J. W. King, and D. F. Williams. 1995. Continental climate response to orbital forcing from biogenic silica records in Lake Baikal. Nature 378: 769-771.

Conley, D. J., and C. L. Schelske. 1993. Potential role of sponge spicules in influencing the silicon biogeochemistry of Florida lakes. Canadian Journal of Fisheries and Aquatic Sciences 50(2): 296-302.

Creager, C., J. Butcher, E. Welch, G. Wortham, and S. Roy. 2006. Technical approach to develop nutrient numeric endpoints for California. 137 pp, Tetra Tech, Inc., Lafayette, CA.

Curtis, C. J., S. Juggins, G. Clarke, R. W. Battarbee, M. Kernan, J. Catalan, R. Thompson, and M. Posch. 2009. Regional influence of acid deposition and climate change in European mountain lakes assessed using diatom transfer functions. Freshwater Biology 54(12): 2555-2572.

Curtis, C. J., R. Flower, N. Rose, J. Shilland, G. L. Simpson, S. Turner, H. D. Yang, and S. Pla. 2010. Palaeolimnological assessment of lake acidification and environmental change in the Athabasca Oil Sands Region, Alberta. Journal of Limnology 69: 92-104.

D'Elia, C. F., J. G. Sanders, and W. R. Boynton. 1986. Nutrient enrichment studies in a coastal plain estuary: Phytoplankton growth in large-scale, continuous cultures. Canadian Journal of Fisheries and Aquatic Sciences 43(2): 397-406.

Douglas, M. S., J. P. Smol, and W. Blake Jr. 1994. Marked post-18th century environmental change in high-arctic ecosystems. Science 266: 416-419.

Driscoll, C. T., G. B. Lawrence, A. J. Bulger, T. J. Butler, C. S. Cronan, C. Eagar, K. F. Lambert, G. E. Likens, J. L. Stoddard, and K. C. Weathers. 2001. Acidic deposition in the northeastern United States: Sources and inputs, ecosystem effects, and management strategies. BioScience 51(3): 180-198.

Dugdale, R. C. 1967. Nutrient limitation in the sea: Dynamics, identification, and significance. Limnology and Oceanography 12(4): 685-695.

Edwards, L. M., and K. Redmond. 2011. Climate assessment for the Sierra Nevada Network Parks. Natural Resource Report 178 pp, National Park Service, Fort Collins, Colorado.

Eilers, J. M., D. F. Brakke, D. H. Landers, and W. S. Overton. 1989. Chemistry of lakes in designated wilderness areas in the western United States. Environmental Monitoring and Assessment 12(1): 3-21.

Elser, J. J., M. E. S. Bracken, E. E. Cleland, D. S. Gruner, W. S. Harpole, H. Hillebrand, J. T. Ngai, E. W. Seabloom, J. B. Shurin, and J. E. Smith. 2007. Global analysis of nitrogen and phosphorus limitation of primary producers in freshwater, marine and terrestrial ecosystems. Ecology Letters 10(12): 1135-1142.

Elser, J. J., T. Andersen, J. S. Baron, A.-K. Bergstrom, M. Jansson, M. Kyle, K. R. Nydick, L. Steger, and D. O. Hessen. 2009a. Shifts in lake N:P stoichiometry and nutrient limitation driven by atmospheric nitrogen deposition. Science 326: 835-837.

Elser, J. J., M. Kyle, L. Steger, K. R. Nydick, and J. S. Baron. 2009b. Nutrient availability and phytoplankton nutrient limitation across a gradient of atmospheric nitrogen deposition. Ecology 90(11): 3062-3073.

Engle, D. L., and J. M. Melack. 1997. Assessing the potential impact of acid deposition on high altitude aquatic ecosystems in California: Integrating ten years of investigation. 186 pp, California Air Resources Board.

EPA. 2000. National air pollutant emission trends 1900-1998. 238 pp, United States Environmental Protection Agency, Research Triangle Park, NC.

Fenn, M. E., J. S. Baron, E. B. Allen, H. M. Rueth, K. R. Nydick, L. Geiser, W. D. Bowman, J. O. Sickman, T. Meixner, D. W. Johnson, and P. Neitlich. 2003. Ecological effects of nitrogen deposition in the Western United States. BioScience 53(4): 404-420.

Fott, J., J. Vukic, and N. L. Rose. 1998. The spatial distribution of characterized fly-ash particles and trace metals in lake sediments and catchment mosses: Czech Republic. Water Air and Soil Pollution 106(3-4): 241-261.

Francoeur, S. N. 2001. Meta-analysis of lotic nutrient amendment experiments: detecting and quantifying subtle responses. Journal of the North American Benthological Society 20(3): 358-368.

Galloway, J. N., and E. B. Cowling. 2002. Reactive nitrogen and the world: 200 years of change. AMBIO: A Journal of the Human Environment 31(2): 64-71.

Galman, V., J. Rydberg, and C. Bigler. 2009. Decadal diagenetic effects on δC-13 and δN-15 studied in varved lake sediment. Limnology and Oceanography 54(3): 917-924.

Gibson, G., R. Carlson, J. Simpson, E. Smeltzer, J. Gerritson, S. Chapra, S. Heiskary, J. Jones, and R. Kennedy. 2000. Nutrient criteria technical guidance manual: Lakes and reservoirs. 232 pp, Environmental Protection Agency, Washington, DC.

Goldman, C. R. 1988. Primary productivity, nutrients, and transparency during the early onset of eutrophication in ultra-oligotrophic Lake Tahoe, California-Nevada Limnology and Oceanography 33(6): 1321-1333.

Goldman, C. R., A. D. Jassby, and S. H. Hackley. 1993. Decadal, interannual and seasonal variability in enrichment bioassays at Lake Tahoe, California-Nevada, USA. Canadian Journal of Fisheries and Aquatic Sciences 50(7): 1489-1496.

Goodridge, J. 1997. Historic rain records of California. 20 pp, California Department of Water Resources, Mendocino, CA.

Gran, G. 1952. Determination of the equivalent point in potentiometric tirations: Part 2. Analyst 77: 661-671.

Grover, J. P. 1989. Phosphorus-dependent growth kinetics of 11 species of freshwater algae. Limnology and Oceanography 34(2): 341-348.

Hamlet, A. F., P. W. Mote, M. P. Clark, and D. P. Lettenmaier. 2005. Effects of temperature and precipitation variability on snowpack trends in the western United States. Journal of Climate 18(21): 4545-4561.

Heard, A. M., L. A. H. Starcevich, J. Sickman, M. G. Rose, and D. W. Schweizer. 2012. Sierra Nevada Network lake monitoring protocol. Natural Resource Report NPS/SIEN/NRR-2012/551, National Park Service, Fort Collins, Colorado.

Helsel, D. R., and R. M. Hirsch. 2002. Statistical methods in water resources techniques of water resources investigations, Book 4, chapter A3. 522 pp. U.S. Geological Survey.

Helsel, D. R. 2005. Nondetects and data analysis: Statistics for censored environmental data, First ed. John Wiley and Sons, Inc., Hoboken, New Jersey.

Henriksen, A., B. L. Skjelvale, J. Mannio, A. Wilander, H. Ron, C. Curtis, J. P. Jensen, E. Fjeld, and T. Moiseenko. 1998. Northern European lake survey, 1995: Finland, Norway, Sweden, Denmark, Russian Kola, Russian Karelia, Scotland and Wales. Ambio 27(2): 80-91.

Hicks, B. B., R. P. Hosker Jr, T. P. Meyers, and J. D. Womack. 1991. Dry deposition inferential measurement techniques - I. Design and tests of a prototype meteorological and chemical system for determining dry deposition. Atmospheric Environment. Part A. General Topics 25(10): 2345-2359.

Holland, E. A., F. J. Dentener, B. H. Braswell, and J. M. Sulzman. 1999. Contemporary and pre-industrial global reactive nitrogen budgets. Biogeochemistry 46(1): 7-43.

Holmes, R. W., M. C. Whiting, and J. L. Stoddard. 1989. Changes in diatom-inferred pH and acid neutralizing capacity in a dilute, high elevation, Sierra Nevada lake since A.D. 1825. Freshwater Biology 21(2): 295-310.

Homyak, P. M. 2012. Nitrogen and phosphorus biogeochemistry of watersheds along the western slope of the Sierra Nevada. Ph.D. Dissertation, 234 pp, University of California, Riverside, CA.

Horvitz, D. G., and D. J. Thompson. 1952. A generalization of sampling without replacement from a finite universe. Journal of the American Statistical Association 47(260): 663-685.

Hu, F. S., D. Kaufman, S. Yoneji, D. Nelson, A. Shemesh, Y. Huang, J. Tian, G. Bond, B. Clegg, and T. Brown. 2003. Cyclic variation and solar forcing of Holocene climate in the Alaskan subarctic. Science 301(5641): 1890-1893.

Kahl, J. S., J. L. Stoddard, R. Haeuber, S. G. Paulsen, R. Birnbaum, F. A. Deviney, J. R. Webb, D. R. DeWalle, W. Sharpe, C. T. Driscoll, A. T. Herlihy, J. H. Kellogg, P. S. Murdoch, K. Roy, K. E. Webster, and N. S. Urquhart. 2004. Have U.S. surface waters responded to the 1990 Clean Air Act Amendments? Environmental Science & Technology 38(24): 484A-490A.

Kapnick, S., and A. Hall. 2012. Causes of recent changes in western North American snowpack. Climate Dynamics 38(9-10): 1885-1899.

Kendall, C. 1998. Tracing nitrogen sources and cycling in catchments, In Isotope tracers in catchment hydrology, edited by C. Kendall and J. J. McDonnell, pp. 519-576, Elsevier Science, Amsterdam.

Landers, D. H., S. M. Simonich, D. Jaffe, L. Geiser, D. H. Campbell, A. Schwindt, C. Schreck, M. Kent, W. Hafner, H. E. Taylor, K. Hageman, S. Usenko, L. Ackerman, J. Schrlau, N. Rose, T. Blett, and M. M. Erway. 2008. The fate, transport, and ecological impacts of airborne contaminants in western National Parks (USA). EPA/600/R-07/138. U.S. Environmental Protection Agency, Office of Research and Development, NHEERL, Western Ecology Division, Corvallis, Oregon.

Lehmann, C. M. B., V. C. Bowersox, and S. M. Larson. 2005. Spatial and temporal trends of precipitation chemistry in the United States, 1985-2002. Environmental Pollution 135(3): 347-361.

Meixner, T., and R. C. Bales. 2003. Hydrochemical modeling of coupled C and N cycling in high-elevation catchments: Importance of snow cover. Biogeochemistry 62(3): 289-308.

Melack, J. M., C. A. Ochs, and J. L. Stoddard. 1985. Major ion chemistry and sensitivty to acid precipitation of Sierra Nevada lakes. Water Resources Research 21(1): 27-32.

Meyers, P. A. 2003. Applications of organic geochemistry to paleolimnological reconstructions: A summary of examples from the Laurentian Great Lakes. Organic Geochemistry 34(2): 261-289.

Meyers, T. P., P. Finkelstein, J. Clarke, T. G. Ellestad, and P. F. Sims. 1998. A multilayer model for inferring dry deposition using standard meteorological measurements. Journal of Geophysical Research: Atmospheres 103(D17): 22645-22661.

Michel, T. J., J. E. Saros, S. J. Interlandi, and A. P. Wolfe. 2006. Resource requirements of four freshwater diatom taxa determined by in situ growth bioassays using natural populations from alpine lakes. Hydrobiologia 568: 235-243.

Michelutti, N., M. S. V. Douglas, and J. P. Smol. 2003. Diatom response to recent climatic change in a high arctic lake (Char Lake, Cornwallis Island, Nunavut). Glob. Planet. Change 38(3-4): 257-271.

Monod, J. 1950. La technique de culture continue, theorie et applications. Ann. Inst. Pasteur, Paris 79(390-410).

Morris, D. P., and W. M. Lewis. 1988. Phytoplankton nutirent limitation in Colorado mountain lakes. Freshwater Biology 20(3): 315-327.

Nanus, L., D. H. Campbell, and M. W. Williams. 2005. Sensitivity of alpine and subalpine lakes to acidification from atmospheric deposition in Grand Teton National Park and Yellowstone National Park, Wyoming. Scientific Investigations Report: 2005-5023. 41 pp, US Geological Survey, Reston, Virginia.

Nanus, L., M. W. Williams, D. H. Campbell, E. M. Elliott, and C. Kendall. 2008. Evaluating regional patterns in nitrate sources to watersheds in national parks of the Rocky Mountains using nitrate isotopes. Environmental Science & Technology 42(17): 6487-6493.

Nanus, L., M. W. Williams, D. H. Campbell, K. A. Tonnessen, T. Blett, and D. W. Clow. 2009. Assessment of lake sensitivity to acidic deposition in national parks of the Rocky Mountains. Ecological Applications 19(4): 961-973.

Nanus, L., D. W. Clow, J. E. Saros, V. C. Stephens, and D. H. Campbell. 2012. Mapping critical loads of nitrogen deposition for aquatic ecosystems in the Rocky Mountains, USA. Environmental Pollution 166(0): 125-135.

National Park Service. 1998. Geospatial vegetation data for the Yosemite National Park Inventory Project, Yosemite National Park and environs. Geospatial Dataset-2167311.

National Park Service. 2009. Geospatial vegetation information for the Sequoia and Kings Canyon National Parks Vegetation Inventory Project Sequoia and Kings Canyon National Parks and environs. Geospatial Dataset-2168871.

National Research Council. 2004. Air quality management in the United States. The National Academies Press, Washington DC.

Nelson, C. E., and C. A. Carlson. 2011. Differential response of high-elevation planktonic bacterial community structure and metabolism to experimental nutrient enrichment. PLoS ONE 6(3): e18320.

Nilsson, J., and P. Grennfelt. 1988. Critical loads for sulphur and nitrogen, in UNECE Nordic Council Workshop Report, Skolster, Sweden.

NPS Geologic Resources Inventory Program. 2006. Digital geologic map of the Yosemite quadrangle, Californa, Nantional Park Service Geologic Resources Inventory Program, Lakewood, CO. Geospatial dataset-1041507.

NPS Geologic Resources Inventory Program. 2013. Digital geologic map of Sequoia and Kings Canyon National Parks and vicinity, California, National Park Service Geologic Resources Inventory. Geospatial Dataset-2194511.

Nydick, K. R., B. M. Lafrancois, J. S. Baron, and B. M. Johnson. 2004. Nitrogen regulation of algal biomass, productivity, and composition in shallow mountain

lakes, Snowy Range, Wyoming, USA. Canadian Journal of Fisheries and Aquatic Sciences 61: 1256-1268.

Ohte, N., S. D. Sebestyen, J. B. Shanley, D. H. Doctor, C. Kendall, S. D. Wankel, and E. W. Boyer. 2004. Tracing sources of nitrate in snowmelt runoff using a high-resolution isotopic technique. Geophys. Res. Lett. 31(21).

Pardo, L. H., M. J. Robin-Abbott, and C. T. Driscoll. 2011. Assessment of nitrogen deposition effects and empirical critical loads of nitrogen for ecoregions of the United States. USDA Forest Service, Newton Square, PA.

Pedersen, M. F., and J. Borum. 1996. Nutrient control of algal growth in estuarine waters. Nutrient limitation and the importance of nitrogen requirements and nitrogen storage among phytoplankton and species of macroalgae. Marine ecology progress series. Oldendorf 142(1): 261-272.

Pinowska, A., R. J. Stevenson, A. R. Albertin, J. O. Sickman, and M. Anderson. 2007. Integrated interporetation of survey and experimental approaches for determining nutrient thresholds for macroalgae in Florida springs. Florida Department of Environmental Protection, Tallahassee, Florida.

Pla, S., D. Monteith, R. Flower, and N. Rose. 2009. The recent palaelimnology of a remote Scottish loch with special reference to the relative impacts of regional warming and atmospheric contamination. Freshwater Biology 54: 505-523.

Porinchu, D. F., A. P. Potito, G. M. MacDonald, and A. M. Bloom. 2007. Subfossil chironomids as indicators of recent climate change in Sierra Nevada, California, lakes. Arctic, Antarctic, and Alpine Research 39(2): 286-296.

Porter, E., and S. Johnson. 2007. Translating science into policy: Using ecosystem thresholds to protect resources in Rocky Mountain National Park. Environmental Pollution 149(3): 268-280.

R Development Core Team. 2011. R: A language and environment for statistical computing. R Foundation for Statistical Computing: Vienna, Austria. http://www.R-project.org.

Raddum, G. G., A. Fjellheim, and B. L. Skjelkvale. 2001. Improvements in water quality and aquatic ecosystems due to reduction in sulphur deposition in Norway. Water, Air, and Soil Pollution 130(1-4): 87-98.

Rigler, F. H. 1956. A tracer study of the phosphorus cycle in lake water. Ecology 37(3): 550-562.

Ritz, C., and J. C. Streibig. 2005. Bioassay analysis using R. Journal of Statistical Software 12(5): 1-22.

Ritz, C. 2010. Toward a unified approach to dose-response modeling in ecotoxicology. Environmental Toxicology and Chemistry 29(1): 220-229.

Rose, N. L. 1994. A note on further refinements to a procedure for the extraction of carbonaceous fly-ash particles from sediments. Jounal of Paleolimnology 11: 201-204.

Rose, N. L., and S. Juggins. 1994. A spatial relationship between carbonaceous particles in lake sediments and sulphur deposition. Atmos. Environ. 28(2): 177-183.

Rose, N. L. 1995. Carbonaceous particle record in lake sediments from the Arctic and other remote areas of the Northern Hemisphere. Science of The Total Environment 160/161(0): 487-496.

Rose, N. L., S. Harlock, P. G. Appleby, and R. W. Battarbee. 1995. Dating of recent lake sediments in the United Kingdom and Ireland using spheroidal carbonaceous particle (SCP) concentration profiles. Holocene 5: 328-335.

Rose, N. L., and S. Harlock. 1998. The spatial distribution of characterised fly-ash particles and trace metals in lake sediments and catchment mosses in the United Kingdom. Water Air and Soil Pollution 106(3-4): 287-308.

Rose, N. L., S. Harlock, and P. G. Appleby. 1999. The spatial and temporal distributions of spheroidal carbonaceous fly-ash particles (SCP) in the sediment records of European mountain lakes. Water Air and Soil Pollution 113(1-4): 1-32.

Rose, N. L., E. Shilland, T. Berg, K. Hanselmann, R. Harriman, K. Koinig, U. Nickus, B. S. Trad, E. Stuchlik, H. Thies, and M. Ventura. 2001. Relationships between acid ions and carbonaceous fly-ash particles in deposition at European mountain lakes. Water Air and Soil Pollution 130(1-4): 1703-1708.

Rose, N. L., and D. T. Monteith. 2005. Temporal trends in spheroidal carbonaceous particle deposition derived from annual sediment traps and lake sediment cores and their relationship with non-marine sulphate. Environmental Pollution 137(1): 151-163.

Rose, N. L. 2008. Quality control in the analysis of lake sediments for spheroidal carbonaceous particles. Limnology and Oceanography-Methods 6: 172-179.

Rouillard, A., N. Michelutti, P. Rosen, M. S. V. Douglas, and J. P. Smol. 2012. Using paleolimnology to track Holocene climate fluctuations and aquatic ontogeny in poorly buffered High Arctic lakes. Paleogeogr. Paleoclimatol. Paleoecol. 321: 1-15.

Saros, J., D. Clow, T. Blett, and A. Wolfe. 2011. Critical nitrogen deposition loads in high-elevation lakes of the western US inferred from paleolimnological records. Water, Air, & Soil Pollution 216(1): 193-202.

Schindler, D. W. 1974. Eutrophication and recovery in experimental lakes: Implications for lake management. Science 184(4139): 897-899.

Schlesinger, W. H. 1997. Biogeochemistry: An analysis of global change, 2nd ed. Academic Press, San Diego, CA.

Schwartz, S. S. 1984. Life history strategies in Daphnia: A review and predictions. Oikos 42(1): 114-122.

Seastedt, T. R., W. D. Bowman, T. N. Caine, D. McKnight, A. Townsend, and M. W. Williams. 2004. The landscape continuum: A model for high-elevation ecosystems. BioScience 54(2): 111-121.

Sickman, J., S. D. Cooper, J. M. Melack, and L. Meeker. 1999. Effects of experimental acid and nutrient additions on the phytoplankton of Emerald Lake, Sierra Nevada, California, p. 66, UC Santa Barbara.

Sickman, J. O. 1989. Characterization of year-round sensitivity of California 's montane lakes to acidic deposition. 120 pp, California Air Resources Board, Santa Barbara, CA.

Sickman, J. O., A. Leydecker, and J. M. Melack. 2001. Nitrogen mass balances and abiotic controls on N retention and yield in high-elevation catchments of the Sierra Nevada, California, United States. Water Resources Research 37(5): 1445-1461.

Sickman, J. O., A. Leydecker, C. C. Y. Chang, C. Kendall, J. M. Melack, D. M. Lucero, and J. Schimel. 2003a. Mechanisms underlying export of N from high-elevation catchments during seasonal transitions. Biogeochemistry 64(1): 1-24.

Sickman, J. O., J. M. Melack, and D. W. Clow. 2003b. Evidence for nutrient enrichment of high-elevation lakes in the Sierra Nevada, California. Limnology and Oceanography 48(5): 1885-1892.

Sickman, J. O., D. Bennett, D. M. Lucero, T. J. Whitmore, and W. F. Kenney. In press. Diatom-inference models for acid-neutralizing capacity and nitrate based on a 41-lake calibration dataset from the Sierra Nevada, California, USA. Journal of Paleolimnology.

Smith, S. J., J. van Aardenne, Z. Klimont, R. J. Andres, A. Volke, and S. Delgado Aria. 2011. Anthropogenic sulfur dioxide emissions: 1850-2005. Atmospheric Chemistry and Physics 11: 1101-1116.

Smith, V. H., and D. W. Schindler. 2009. Eutrophication science: Where do we go from here? Trends in Ecology & Evolution 24(4): 201-207.

Smol, J. P. 2010. The power of the past: Using sediments to track the effects of multiple stressors on lake ecosystems. Freshwater Biology 55: 43-59.

Sorvari, S., A. Korhola, and R. Thompson. 2002. Lake diatom response to recent Arctic warming in Finnish Lapland. Global Change Biology 8(2): 171-181.

Stanko, K. M., and J. W. Fitzgerald. 1990. Sulfur transformations in forest soils collected along an elevational gradient. Soil Biology and Biochemistry 22(2): 213-216.

State Water Resources Control Board, and California Environmental Protection Agency. 2011. Scoping document: Nutrient policy. State Water Resources Control Board, Sacramento, CA.

Sterner, R. W. 2008. On the phosphorus limitation paradigm for lakes. International Review of Hydrobiology 93(4-5): 433-445.

Stevens, D. L., and A. R. Olsen. 2003. Variance estimation for spatially balanced samples of environmental resources. Environmetrics 14(6): 593-610.

Stevens, D. L., and A. R. Olsen. 2004. Spatially balanced sampling of natural resources. Journal of the American Statistical Association 99(465): 262-278.

Stoddard, J. L., D. S. Jeffries, A. Lukewille, T. A. Clair, P. J. Dillon, C. T. Driscoll, M. Forsius, M. Johannessen, J. S. Kahl, J. H. Kellog, A. Kemp, J. Mannio, D. T. Monteith, P. S. Murdoch, S. Patrick, A. Rebsdorf, B. L. Skelkvale, M. P. Stainton, T. Traaen, H. van Dam, K. E. Webster, J. Wieting, and A. Wilander. 1999. Regional trends in aquatic recovery from acidification in North America and Europe. Nature 401: 575-578.

Street, J. H., R. S. Anderson, and A. Paytan. 2012. An organic geochemical record of Sierra Nevada climate since the LGM from Swamp Lake, Yosemite. Quaternary Science Reviews 40(0): 89-106.

Sullivan, T. J., B. J. Cosby, K. A. Tonnessen, and D. W. Clow. 2005. Surface water acidification responses and critical loads of sulfur and nitrogen deposition in Loch Vale watershed, Colorado. Water Resources Research 41(1).

Theobald, D. M., J. S. Baron, P. Newman, B. Noon, J. B. Norman, I. Leinwand, S. E. Linn, R. Sherer, K. E. Williams, and M. D. Hartman. 2010. A natural resource

condition assessment for Rocky Mountain National Park. Natural Resource Report NPS/NRPC/WRD/NRR - 2010/228, National Park Service, Fort Collins, CO.

Tonnesen, G., Z. Wang, M. Omary, and C.-J. Chien. 2007. Assessment of nitrogen deposition: Modeling and habitat assessment. California Energy Commission, PIER Energy-Related Environmental Research: CEC-500-2006-032.

UNECE. 1999. The 1999 Gothenburg protocol to abate acidification, eutrophication, and ground-level ozone. United Nations Economic Commission for Europe, Gothenberg, Sweden.

Valderrama, J. C. 1981. The simultaneous analysis of total nitrogen and total phoshporus in natural waters. Marine Chemistry 10: 109-122.

Vicars, W. C., and J. O. Sickman. 2011. Mineral dust transport to the Sierra Nevada, California: Loading rates and potential source areas. Journal of Geophysical Research-Biogeosciences (2005-2012) 116: G1.

Vitousek, P. M. 2004. Nutrient cycling and limitation, Hawai'i as a model system. Princeton University Press, New Jersey.

Wessels, M., K. Mohaupt, R. Kummerlin, and A. Lenhard. 1999. Reconstructing past eutrophication trends from diatoms and biogenic silica in the sediment and the pelagic zone of Lake Constance, Germany. Journal of Paleolimnology 21(2): 171-192.

Wetzel, R. G., and G. E. Likens. 2000. Limnological Analyses, Third ed. Springer, New York, New York.

Whiting, M. C., D. R. Whitehead, R. W. Holmes, and S. A. Norton. 1989. Paleolimnological reconstruction of recent acidity changes in four Sierra Nevada lakes. Jounal of Paleolimnology 2(4): 285-304.

Wigington Jr, P. J., T. D. Davies, M. Tranter, and K. N. Eshleman. 1992. Comparison of episodic acidification in Canada, Europe and the United States. Environmental Pollution 78(1-3): 29-35.

Wik, M., and I. Renberg. 1991. Recent atmospheric deposition in Sweden of carbonaceous particles from fossil-fuel combustion surveyed using lake sediments. Ambio 20(7): 289-292.

Williams, J. C. 1997. Energy and the making of modern California, First ed. The University of Akron Press, Akron, Ohio.

Williams, M. W., and K. A. Tonnessen. 2000. Critical loads for inorganic nitrogen deposition in the Colorado Front Range, USA. Ecological Applications 10(6): 1648-1665.

Williamson, C., C. Salm, S. L. Cooke, and J. E. Saros. 2010. How do UV radiation, temperature, and zooplankton influence the dynamics of alpine phytoplankton communities? Hydrobiologia 648(1): 73-81.